

INFORMATION TO USERS

This manuscript has been reproduced from the microfilm master. UMI films the text directly from the original or copy submitted. Thus, some thesis and dissertation copies are in typewriter face, while others may be from any type of computer printer.

The quality of this reproduction is dependent upon the quality of the copy submitted. Broken or indistinct print, colored or poor quality illustrations and photographs, print bleedthrough, substandard margins, and improper alignment can adversely affect reproduction.

In the unlikely event that the author did not send UMI a complete manuscript and there are missing pages, these will be noted. Also, if unauthorized copyright material had to be removed, a note will indicate the deletion.

Oversize materials (e.g., maps, drawings, charts) are reproduced by sectioning the original, beginning at the upper left-hand corner and continuing from left to right in equal sections with small overlaps.

ProQuest Information and Learning
300 North Zeeb Road, Ann Arbor, MI 48106-1346 USA
800-521-0600

UMI[®]

**Kinetics and Mechanisms of Morphological Transitions
in Block Copolymer Aggregates and Sodium Dodecyl Sulfate
as a Morphogenic Agent**

by

Susan Elizabeth Burke

A thesis

submitted to the Faculty of Graduate Studies and Research
in partial fulfillment of the requirements for the degree of

Master of Science

Department of Chemistry
McGill University
Montreal, Quebec
Canada, H3A 2K6

© Susan Elizabeth Burke

March 2001



**National Library
of Canada**

**Acquisitions and
Bibliographic Services**

**385 Wellington Street
Ottawa ON K1A 0N4
Canada**

**Bibliothèque nationale
du Canada**

**Acquisitions et
services bibliographiques**

**385, rue Wellington
Ottawa ON K1A 0N4
Canada**

Your file Votre référence

Our file Notre référence

The author has granted a non-exclusive licence allowing the National Library of Canada to reproduce, loan, distribute or sell copies of this thesis in microform, paper or electronic formats.

The author retains ownership of the copyright in this thesis. Neither the thesis nor substantial extracts from it may be printed or otherwise reproduced without the author's permission.

L'auteur a accordé une licence non exclusive permettant à la Bibliothèque nationale du Canada de reproduire, prêter, distribuer ou vendre des copies de cette thèse sous la forme de microfiche/film, de reproduction sur papier ou sur format électronique.

L'auteur conserve la propriété du droit d'auteur qui protège cette thèse. Ni la thèse ni des extraits substantiels de celle-ci ne doivent être imprimés ou autrement reproduits sans son autorisation.

0-612-70389-4

Canada

Abstract

The kinetic and mechanistic details involved in the morphological transitions occurring in aggregates prepared from the copolymer polystyrene-*b*-poly(acrylic acid) (PS-*b*-PAA) in dioxane-water mixtures and the ability of sodium dodecyl sulfate to induce architectural changes in these aggregates are described in this dissertation. The kinetics of the sphere-to-rod, rod-to-sphere, and vesicle-to-rod transitions were determined by following the change in the solution turbidity as a function of time after the transitions were induced by a sudden jump in one of the solvent components of the system. The kinetics of each transition was explored as a function of the initial solvent composition, the magnitude of the solvent content jump, and the initial polymer concentration. In another study, the amphiphile, sodium dodecyl sulfate (SDS), was found to induce morphological transitions in the copolymer aggregates at lower water contents than those required in the absence of surfactant. The effect was studied as a function of SDS concentration, solvent composition, and copolymer concentration.

Résumé

Ce mémoire fait l'objet des détails d'ordre cinétique et mécanistique mis en jeu lors des transitions morphologiques ayant lieu dans certains agrégats. Ces derniers sont en fait des copolymères polystyrène-*b*-poly(acid acrylique) (PS-*b*-PAA) en solution (dioxane/eau). L'abilité du dodécylsulfate de sodium à induire des changements architecturaux est aussi discutée dans le présent mémoire. Les cinétiques des transitions sphère-cylindre, cylindre-sphère, et vésicule-cylindre ont été déterminées en suivant le changement de turbidité en fonction du temps après que les transitions eurent été induites par une subite augmentation de l'un des solvants du système. Les cinétiques de chaque transition ont été explorées en fonction de la composition initiale du solvant, de l'ampleur de cette addition brutale en solvant, ainsi que de la concentration initiale en polymère. Dans une autre étude, il fut trouvé qu'un amphiphile, le dodécylsulfate de sodium (DSS), induit des transitions morphologiques dans les agrégats de copolymères, et ce avec des taux en eau plus bas que ceux requis en absence de surfactants. Cet effet fut étudié en fonction de la concentration en DSS, de la composition du système, et de la concentration en copolymères.

Foreward

In accordance with Thesis Specifications of the “Guidelines for Thesis Preparation” (Faculty of Graduate Studies and Research, McGill University), the following text is cited:

“Candidates have the option of including, as part of the thesis, the text of one or more papers submitted, or to be submitted, for publication, or the clearly-duplicated text of one or more published papers. These texts must be bound together as an integral part of the thesis.

If this option is chosen, **connecting texts that provide logical bridges between the different papers are mandatory**. The thesis must be written in such a way that it is more than a mere collection of manuscripts; in other words, results of a series of papers must be integrated.

The thesis must still conform to all other requirements of the “Guidelines for Thesis Preparation”. **The thesis must include:** a table of contents, an abstract in English and French, an introduction which clearly states the rational and objectives of the research, a comprehensive review of the literature, a final conclusion and summary, and a thorough bibliography or reference list.

Additional material must be provided where appropriate (e.g., in appendices) and in sufficient detail to allow a clear and precise judgement to be made of the importance and originality of the research reported in the thesis.

In the case of manuscripts co-authored by the candidate and others, **the candidate is required to make an explicit statement in the thesis as to who contributed to such work and to what extent**. The supervisor must attest to the accuracy of such statement at the doctoral oral defence. Since the task of the examiners is made more difficult in these cases, it is in the candidate's interest to clearly specify the responsibilities of all the authors of the co-authored papers.”

This dissertation is written in the form of 3 original papers, each of which comprises one chapter. In addition, an introduction to this work is provided in the first chapter and general conclusions are given in chapter 5. Following normal procedures, the papers have been submitted or will be submitted shortly for publication in scientific journals. A list of papers contained within each chapter is given below:

Chapter 2: submitted to *Langmuir* (in a slightly modified form)

Chapter 3: submitted to *Polymer* (in a slightly modified form)

Chapter 4: to be submitted

Contributions of Authors

All of the papers were co-authored by the research director Dr. Adi Eisenberg. Other than the supervision, advice, and direction of Dr. Eisenberg, all of the work presented in this dissertation was performed by the author.

Acknowledgements

I would like to express a sincere thank you to Professor Eisenberg for providing me with the opportunity to carry out research in his laboratory. His guidance and support of my research are much appreciated. I would also like to thank him for his sound advice and fruitful discussions during the process of preparing my thesis.

I would also like to acknowledge a few other professors in the Department of Chemistry who have assisted me over the past year and a half. A special thank you goes to Professors Lennox and Damha for providing much needed support, advice, and assistance with administrative red tape. I graciously thank Professor Barrett for proof reading the introductory chapter of this dissertation.

My heart-felt gratitude is extended to Professor Palepu (St. Francis Xavier University) for helping me to discover my passion for doing chemical research while working in his laboratory during my undergraduate years. His guidance and genuine concern for me have helped to improve my confidence and abilities as a scientist. I will always be grateful for his friendship and advice. He is also acknowledged for providing useful comments about the results discussed in this dissertation.

My deepest appreciation is for my extraordinary family. Their love and support continue to lift me to new heights. I have been truly blessed with the most wonderful parents, Terrence and Patricia Burke. I thank them for always encouraging me to make my own choices because it is my own mistakes and successes that have proven to be my best teachers. I thank my sister, Nancy, for always being my very best friend.

I have been very fortunate to work with a wonderful group of scientists: Hongwei, Patrick, Sachiko, Carl, Owen, Amira, Michael, Laibin, Neil, Muriel, Izabel, Candice, and Pierre. I appreciate their willingness to share their expertise on everything from experimental design to how to make the computers work. It was my pleasure to have worked with them. A special thank you is extended to Hongwei for his assistance in the early stages of my research project and to Patrick for reviewing parts of my thesis.

I am especially grateful for the wonderful friendship of Ozzy, Sachiko, Patrick, Mohua, Amira, and Lana. Their support, encouragement, and ability to make me laugh is much appreciated and will never be forgotten. ☺

A sincere thank you is expressed to Renée Charron, Chantal Marotte, Paulette Henault, Carol Brown, Sandra Aerssen, and Fay Nurse for their administrative assistance and cheerful dispositions.

I am grateful to Fred Kluck for providing technical assistance in relation to my experimental design problems and to Jeannie Mui for providing valuable advice and assistance in the operation of the electron microscopes. I also thank Olivier Bourrier for French translation of the abstract.

I also gratefully acknowledge the Natural Sciences and Engineering Research Council of Canada and McGill University for providing financial support in the form of scholarships.

Table of Contents

Abstract.....	ii
Résumé.....	iii
Foreward.....	iv
Acknowledgements.....	vii
Table of Contents.....	ix
List of Tables.....	xii
List of Figures.....	xiii
List of Symbols.....	xv
Chapter 1. General Introduction.....	1
1.1 Introduction.....	1
1.2 Introduction to Polymers.....	2
1.2.1 Basic Definitions.....	2
1.2.2 Polymerization.....	3
1.2.3 Anionic Polymerization.....	4
1.2.4 Post-Polymerization Characterization.....	6
1.3 Introduction to Surfactants.....	7
1.4 Surfactant Aggregates in Solution.....	8
1.4.1 Micellization.....	9
1.4.2 Mechanism and Thermodynamics of Micellization.....	9
1.4.3 Kinetics of Micelle Formation.....	11
1.4.4 Polymorphism in Surfactant Aggregates.....	13
1.4.5 Morphological Transformation.....	15
1.5 Block Copolymer Aggregates in Solution.....	16
1.5.1 Micellization of Block Copolymer Molecules.....	16
1.5.2 Thermodynamics and Kinetics of Block Copolymer Micellization.....	17
1.5.3 Multiple Morphologies from Block Copolymers in Solution.....	19
1.5.4 Effect of Additives on the Morphology of Block Copolymer Aggregates...	22
1.6 Characterization Methods Employed.....	24
1.6.1 Solution Turbidity Measurements.....	24

1.6.2 Transmission Electron Microscopy.....	25
1.7 Objectives of This Thesis.....	26
1.8 References.....	27
Chapter 2. Kinetics and Mechanisms of the Sphere-to-Rod and Rod-to-Sphere Transitions in the Ternary System PS₃₁₀-b-PAA₅₂ / Dioxane / Water...	34
2.1 Introduction.....	35
2.2 Experimental Section.....	38
2.3 Results and Discussion.....	40
2.3.1 Change in Aggregate Size and Shape.....	40
2.3.2 Mechanisms.....	43
2.3.3 Transition Kinetics.....	45
2.3.4 Factors Influencing the Kinetics.....	47
2.3.4.1 Effect of Initial Solvent Composition.....	47
2.3.4.2 Effect of the Solvent Jump Magnitude.....	53
2.3.4.3 Effect of the Initial Polymer Concentration.....	54
2.4 Conclusions.....	56
2.5 References.....	57
Chapter 3. Kinetic and Mechanistic Details of the Vesicle to Rod Transition in Aggregates of PS₃₁₀-b-PAA₅₂ in Dioxane-Water Mixtures.....	61
3.1 Introduction.....	62
3.2 Experimental.....	66
3.3 Results and Discussion.....	67
3.3.1 Transition Region and Aggregate Dimensions.....	67
3.3.2 Interpretation of Dimensional and Structural Changes.....	69
3.3.3 Mechanism of Morphological Change.....	70
3.3.4 Transition Kinetics.....	71
3.3.5 Factors Effecting the Transition Kinetics.....	72
3.3.5.1 The Initial Solvent Composition.....	72
3.3.5.2 The Size of the Dioxane Content Jump.....	74
3.3.5.3 The Initial Polymer Concentration.....	75
3.4 Comparison of the Results with Those of Other PS-b-PAA Aggregate	

Transitions.....	76
3.5 Conclusions.....	79
3.6 References.....	80
Chapter 4. Effect of Sodium Dodecyl Sulfate on the Morphology of Polystyrene-b-Poly(Acrylic Acid) Aggregates in Dioxane-Water Mixtures.....	84
4.1 Introduction.....	85
4.2 Experimental.....	87
4.3 Results and Discussion.....	88
4.3.1 General Description of the Effect of SDS.....	88
4.3.2 Effect of SDS at Different Solvent Compositions and Polymer Concentrations.....	92
4.3.3 Effect of the Solution Preparation Method.....	95
4.4 Conclusions.....	98
4.5 References.....	99
Chapter 5. Conclusions, Contributions to Original Knowledge, and Suggestions for Future Work.....	103
5.1 Conclusions and Contributions to Original Knowledge.....	103
5.1.1 Kinetics and Mechanisms of Morphological Transitions.....	103
5.1.2 Effect of Sodium Dodecyl Sulfate on Block Copolymer Aggregates.....	105
5.2 Suggestions for Future Work.....	106
5.2.1 Suggestions for Research on Kinetics and Mechanisms of Morphological Change.....	106
5.2.2 Suggestions for Future Work on the Effect of Surfactants on PS-b-PAA Aggregates.....	108
5.3 References.....	108

List of Tables

Table 1.1 Examples of surfactant names and structural formula	8
Table 1.2 Critical packing parameters for surfactants and the structures they form	14
Table 2.1 Kinetic parameters for the sphere-to-rod transition in PS ₃₁₀ -b-PAA ₅₂ aggregates in dioxane-water mixtures	48
Table 2.2 Kinetic parameters for the rod-to-sphere transition in PS ₃₁₀ -b-PAA ₅₂ aggregates in dioxane-water mixtures	49
Table 3.1 Kinetic results for the vesicle-to-rod transition of PS ₃₁₀ -b-PAA ₅₂ aggregates in dioxane-water mixtures	74
Table 3.2 General trends in the relaxation times	78
Table 4.1 Comparison of the morphological boundaries between regions of spheres (S), spheres+rods (S+R), rods (R), rods+vesicles (R+V), and vesicles (V) for aggregates prepared from 1.0 wt % PS ₃₁₀ -b-PAA ₅₂ in the presence of various additives in dioxane-water mixtures	90
Table 4.2 Effect of polymer concentration on the morphological boundaries between the regions of spheres (S), spheres+rods (S+R), rods (R), rods+vesicles (R+V), and vesicles (V) for PS ₃₁₀ -b-PAA ₅₂ aggregates in the presence of SDS	95

List of Figures

Figure 1.1 Copolymer architectures	3
Figure 1.2 A schematic of the polymerization of PS- <i>b</i> -PtBuA.	5
Figure 1.3 Various morphologies formed from asymmetric, amphiphilic block copolymers in solution	20
Figure 2.1 A partial morphological phase diagram for PS ₃₁₀ - <i>b</i> -PAA ₅₂ in dioxane-water mixtures. S: spheres, S + R: spheres and rods, R: rods, R + V: rods and vesicles. The solid line scale shows the water content range covered at a given polymer concentration. The dashed lines with arrows indicate the forward and reverse solvent jumps at 1.0 wt % polymer.	42
Figure 2.2 Dependence of the solution turbidity on the polymer concentration for spheres and rods in water. (Error in turbidity of ± 0.01 units)	43
Figure 2.3 Micrographs of the aggregates at different time points during the sphere-to-rod transition occurring in solutions of 1.0 wt % PS ₃₁₀ - <i>b</i> -PAA ₅₂ in dioxane-water mixtures.	44
Figure 2.4 Micrographs of the aggregates at different time points during the rod-to-sphere transition occurring in solutions of 1.0 wt % PS ₃₁₀ - <i>b</i> -PAA ₅₂ in dioxane-water mixtures.	45
Figure 2.5 (A) Effect of the initial solvent composition on the kinetics of the sphere-to-rod transition in PS ₃₁₀ - <i>b</i> -PAA ₅₂ aggregates in dioxane-water mixtures. The initial polymer concentration is 1.0 wt %. (B) Effect of the magnitude of the dioxane jump on the kinetics of the sphere-to-rod transition in PS ₃₁₀ - <i>b</i> -PAA ₅₂ aggregates in dioxane-water mixtures. The initial polymer concentration is 1.0 wt %. (C) Effect of the initial polymer concentration on the kinetics of the sphere-to-rod transition from 11.5 to 12.0 wt % H ₂ O in PS ₃₁₀ - <i>b</i> -PAA ₅₂ aggregates.	48
Figure 2.6 (A) Effect of the initial solvent composition on the kinetics of the rod-to-sphere transition in PS ₃₁₀ - <i>b</i> -PAA ₅₂ aggregates in dioxane-water mixtures. The initial polymer concentration is 1.0 wt %. (B) Effect of the magnitude of the dioxane jump on the kinetics of the rod-to-sphere transition in PS ₃₁₀ - <i>b</i> -PAA ₅₂ aggregates in dioxane-water mixtures. The initial polymer concentration is 1.0 wt	

%. (C) Effect of the initial polymer concentration on the kinetics of the rod-to-sphere transition from 12.0 to 11.5 wt % H₂O in PS₃₁₀-b-PAA₅₂ aggregates. 49

Figure 3.1 Dependence of the solution turbidity on the polymer concentration for vesicular aggregates in water. The line illustrates the linear fit at lower concentrations. (error in turbidity of ± 0.01 units) 69

Figure 3.2 Micrographs of the aggregate morphologies at various time points during the transition from 29.0 to 26.4 wt % H₂O in a 1.0 wt % PS₃₁₀-b-PAA₅₂ solution. (A: 0s, B: 5s, C: 11s, D: 17s, E: 25s). 71

Figure 3.3 (A) Effect of the initial solvent composition on the kinetics of the vesicle-to-rod transition in PS₃₁₀-b-PAA₅₂ aggregates in dioxane-water mixtures. The initial polymer concentration is 1.0 wt %. (B) Effect of the magnitude of the dioxane jump on the kinetics of the vesicle-to-rod transition in PS₃₁₀-b-PAA₅₂ aggregates in dioxane-water mixtures. The initial polymer concentration is 1.0 wt %. (C) Effect of the initial polymer concentration on the kinetics of the vesicle-to-rod transition from 28.0 to 27.0 wt % H₂O in PS₃₁₀-b-PAA₅₂ aggregates. 73

Figure 4.1 Micrographs of the morphologies observed for aggregates prepared from 1.0 wt % PS₃₁₀-b-PAA₅₂ aggregates in solutions of 11.5 wt % H₂O and increasing concentrations of SDS. (A: 2.0 mM, B: 5.1 mM, C: 9.2 mM, D: 11.0 mM, E: 17.1 mM) 89

Figure 4.2 Morphological phase diagram for aggregates prepared from PS₃₁₀-b-PAA₅₂ in dioxane-water mixtures in the presence of SDS. The small symbols represent points obtained from turbidity studies (● spheres, ● spheres and rods, ◆ rods, ⊙ rods and vesicles, ○ vesicles). The ▲ symbol represents the position of phase boundaries determined from increasing water content. The solid lines represent the phase boundaries determined from turbidity and TEM studies. The dashed lines are visual guides. 93

Figure 4.3 Morphological transitions examined by turbidity measurements for 1.0 wt % PS₃₁₀-b-PAA₅₂ in dioxane-water mixtures with a fixed SDS concentration of 11.7 mM. The arrows indicate the transition boundaries determined from experiments in which the solvent composition was held constant while the SDS concentration was increased. 96

List of Symbols

PS-b-PAA	polystyrene-b-poly(acrylic acid)
S	surfactant molecule or spherical aggregates
N	aggregation number
CMC	critical micelle concentration
τ	relaxation time
PS-b-PMMA	polystyrene-b-poly(methyl methacrylate)
LCVs	large compound vesicles
TEM	transmission electron microscopy
χ	Flory interaction parameter
Y	turbidity
SDS	sodium dodecyl sulfate
TDA	tridecanoic acid
CWC	critical water content
C	turbidity at infinite time
R	rods
R+V	rods and vesicles
S+R	spheres and rods

***Dedicated
in
loving memory
to***

Thomas and Agnes Burke

**Yea, though I walk through the valley of the shadow
of death, I will fear no evil, for thou art with me,
thy rod and thy staff they comfort me.**

- Psalm 23: 4

Chapter 1

General Introduction

1.1 Introduction

One of the most intriguing solution properties of block copolymers is their ability to form micelles in a solvent that is selective for one of the blocks. Over the past few decades, extensive investigations of this phenomenon over the past few decades, have led to the publication of several book chapters and review articles devoted to this topic, which are in addition to an extensive collection of original literature.¹⁻¹⁰

Until recently, small molecule surfactants were the only species known to form, systematically, self-assembled aggregates of multiple morphologies in solution.¹¹⁻¹⁶ However, in 1995 Zhang and Eisenberg showed that a number of morphologies, such as spheres, rods, vesicles, and reverse micelles, are obtained in solution from an asymmetric, amphiphilic diblock copolymer.¹⁷ Within the past few years, many studies have been devoted to the investigation of block copolymer systems that form multiple morphologies in solution; many other studies will be discussed throughout the remainder of this chapter.¹⁸⁻²⁸ These studies have revealed important information about such things as the factors that influence aggregate architecture, alternative means of preparing multiple block copolymer morphologies, as well as some of the thermodynamic and kinetic aspects of morphological transitions. This thesis focuses on the kinetics and mechanisms of three morphological transformations, which have been explored with the aid of turbidity measurements and transmission electron microscopy. These techniques were also employed in order to investigate the influence of a small molecule surfactant on the architecture of diblock copolymer aggregates in solution.

This chapter is meant to provide some introductory information as the basis for the chapters that follow. It is divided into seven sections, beginning with an introduction to polymers, as well as the methods used in the synthesis and characterization of macromolecules. This is followed by a fundamental definition of small molecule surfactants. The next two sections draw comparisons between the micellization and phase behavior of surfactant and block copolymer aggregates. The characterization techniques

used to carry out the experimental work for this thesis are reviewed in section six. The chapter is concluded with a description of the main objectives of this thesis.

1.2 Introduction to Polymers

1.2.1 Basic Definitions

The word polymer is derived from the Greek words “poly”, which means many and “mer”, which is equivalent to the English definition of the word part. Polymers are macromolecules that are prepared from a large number of monomers, which are referred to as repeat units when they are covalently bonded together to form a macromolecule.²⁹ A monomer is defined as any small molecule containing two or more bonding sites; this quality makes them capable of linking to other monomer units in a chain. Polymers characteristically have at least one dimension with a length in the nanometer to micrometer range.³⁰

Polymers are broadly defined as being either naturally occurring or synthetically prepared. Natural polymers include such things as proteins, polysaccharides, and polynucleotides etc. Polyamides, polyesters, polycarbonates, and polyalkylenes are some examples of synthetic polymers. There are several other means that are commonly used to classify polymers including those based upon the kinetics of polymerization, the synthesis mechanism, processing characteristics (i.e. thermoplastics, thermosets), electrical charge, as well as the number of different monomer species incorporated into the polymer. There are three general categories of polymers as defined by the number of different monomer species they contain: homopolymers, copolymers, and terpolymers. Those polymers prepared from one monomer species are referred to as homopolymers. Polymers composed of two or three different types of monomers are referred to as copolymers and terpolymers respectively.²⁹

A substantial amount of control can be exercised over the procedures used to synthesize copolymers; this results in the ability to prepare a host of copolymer architectures. There are four main categories of architectures: statistical, alternating, graft, and block copolymers (Figure 1). Statistical copolymers have a sequence distribution of the two types of monomers that is dictated by their reactivity ratios. Alternating copolymers consist of equimolar quantities of the two monomers. The characteristic feature of these copolymers is the regular alternating sequence of each

monomer type. In the case of graft copolymers, blocks composed of one monomer are attached as branches to a polymer backbone, which is prepared solely from units of the other monomer. Block copolymers are defined by the alternating series of blocks that are constructed from a sequential number of units of a given monomer. The most common types of block copolymers are diblocks, copolymers with one block of each monomer, and triblock copolymers, which have one block of a given monomer attached to both ends of a block of a second monomer.^{29,30} It is noteworthy that it is possible to synthesize many other types of block copolymers including, four arm starblocks, random multiblocks, as well as some more complicated architectures studied by Hadjichristidis et al. such as 3-miktoarm starblock copolymers, and super H-shaped block copolymers.³¹ The physico-chemical character of any of these block copolymers greatly depends upon the composition of each block. For example, it is quite common for block copolymers to be composed of both hydrophobic and hydrophilic blocks, which gives them amphiphilic character. This thesis deals with one such diblock copolymer, polystyrene₃₁₀-b-poly(acrylic acid)₅₂.

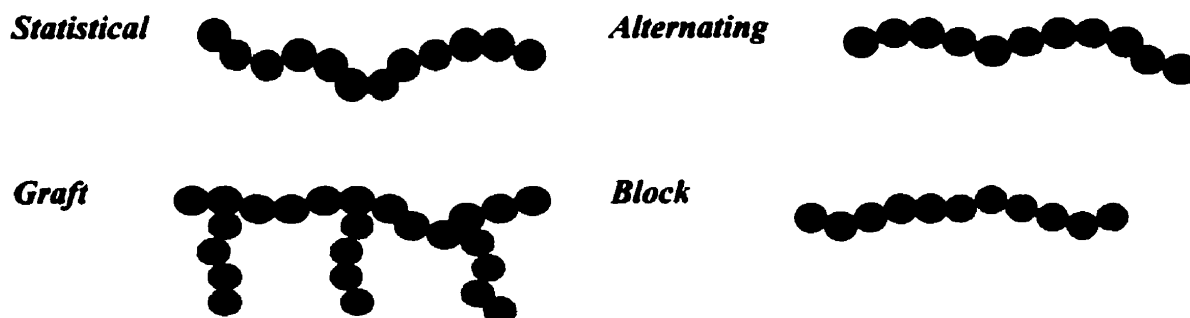


Figure 1: Copolymer architectures

1.2.2 Polymerization

As mentioned in the previous section, it is possible to classify polymers based upon the kinetics of polymerization. Under this classification scheme, step-growth polymerization is defined as a process involving the random reaction of two species that can be a combination of a monomer, an oligomer, or a long-chain molecule. Polymers of high molar mass are formed only near the end of the reaction when most of the monomer supply has been consumed. In contrast, chain-growth (addition) polymerization involves

an initiation step, which produces an active center. This is followed by a series of chain extension reactions during which individual monomers attach to the active end of the chain. This active species may be either a free radical or an ionic site. High molar mass polymer chains are characteristically formed in the early stages of a chain-growth polymerization.²⁹

Chain-growth polymerization processes have not only been employed in the preparation of homopolymers, but have also been extensively used to form copolymers of various architectures.²⁹ The polystyrene-*b*-poly(acrylic acid) copolymer is most frequently prepared by sequential anionic copolymerization.^{32,33} The details of this procedure are provided in the following section.

1.2.3 Anionic Polymerization

The preparation of polystyrene-*b*-poly(acrylic acid) (PS-*b*-PAA) begins with the sequential anionic polymerization of styrene and tert-butyl acrylate to form polystyrene-*b*-poly(tert-butyl acrylate). This type of copolymerization process involves the initiation of one of the monomers, in this case styrene, by an electropositive initiator to form a “living” carbanion. The living nature of the reaction arises from the fact that there is no formal termination step. In general, anionic initiation requires the monomer to possess electron withdrawing substituents in order to promote the formation of a stable carbanion. However, the carbanion is highly sensitive to trace amounts of certain impurities such as water, oxygen, alcohols, and carbon dioxide. As long as the reaction is carried out in an inert environment, the propagation of the chain will continue until all of the monomer is consumed. At this point, the second monomer is added to the reaction flask. The living end of the first block initiates the formation of the second.³²

The first successful attempt at the preparation of PS-*b*-PtBuA was made by Hautekeer et al. (Figure 2).³³ This method was used by Shen et al. to prepare the PS₃₁₀-*b*-PAA₅₂ block copolymer used for the studies discussed in this thesis.³⁴ The synthesis was carried out in ultra dry glassware in the presence of nitrogen gas or vacuum to prevent premature termination of the polymer chains. The initiator, (α -methylstyryl)-lithium, is prepared in the reaction flask, containing lithium chloride, by reacting sec-butyllithium with a slight excess of α -methylstyrene at room temperature in dry tetrahydrofuran

(THF). The *sec*-butyllithium serves to eliminate any impurities in the system and then to activate the α -methylstyrene. The success of the initiation, which is carried out at $-20\text{ }^{\circ}\text{C}$ to prevent the polymerization of α -methylstyrene, is indicated by a deep red color characteristic of the α -methylstyryl ion. The solution temperature is lowered to $-78\text{ }^{\circ}\text{C}$, after which the styrene monomer is added dropwise with constant stirring. The formation of the styrene carbanion causes a change in the solution colour from red to pale orange. However, when the concentration of free styrene is completely depleted, the solution reverts back to a red colour due to the reaction of the remaining α -methylstyrene with the living chains. It must be noted that it is common for a few of the α -methylstyrene molecules to polymerize before the styrene is added; therefore, the polymer chains usually have more than one repeat unit of α -methylstyrene at the beginning and the end of the styrene block.³²

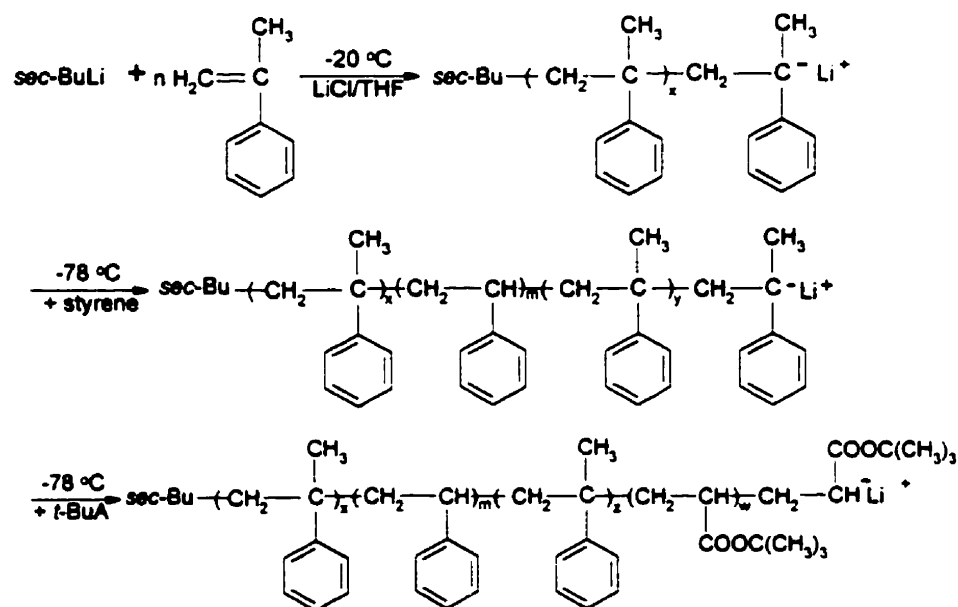


Figure 2: A schematic of the polymerization of PS-*b*-PtBuA.

Following the preparation of the polystyrene block, the *tert*-butyl acrylate is added. The polymerization of this monomer is initiated by the living end of the first block. Because of the possibility of an attack on the carbonyl group of the tertiary hydrogen atom of *tert*-butyl acrylate, either by the polystyryllithium or the polyacrylate type ion pairs, LiCl is present in the system to coordinate with the anions preventing any

side reactions. Once all of the tert-butyl acrylate has been polymerized, a small amount of methanol is added to the system to terminate the reaction. The polymer is recovered by precipitating it into a methanol-water mixture.³²

The block copolymer is converted to polystyrene-*b*-poly(acrylic acid) through hydrolysis. The PS-*b*-PtBuA is dissolved in toluene along with *p*-toluenesulfonic acid. The solution is refluxed for twenty-four hours, and the polymer is then recovered by precipitation into methanol.³²

The number of repeat units incorporated into each of the copolymer blocks is determined from the post-polymerization analysis carried out using two samples, one withdrawn from the reaction flask soon after the polymerization of the first block, and one taken after the termination of the second copolymer block.

1.2.4 Post-Polymerization Characterization

A typical synthetic polymer sample contains chains with a wide distribution of chain lengths, hence an exact molar mass cannot be assigned to the polymer. This occurs because the polymerization process is essentially a series of random events, and as mentioned earlier, there are a number of side reactions and premature termination processes that can occur throughout the polymerization. In order to deal with this distribution of chain lengths, it is most common to define an average molar mass. There are three conventional means of defining an average molar mass, which include the number average, the weight average, and the *z*-average molar masses.

The number average molar mass $\langle M \rangle_n$ is a measure of the number of molecules present in the sample.²⁹

$$\langle M \rangle_n = \frac{\sum N_i M_i}{\sum N_i} = \frac{\sum w_i}{\sum (w_i / M_i)} \quad (1)$$

Here, N_i is the number of polymer molecules of species *i* of molar mass m_i . This quantity can be obtained by using colligative methods of analysis (i.e. osmometry, cryoscopy, ebulliometry). The weight w_i of all polymer molecules with a molar mass of M_i can be measured using light scattering techniques and this value is needed to calculate the weight average molar mass.

$$\langle M \rangle_w = \frac{\sum N_i M_i^2}{\sum N_i M_i} = \frac{\sum w_i M_i}{\sum w_i} \quad (2)$$

The z average molar mass is most frequently determined from gel permeation chromatography measurements, but in the past ultra centrifugation was also employed. This value is useful for discussing the mechanical properties of polymers.

$$\langle M \rangle_z = \frac{\sum N_i M_i^3}{\sum N_i M_i^2} = \frac{\sum w_i M_i^2}{\sum w_i M_i} \quad (3)$$

The extent of the distribution of chain lengths in a given polymer sample is often described by the heterogeneity index, which is actually a ratio of the weight average molar mass to the number average molar mass. The number of monomer units in any given chain is expressed by the average degree of polymerization, the ratio of the molar mass of the monomer to the average molar mass.²⁹

As mentioned in the description of block copolymers, these macromolecules can be amphiphilic if one of the blocks is made from hydrophilic repeat units and the other block from hydrophobic components. These types of copolymers often display similar characteristics to a class of small molecule species known as surfactants.

1.3 Introduction to Surfactants

SURFace ACTive AgeNTS (surfactants) are a special class of chemical species that have the ability to adsorb onto a surface or an interface and also to self-assemble into colloidal aggregates in solution at relatively low concentrations.³⁵ Surfactants have a characteristic structure composed of a lypophilic “tail” component and a lypophobic portion know as a “headgroup”. Hence, these molecules have a dual affinity for both polar and nonpolar solvents, and are thus referred to as amphiphiles. The surfactant tail can be prepared from a number of different materials such as a linear alkyl chain (eight to eighteen carbon atoms), a branched alkyl chain, an alkybenzene chain, or a fluoroalkyl group etc. The headgroup can be cationic, anionic, nonionic, or zwitterionic in nature.^{35,36} Some example of surfactant structures are shown in Table 1.³⁶

Table 1: *Examples of surfactant names and structural formula*

Name	Formula	Charge
Sodium Dodecyl Sulfate	$C_{12}H_{25}OSO_3Na$	Anionic
Hexadecyltrimethylammonium Bromide	$C_{16}H_{32}N(CH_3)_3Br$	Cationic
Dodecyldimethylpropane sultaine	$C_{12}H_{25}N(CH_3)_2(CH_2)_3SO_3$	Zwitterionic
Decylglucoside	$C_{10}H_{21}C_6O_6H_{11}$	Neutral

When surfactant molecules are dissolved in a polar solvent, the lypophilic groups cause an unfavorable distortion of the liquid structure. In the case of an aqueous environment, the presence of the surfactant leads to an ordering of the water molecules, producing a decease in the entropy and hence an increase in the free energy of the system. Thus, due to the amphiphilic nature of surfactant molecules, they must find a means of reducing the energy of the system when they are in solution. The most cost effective way of accomplishing this, at low surfactant concentrations, is to absorb onto a surface or an interface. Because of the fact that less work required to bring surfactant molecules to the interface, as opposed to water molecules, the presence of the surfactant reduces the amount of work needed to increase the interfacial area, which leads to a decrease in the interfacial tension.³⁷ However, when all the available sites at the interface are saturated, the overall reduction in the energy of the system continues via other mechanisms such as crystallization, liquid crystal formation, bilayer and vesicle formation, and micellization.³⁴

1.4 Surfactant Aggregates in Solution

1.4.1 Micellization

Micellization can result at higher concentrations of the surfactant, after the saturation of the interface, because the intra-molecular surfactant interactions begin to have an influence on the solution behavior of these molecules. As the concentration of the surfactant added to the solution is increased, there comes a point, known as the critical micelle concentration, where the self-interactions of both the surfactant and solvent molecules dominate over the surfactant-solvent interactions. Too much crowding at the interface leads to the formation of surfactant aggregates known as micelles, which may contain as many as 200 molecules. The micellization phenomenon in highly polar media, such as water, is a result of the hydrophobic effect. This effect is based upon the

behavior of hydrocarbons in water. The presence of a hydrocarbon molecule in water, at room temperature, causes an unfavorable change in the entropy of the system because it induces an increase in the degree of structuring of the water molecules. An isolated hydrocarbon molecule forms a cavity in the water structure. The cavity walls are lined with water molecules that have a more ordered bonding pattern than those in the bulk solution. Thus, the main feature of the hydrophobic effect is the influence the hydrocarbon molecule has on the degree of ordering of the water molecules in their immediate surroundings. Another aspect of this effect is the extent to which the hydrocarbon molecule disrupts the extensive hydrogen-bonding pattern of water. The large negative entropy of the highly ordered water structure surrounding the hydrocarbon molecules outweighs the slightly favorable energy change associated with this process. In the case of pure hydrocarbons, the unfavorable free energy change would lead to phase separation. However, the amphiphilic nature of surfactants prevents phase separation, and instead promotes micellization. The removal of the hydrocarbon tail from the water environment breaks up the ordered water structure in the cavity, which causes an increase in the entropy. The reorganization of these water molecules slightly counteracts this favorable entropy change. Micellization is also associated with a decrease in the enthalpy because of the creation of the hydrophobic environment (i.e. the core) where the surfactant tails prefer to reside. Overall, the micellization process is associated with a favorable change in the Gibbs free energy of the system. It must be noted that the electrostatic repulsions between the head groups of the surfactant molecules within a micelle, along with the restriction of the core size as a result of the finite length of the hydrophobic chain prevent the aggregates from becoming infinitely large. However, the micelles are not static species; in fact, they are very dynamic and, as a result, there is a constant exchange of monomers between the aggregate and solution phase.³⁷

1.4.2 Mechanism and Thermodynamics of Micellization

The self-assembly of surfactant molecules to form micelles is a thoroughly characterized process. The aggregation is generally described as a step-wise association. However, since micelles have aggregation numbers on the order of 100 surfactant molecules, it is virtually impossible to define an equilibrium constant for each step.

Several models have been devised to approximately characterize the phenomenon of micellization; this includes the isodesmic, phase separation, and closed-association models. The most widely accepted model is that of closed-association. It relates the free energy of micellization to the critical micelle concentration and also incorporates the initial and final cooperative features associated with micelle formation.³⁹

Closed-association is described as a dynamic equilibrium between individual surfactant molecules S and micelles S_N of a given aggregation number N .



Hence, the equilibrium constant K_N as:

$$K_N = \frac{[S_N]}{[S]^N} \quad (5)$$

In this case, the total surfactant concentration $[S]_T$ is expressed in terms of the moles of monomer with the equation

$$[S]_T = N[S_N] + [S] = NK_N [S]^N + [S]. \quad (6)$$

The previous two expressions are used to obtain a solution for the derivative $\partial\{N[S_N]\}/\partial[S]_T$, which describes the fraction of added surfactant that is incorporated into a micelle. The point at which a monomer is just as likely to enter a micelle as to remain in solution is considered to be the critical micelle concentration.³⁹

$$\left. \frac{\partial\{N[S_N]\}}{\partial[S]_T} \right|_{CMC} = \left. \frac{\partial[S]}{\partial[S]_T} \right|_{CMC} = 0.5 \quad (7)$$

Solving for the inverse of this equation, $\partial[S]_T/\partial[S] = 2$ in equation (6), we

find $[S]_{CMC}^{N-1} = (N^2 K_N)^{-1}$, where $[S]_{CMC}$ is the monomer concentration at the CMC.

$$CMC = [S]_{CMC} (1 + N^{-1}) = (N^2 K_N)^{-1/(N-1)} (1 + N^{-1}) \quad (8)$$

Taking the logarithm of this equation and assuming that the aggregation number is greater than 1 leads to a relation that can be used to express the standard free energy of micellization.

$$\ln CMC \cong -\frac{1}{N} \ln K_N \quad (9)$$

$$RT \ln CMC \cong RT \ln [S]_{CMC} = \frac{-RT}{(N-1)} \ln \left(\frac{K_N}{N^2} \right) = \frac{1}{N-1} (N \Delta G_{mic}^o - 2R \ln N) \cong \Delta G_{mic}^o \quad (10)$$

The standard enthalpy of micellization is obtained by using the Gibbs-Helmholtz equation in combination with the above expression for the Gibbs free energy.

$$\Delta H_{mic}^{\circ} = -RT^2 \frac{\partial}{\partial T} \ln CMC \quad (11)$$

The standard entropy of micellization is expressed as follows:

$$\Delta S_{mic}^{\circ} = -RT \frac{\partial}{\partial T} \ln CMC - R \ln CMC \quad (12)$$

Hence, the temperature dependence of the critical micelle concentration is determined by the relative contributions of the enthalpy and entropy of micellization.³⁹

The above expressions are derived for nonionic surfactant species. When dealing with charged species, for example anionic surfactants, the equilibrium equation involves a relationship between the surfactant molecules S^- , counterions C^+ , and micelles S_N .



The standard Gibbs free energy for such systems is given as:

$$\Delta G_{mic}^{\circ} = -\frac{RT}{N} \ln[S_N^{-P}] + RT \ln[S^{-1}] + RT \left(1 - \frac{P}{N}\right) \ln[C^+]. \quad (14)$$

It is most commonly found that micelle formation is exothermic in nature and is favored by a decrease in temperature. However, the enthalpy of micellization be a positive value. In any event, micellization is accompanied by a rather large positive entropic contribution, which compensates for any positive enthalpy term; hence surfactant self-assembly is primarily driven by entropy.³⁹

1.4.3 Kinetics of Micelle Formation

The kinetics of micelle formation were first studied by Aniansson et al. based upon the step-wise association mechanism.⁴⁰ They established that this process consists of two relaxation phenomena. The fast process generally occurs over a microsecond range and involves the exchange of monomeric surfactants between the micelles and the bulk micellar solution.



In this case, S is a surfactant molecule and S_N and S_{N+1} are micelles of N and $N+1$ surfactant molecules respectively. The rate-limiting step is the formation-breakdown of the micelles. This entails a series of step-wise events, which involves one molecule at a time associating with or dissociating from an aggregate. The exchanges process takes millisecond s to complete.

An expression for the relaxation time for each step has been derived based upon a number of valid assumptions: the perturbation imposed on the system to study the kinetics is small, there is no exchange of monomers between micelles and oligomers, and the rate constants for k_N^+ and k_N^- are independent of N and hence can be expressed simply as k^+ and k^- respectively. The relaxation time for the exchange process is represented by the following equation.^{40,41}

$$\tau_1^{-1} = \frac{k^-}{\sigma^2} \left(1 + \frac{\sigma^2}{N} a \right) \quad (16)$$

Here, σ^2 is the variance in the micellar size distribution, N is the aggregation number, and a involves a relation between the total surfactant concentration S_{tot} and the equilibrium value of the free monomer concentration \bar{S} above the CMC.

$$a = \frac{S_{tot} - \bar{S}}{\bar{S}} \quad (17)$$

The relaxation time for micelle formation-breakdown is also dependent on the assumption that only a small perturbation is employed.

$$\tau_2^{-1} \cong N^2 \left(R S_N^- \right)^{-1} \left(1 + \frac{\sigma^2}{N} a \right)^{-1} \quad (18)$$

$$R = \sum_{N_1+1}^{N_2} \left(k_N^- \bar{S}_N^- \right)^{-1} \quad (19)$$

Here, \bar{S}_N^- is the equilibrium concentration of aggregates S_N . It must be noted that in the case of ionic surfactants, expressions for the degree of ionization of the micelles, and the activity coefficients of the total 1-1 electrolyte must be incorporated into the relaxation time equations.⁴¹

1.4.4 Polymorphism in Surfactant Aggregates

Ultimately, the major forces that control the self-assembly of amphiphiles are derived from the opposing forces that are most prevalent at the hydrocarbon-water interface, which include the hydrophobic interactions that induce micellization and the repulsion among the head groups.¹³ In order for surfactant aggregates to be thermodynamically stable in solution, the total interaction energy resulting from the two opposing interfacial interactions must be at a minimum, which leads to the concept of the optimal surface area per molecule at the interface (a_o). It is defined in terms of the total free energy per molecule within the aggregate

$$\mu^o = \gamma a + \frac{K}{a} \quad (20)$$

In this case, K is a constant, γ is the interfacial free energy per unit area, and “ a ” is the surface area occupied by the head group. In order for equilibrium conditions to be met, the interfacial free energy must be minimized; hence, the first derivative of the free energy with respect to the surface area of the head group must be zero, which leads to the following expression:





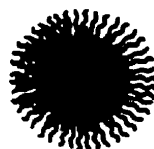
$$\mu^o = 2\gamma a_o \text{ and } a_o = \sqrt{\frac{K}{\gamma}} \quad (21)$$

The optimal surface area per molecule not only represents a balance between the interactions within the surfactant molecule, among individual monomers, and among the other species making up the system, but also contributes to the determination of the overall equilibrium morphology of the aggregates such as spheres, rods, vesicles, and bilayers. Israelachvili et al. developed a geometric treatment for surfactant aggregation to explain the concept of polymorphism in these systems.⁴² It relates the free energy of association to the optimal surface area per molecule (a_o), the volume of the hydrophobic tail (v), and the chain length of maximum extension of a tail within the core (l_c). Since these properties can be measured for a given system, the geometric treatment is used to predict the size and shape of aggregates that yield the minimum free energy. This property is defined in terms of a critical packing parameter P_c .

$$P_c = \frac{v}{a_o l_c} \quad (22)$$

In fact, it has been found that a given aggregate architecture has a characteristic value of P_c as indicated in Table 2.¹³ It is interesting to note that since μ_o is essentially the same for a number of different structures, the overall optimal geometry is determined by the entropy of the system, which favors the structure with the smallest aggregation number.¹³

Table 2: Critical packing parameters for surfactants and the structures they form

Type of Surfactant	Critical Packing Parameter	Morphological Classification	Structure
Single-Chained Surfactants with Large Head Group Area	$< 1/3$	Spherical Micelles	
Single-Chained Surfactants with Small Head Group Area	$1/3-1/2$	Cylindrical Micelles	
Double-Chained Surfactants with Large Head Group Area	$1/2-1$	Flexible Bilayers & Vesicles	
Double-Chained Surfactants with Small Head Group Area (anionic surfactants with high salt content, saturated frozen chains)	~ 1	Planar Bilayers	
Double-Chained Surfactants with Small Head Group Areas (nonionic surfactants, poly (cis) unsaturated chains, high temperature)	~ 1	Inverted Micelles	

The dynamic nature of the surfactant aggregates arise from the fact that the amphiphilic molecules are held together by fairly weak forces such as van der Waals, hydrogen bonding, hydrophobic, and electrostatic interactions. Any factor that can perturb these forces has the potential to change the size and shape of the surfactant aggregates. Hence, the three structural characteristics that determine the critical packing parameter are not only influenced by the nature of the surfactant molecules, but are also

affected, to a large extent, by the solution environment of the system. For example, simple, single tail surfactants with relatively large head groups generally form spherical micelles, but can be induced to form extended bilayers, large vesicles, or inverted micellar structures by altering the ionic strength of the head group region with a change in the solution pH, or the introduction of a high salt concentration. Increasing the temperature of a solution containing surfactant molecules with a chain length of greater than sixteen carbon atoms greatly effects the chain motion, which allows for trans-gauche isomerization, thus leading to a decrease in the value of l_c and ultimately producing a change in the structure of the aggregates. The minimum interfacial area occupied by the surfactant head group is also subject to modification by changing the nature of or solvation of the ions with the addition of complexing or cryptating species, which increase the value of a_0 , which results in an increase in the critical packing parameter, and therefore a change in the aggregate morphology.¹³

1.4.5 Morphological Transformation

There has been a steady increase in the in the amount of literature available about structural transitions in surfactant aggregate systems, involving such processes as the sphere-to-rod, sphere-to-vesicle, vesicle-to-sphere transitions, as well as the fusion of two smaller vesicles to produce one large vesicle etc.⁴³⁻⁴⁸ However, only a few investigations have been dedicated to studying the kinetics of these transitions.⁴⁹⁻⁵⁵ The initial study into the kinetics of the sphere to rod transition was carried out by Harada et al. using aqueous solutions of hexadecyl trimethyl ammonium bromide.⁵⁰ An increase in the surfactant concentration was employed to induce the transition near the sphere to rod boundary, and the structural changes were monitored using conductivity and ultrasonic velocity measurements. This process involves a two-step mechanism in which the fast step corresponds to the successive association of monomers to the spherical micelles in the time range of tens of milliseconds. The slower step takes place over hundreds of milliseconds and is due to the overall formation and dissociation of the rod-like micelles. Michels et al. recently employed temperature jump studies with light scattering detection to measure the relaxation times associated with the sphere to rod transition in aqueous sodium dodecyl sulfate solutions containing sodium chloride.⁵¹ Spherical SDS micelles

are known to grow into cylindrical aggregates when the ionic strength of the system is high. This process was found to occur via the same mechanism described by Harada et al.^{50,51}

The most widely studied morphological transition is the transformation of spherical micelles into vesicles and the reverse process.⁵²⁻⁵⁵ The mechanism most frequently encountered for the formation of vesicles from spheres consists of two steps. The first event in the transition is the fast growth of the micelles to form disk-like aggregates. These intermediate structures are unstable because they prefer to have a slight curvature as opposed to a planar structure, which leads to the disjoining of the disc bilayer film. The slow process involves the cooperative adsorption of free surfactant molecules to the inner hydrophobic surface to form a bilayer of the vesicle wall. Vesicle deformation has been shown to occur more quickly than the formation process. The breakdown of vesicles is believed to occur via a multi-step process involving the initial loss of surfactant molecules from the outside wall of the vesicle. This leads to the formation of an unstable bilayer structure that dissociates into smaller disc structures; the individual molecules in the discs eventually reorganize into micelles. It is interesting to note that Campbell et al. have studied the kinetics of the micelle to vesicle transition in a mixed system of sodium xylenesulfonate and poly(oxy ethylene (4)) lauryl ether, and have found that in this case, it occurs via a single relaxation process involving growth by monomeric association.⁵⁵

1.5 Block Copolymer Aggregates in Solution

1.5.1 Micellization of Block Copolymer Molecules

The amphiphilic nature exhibited by a wide variety of synthetic block copolymers has contributed to their surfactant-like behavior in solution.¹⁰ Hence, the vast history of surfactant science has paved the way to the understanding and the utilization of the colloidal properties observed in solutions containing amphiphilic block copolymers. One of the mostly widely studied of the phenomena that are associated with such systems is the self-assembly of these molecules to form micelles. As in the case of surfactants, in order for the micellization of block copolymer molecules to occur, two opposing forces must exist in the system. This involves an attractive force between the amphiphiles

leading to aggregation, and a repulsive force that prevents the micelles from growing infinitely. The attractive force is believed to stem from the hydrophobic effect, which originates from the behavior of the solvent molecules upon removal of the insoluble segments from the bulk solvent environment. In the case of ionic species, the repulsive forces tend to arise mainly from electrostatic interactions, while for neutral species, the preference for hydration as opposed to self-association contributes to the repulsion.¹⁰

It has been found that dissolving a block copolymer in a solvent favorable for only one of the blocks, results in the formation of micellar aggregates most frequently of spherical shape, which contain a swollen core composed of the insoluble blocks surrounded by a flexible shell of the soluble blocks.¹⁰ Depending on the relative lengths of each block, the micelles can be star-like or crew-cut. The main difference between the two types of micelles is that the size of the corona is larger than the core radius in star-like micelles, while the opposite is true for crew-cut micelles.⁵⁶ Detailed investigations into the physico-chemical nature of the micellization of amphiphilic block copolymers have recently appeared in the literature and will be discussed in the following sections.¹⁰

1.5.2 Thermodynamics and Kinetics of Block Copolymer Micellization

There are two possible association models, open and closed-association, that have been proposed as possible mechanisms for the micellization of block copolymer molecules into colloidal aggregates. Since block copolymer micelles have been found to have a distinctive critical micelle concentration (CMC), the closed-association model is most applicable, as in the case of surfactants, because open-association does not lead to a definite CMC.¹⁰ The details of the closed-association model are outlined in section 1.4.2 and are applied to block copolymer systems without modification.¹⁰ Therefore, in terms of the thermodynamics of micellization, the most important product of this model is the simplified equation relating the standard Gibbs free energy to the critical micelle concentration.

$$\Delta G_m^\circ = RT \ln CMC \quad (23)$$

Although the thermodynamics of the closed-association process, which governs micelle formation in block copolymer systems, has been well studied, it has only been within the past few years that the kinetics of block copolymer micellization have been

investigated.⁵⁷⁻⁶³ This process is described as being very similar to the micellization of surfactant molecules in the sense that it is widely believed to be a two-step process with common mechanistic details. The first step involves the quick association of block copolymer molecules to form pseudo-equilibrium structures. During this step, the population of the aggregates tends to increase at the expense of an increase in their size. The second step is much slower than the first. At this stage the micelles tend to grow in size, with the loss of some of the pseudo-equilibrium aggregates, and the core blocks adjust to their equilibrium conformation. One of the advantages of micellization in macromolecular systems is that the process tends to be significantly slower than that of surfactant molecules; hence, it is easily followed by standard analytical techniques. The slow nature of this process is often attributed to the chain dynamics of the macromolecule chains.

As pointed out above, the kinetics of micellization in block copolymer systems is greatly influenced by the chain mobility. Thus, knowledge of the chain dynamics in a copolymer system is important if one is to fully understand the details of micelle formation. The exchange of molecules between the solvent and the micelles has been investigated by a number of groups.⁶⁴⁻⁶⁸ The most frequently encountered conclusion is that the chain dynamics are greatly influenced by the nature of the solvent and the interaction of these molecules with the copolymer. Kent et al. have determined that intramolecular interactions between unlike monomers in the chain can lead to premature weakly ordered micellar phases.⁶⁴ Tsunashima et al. found that chain diffusion is impeded due to strong interchain hydrophobic interactions for the copolymer PS-*b*-PMAA in benzene, which is a good solvent for both blocks. The diffusive motion in conjunction with the internal chain motion is said to lead to deformation of the block copolymer chains during diffusion.⁶⁵ It was also found by Tian et al. that in the case of polystyrene based copolymers in various solvent mixtures, the higher the ratio of the solvent suitable for the PS chains, the more mobile the micellar core becomes. However, at high contents of the nonsolvent, the core tends to be more glassy, and the chain exchange becomes slower.⁶⁶ This complex interaction between the copolymer and the solvent greatly influences the size and shape of the block copolymer aggregates.

1.5.3 Multiple Morphologies from Block Copolymers in Solution

Since the first report¹⁷ in 1995 of the ability to obtain a variety of different architectures from polystyrene-*b*-poly(acrylic acid) in a solvent mixture, there has been a growing interest, world wide, in this phenomenon.¹⁸⁻²⁸ Fundamental knowledge of the physico-chemical properties of the various block copolymer morphologies and the transition between these aggregates is of prime importance for the use of these materials in a wide diversity of applications. Block copolymer aggregates are of particular interest in the pharmaceutical and personal care industry for the delivery a variety of agents including drugs, and dyes.⁶⁹ It is also interesting to note that many of the block copolymer aggregates have architectures that resemble more complicated biological and cellular structures. This inspires the potential use of block copolymer aggregates as model systems for obtaining crucial information about the details involved in a number of biological processes.⁷⁰

The most extensive investigations of block copolymer systems, that form multiple morphologies in solution, have been carried out by Eisenberg et al.⁷¹⁻⁹¹ For the majority of these studies, the asymmetric, amphiphilic diblock copolymers polystyrene-*b*-poly(acrylic acid) and polystyrene-*b*-poly(ethylene oxide) in various mixed solvents were employed.⁷¹⁻⁷⁸ A number of other copolymers, such as polybutadiene-*b*-poly(acrylic acid)⁷⁹, polystyrene-*b*-poly(4-vinylpyridine)⁸⁰, and polystyrene-*b*-poly(methyl methacrylate)-*b*-poly(acrylic acid)⁸¹, have also be found by this group to form aggregates of various structures in solution. Micelle formation is induced in these systems by the slow addition of a solvent selective to the hydrophilic block (i.e. water) to a solution of the copolymer dissolved in a solvent that is favorable for both blocks. To date, more than thirty different morphologies have been identified in these systems including such things as spheres, rods, vesicles, compound micelles, tubules, needles, onions, entrapped vesicles, bilayer structures, etc (Figure 3).²³ A number of these morphologies are under thermodynamic control, but many of them are kinetically controlled.^{82,83}

Several studies have been devoted to examining the physico-chemical properties of these aggregate structures in order to obtain an understanding of the thermodynamic vs. kinetic control of block copolymer morphologies. For example, Zhang et al. have inquired whether certain PS-*b*-PAA aggregate morphologies are formed under

equilibrium or non-equilibrium conditions.⁸² It was found that at a high concentration of the solvent that is suitable for both blocks, in other words, when the aggregates are dynamic enough that chain exchange occurs at a reasonable rate, the morphologies are under thermodynamic control. However, when the polystyrene core becomes increasingly viscous at higher water contents, chain mobility is limited and the structure of the aggregate is influenced more by the kinetics of the system. For those structures that are under equilibrium control, it has been determined that the thermodynamics are governed by the interplay of three components of the free energy of aggregation, which include stretching of the core-forming blocks, interfacial energy between the micellar core and the solvent, and intercorona interactions.⁸²⁻⁸⁴ The balance between these three forces is sensitive to many factors, such as the relative block lengths⁸⁵, the solvent composition⁸⁶, and the presence of additives⁸⁷⁻⁹⁰.

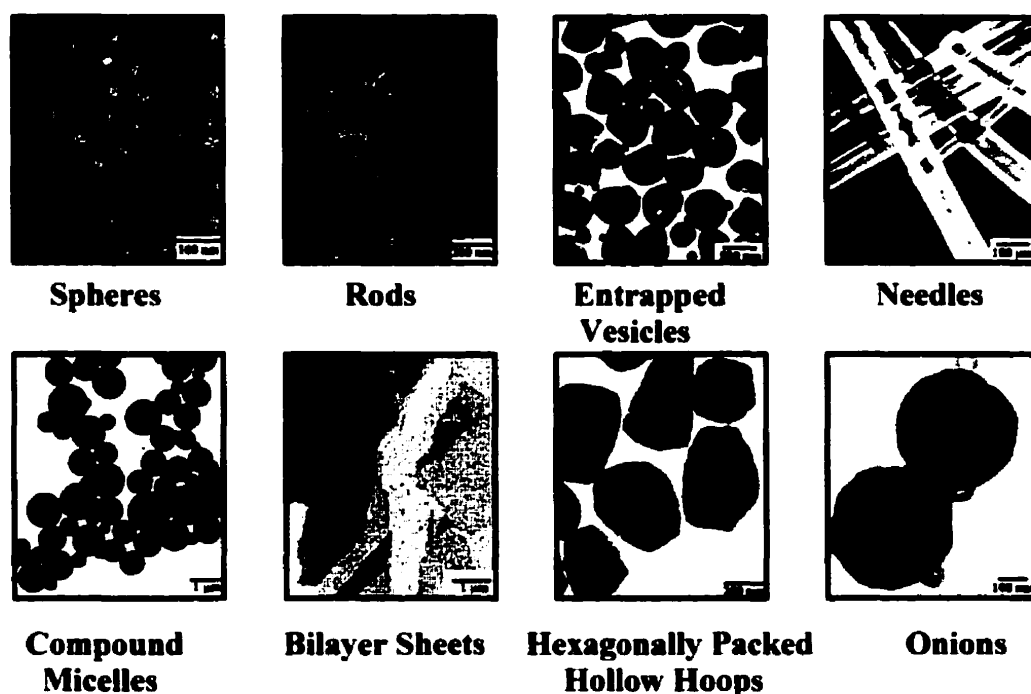


Figure 3: Various morphologies formed from asymmetric, amphiphilic block copolymers in solution.

The kinetics and mechanisms associated with each morphological transition are also of fundamental importance to the complete characterization of self-associating block

copolymer aggregate systems in solution. Chen et al. completed an investigation of the transformation of rods into vesicles that occurs in the aggregates formed in the ternary system PS₃₁₀-b-PAA₅₂ / dioxane / water.⁹¹ A jump in the water content of the system was used to induce the transitions, and the intermediate morphologies were monitored by transmission electron microscopy (TEM). The data obtained for the rod-to-vesicle transition indicates that near the phase boundary the rods tend to become shorter and more plump, with the appearance of some vesicles. As the water content is increased in this region, the vesicle population increases at the expense of the rod population. The results of the TEM studies suggest that the transition mechanism has two steps. The first step involves the flattening of the short rods to form circular or irregular-shaped lamellae. The final step is the closing of the bowl-shaped lamellae to produce vesicles. The first step is found to be the faster of the two. The two relaxation times depend on both the initial water content and the polymer concentration. The relaxation times became longer with an increase in either parameter. However, the size of the water jump was found to have little influence on the transition kinetics.⁹¹

A number of research groups have observed polymorphism in aggregates prepared from several other amphiphilic block copolymers. Their studies have expanded our knowledge of the number of systems that exhibit such behavior and have also contributed to the fundamental understanding of the solution properties of block copolymer aggregates. Liu et al. have obtained multiple morphologies from polystyrene-b-poly(2-cinnamoyl ethyl methacrylate) and polyisoprene-b-poly(2-cinnamoyl ethyl methacrylate) in various organic solvents and solvent blends.⁹²⁻⁹³ This group has also produced hollow aggregates by chemically modifying the self-assembled structures with photo cross-linking followed by treatment with ozone.⁹⁴ The research team led by Maskos have also employed the concept of cross-linking the chains in the micellar core in order to yield a variety of different aggregate structures, such as cylinders, double-shell vesicles and string of vesicles, from the copolymers poly(dimethylsiloxane)-b-poly(ethylene oxide) and poly(1,2-butadiene)-b-poly(ethylene oxide).^{95,96} Several other morphological studies have been carried out with neutral block copolymers. For example, research teams led by Discher, Bates, and Hammer have explored the self-assembly of poly(ethylene oxide)-b-polyethylethylene in water.⁹⁷⁻⁹⁹ Spherical, worm-like, and giant

vesicular structures have been identified in this system. In addition, a great deal of work has been completed on Pluronic copolymers that self-assemble into aggregates of various shapes such as spheres, rods, vesicles, and multilayered vesicles (onions).¹⁰⁰⁻¹⁰³ Several groups have also examined aggregate architectures of block copolymer containing charged species. Webber and coworkers have found that in 2-vinylpyridine based copolymer systems onion-type vesicles can be obtained from spherical aggregates.^{104,105} Förster et al. have shown that micelles of poly(ethylethylene-*b*-styrenesulfonic acid) can be made to fuse to form toroid networks.¹⁰⁶ Li et al. have also worked extensively with polystyrene-*b*-poly(2- β -D-glucopyranosyloxy)ethyl acrylate, which forms an array of aggregate morphologies in solvent mixtures.^{107,108} A number of other groups have focused their attention on block copolymers containing inorganic segments. Various architectures of organometallic nanoaggregates from inorganic block copolymers or hybrid organic-inorganic block copolymers have been observed by the groups of Winnik and Manners.¹⁰⁹⁻¹¹⁰ Möller and coworkers have also studied metal containing nanoaggregates of various shapes, prepared from block copolymers.¹¹¹⁻¹¹² Over the past few years, Antonietti et al. have investigated the morphogenic properties of a variety of different block copolymers including a novel type of chelating species, polystyrene-*b*-poly-*m*-vinylphenylphosphinates.¹¹³⁻¹¹⁴ Some of the aggregates that they observed include disk-like and multilamellar vesicles.

The above discussion clearly indicates that the monomeric composition of block copolymers influences the morphology of the aggregates formed from these molecules in solution. However, the interactions of these block copolymers with small molecule species that are added to the polymer solutions have also been shown to produce several different block copolymer aggregate morphologies.

1.5.4 Effect of Additives on the Morphology of Block Copolymer Aggregates

It has previously been stated that Zhang et al. have shown that ionic additives influence the morphology of the crew-cut micelles.^{87,88} The molar ratio (*R*) of the number of added ions to the number of repeat units in the corona controls the morphology. The effect of ionic species has been investigated for both polystyrene-*b*-poly(acrylic acid) and polystyrene-*b*-poly(4-vinylpyridine) copolymers.⁸⁷⁻⁹⁰

The presence of a simple electrolyte such as sodium chloride (NaCl) in a copolymer solution results in the screening of the electrostatic field along the partially ionized corona chains. The reduction in the corona-chain repulsion decreases their dimensions and stimulates micellar growth. Consequently, the core radius increases with added salt content. The PS chains of the core must stretch, which is subject to an entropic penalty. The aggregates change their morphology (i.e. from spheres to rods) to produce a more thermodynamically favorable structure. For example, the addition of NaCl has been shown to convert a dynamic system of spherical PS₄₁₀-b-PAA₂₅ micelles to rods, vesicles, or large compound vesicles (LCVs).⁸⁸

The addition of hydrochloric acid (HCl) produces morphological transitions in PS₄₁₀-b-PAA₂₅ micelles similar to those produced by NaCl.⁸⁸ In this case, the reduction of coronal repulsion is attributed to protonation of the acrylic acid blocks. Hence, increasing the molar ratio progressively leads to the formation of rods, vesicles, and LCVs. Slightly different results are obtained with the addition of HCl to solutions of PS₃₁₀-b-P4VP₅₈.⁹⁰ The sphere to rod transition is induced at a lower molar ratio than in the case of PS-b-PAA aggregates. A further increase in the HCl content causes a conversion of the rods back to spheres due to the higher charge density. The trend is inverted again with even higher molar ratios as a result of electrostatic shielding.

The use of a base as an additive has the opposite effect of the use of an acid. In this case, strong bases like NaOH serve to increase the charge density of the corona for PS-b-PAA micelles by deprotonating the acrylic acid blocks. The corona-chain repulsion is enhanced, which leads to a decrease in the aggregation number and core diameter. This reverses the morphological transitions leading to spherical micelles with a higher molar ratio of base.⁸⁷⁻⁸⁹

A few other studies have appeared in the literature, which deal with the influence of different small molecule additives on block copolymer morphologies. The aggregates formed from the triblock copolymer poly(ethylene oxide)₂₉-b-poly(propylene oxide)₄₀-b-poly(ethylene oxide)₂₉ in aqueous solution have been shown to undergo morphological transitions with a change in temperature.¹¹⁵ These same transitions have been obtained in this system at lower temperatures with the aid of simple electrolytes such as potassium fluoride and potassium chloride. Talingting et al. studied the use of hydrochloric acid as a

morphogenic agent for polystyrene-*b*-poly(2-vinylpyridine) and poly(2-vinylpyridine)-*b*-poly(ethylene oxide) aggregates in methanol-dioxane-water mixtures.¹⁰⁵ They successfully observed a transformation of spherical micelles into multilayered vesicles. A theoretical discussion by Netz outlines the effects of small ionic species on block copolymer aggregates in solution.²⁴ The effects of small amphiphilic molecules on the solution behavior of block copolymers has been studied independently by Kabanov et al., as well as Zheng and Davis. Kabanov and coworkers introduced various cationic surfactants into aqueous solutions of poly(ethylene oxide)-*b*-poly(sodium methacrylate), which resulted in the spontaneous formation of vesicles due to complex formation.¹¹⁶ It was recently demonstrated by Zheng et al. that nonionic surfactants could partition into spherical micelles formed from Pluronic copolymers leading to the formation of cylindrical aggregates.¹¹⁷

1.6 Characterization Methods Employed

The experimental results discussed throughout this thesis were obtained using two main methods of instrumental analysis: absorbance spectroscopy and transmission electron microscopy. Due to the extensive use of these techniques, the basic principle involved in each are reviewed in the following discussion.

1.6.1 Solution Turbidity Measurements

The formation of aggregates from block copolymer molecules in solution often produces samples that are not optically clear, due to the fact that some of the electromagnetic radiation that passes through the sample is scattered by the copolymer particles.^{118,119} Depending on the size of the particles, the scattering may be Rayleigh or Tyndall in nature. Rayleigh scattering occurs when the dimensions of the scattering particles are less than five percent of the wavelength of incident radiation. Tyndall scattering results when the dimensions of the particles that are causing the scattering are larger than the wavelength of the scattered radiation.¹¹⁸ Since the amount of light scattered depends on the size and shape of the particles, the change in solution turbidity has been extensively employed to detect changes in the dimensions of particles observed in a variety of colloidal systems.

The simplest means of monitoring changes in solution turbidity is by following the absorbance at one wavelength with a spectrometer. In order for this type of experiment to be feasible, the wavelength of choice must be one at which none of the species in solution absorb light. Hence, the absorbance reading is based solely on the contributions from light scattered at 180° for the incident radiation and any light that is passes through the sample without interacting with the molecules and aggregates in the solution.¹¹⁹

1.6.2 Transmission Electron Microscopy

An electron microscope is an optical instrument that employs a beam of electrons to provide high resolution of details in an object.^{120,121} In fact, it is the focusability and extremely short wavelength of the electron beams that provide the high resolving power of an electron microscope. In transmission electron microscopy, the electrons are discharged from an electron gun (point filament) contained within an evacuated system. The beam is concentrated by an electromagnetic lens into a smaller spot (2 to 3 μm), which is passed through the specimen. The reemitted beam is focused by an objective lens to form an intermediate image. This image is deemed to be intermediate because it cannot be viewed directly by the eye. The image is enlarged by one or more projector lenses to form the final image, which is viewed on a fluorescent screen or photosensitive material for photographic processing.^{120,121}

The information that is obtained about a specimen from TEM is derived from the scattering processes that occur when the electron beam travels through the sample. The resultant beam contains some of the original free electrons that have not been altered, and some that have been changed in either velocity or direction or both. There are two types of scattering processes that can occur. Elastic scattering results from the interaction of the electrons and the effective potential field of the nuclei with the sample. It does not involve any loss of energy, and it can be coherent or incoherent in nature. The interaction between the beam electrons and those in the specimen, which results in a loss of energy and absorption, is referred to as inelastic scattering.¹²⁰

The resolution of the electron microscope is expressed using the Rayleigh formula, which is derived by considering the maximum angle of electron scattering that is able to pass through the objective lens.

$$R = \frac{0.61\lambda}{\alpha} \quad (24)$$

Here, R is the size of the resolved object, λ is the wavelength, and α is equal to the effective aperture of the objective lens. The relativistic wavelength of the electrons depends on the accelerating voltage and is given by the modified De Broglie wavelength.

$$\lambda = \frac{h}{[2m_0eE\{1 + eE/2m_0c^2\}]^{1/2}} \quad (25)$$

In this case, h is Planck's constant, m_0 is the rest mass, e is the charge on the electron, E is the accelerating potential and c is the speed of light.¹²¹

Another advantage of the small wavelength of electrons is that the depth of field and depth of focus are very large in electron microscopy. The depth of field is expressed as:

$$D = \frac{d}{\tan \alpha}, \quad (26)$$

where d is the resolution and α is the lens aperture. Interestingly, the depth of focus D_f is related to the depth of field through the magnification M .

$$D_f = \frac{dM^2}{\alpha} \quad (27)$$

The degree to which the dimensional details of an object can be resolved is determined, to a great extent, by these two parameters.¹²⁰

1.7 Objectives of this Thesis

The ability to obtain aggregates of several different architectural shapes from amphiphilic block copolymers in solution is a relatively new concept; and as evident from the previous discussion, very little is known about some of the more fundamental details associated with these types of colloidal aggregates. This is particularly true in the area of the kinetics and mechanisms of morphological transitions and with respect to the use of certain species as morphogenic agents. This thesis addresses these two issues. All

of the experimental work completed for this dissertation was carried out with aggregates prepared from polystyrene₃₁₀-b-poly(acylic acid)₅₂ in dioxane-water mixtures.

The focus of chapter 2 is on the kinetics and mechanisms of the transformation of spherical aggregates into rod-like structures and the reverse process. The addition model of colloidal aggregation has been used to describe these transitions. The mechanisms have been identified with the aid of transmission electron microscopy, while the kinetic parameters were obtained from solution turbidity measurements as a function of time.

Chapter 3 deals with the kinetics and mechanism associated with the transformation of vesicular aggregates into rods. The corresponding forward transition was recently studied by Chen et al.⁹¹ The two transitions are described and their differences are discussed

The use of the amphiphilic species sodium dodecyl sulfate as a morphogenic agent for structural transitions in PS₃₁₀-b-PAA₅₂ / dioxane / water system is outlined in chapter 4. A series of phase diagrams have been constructed to demonstrate the influence of changing the surfactant concentration, the solvent composition, and the copolymer concentration has on the block copolymer aggregates present in this four component system.

In the final chapter, some general conclusions are made about this thesis. The contributions made to original knowledge that have stemmed from this work and some suggestions for future studies are also discussed.

1.8 References

1. Tuzar, Z.; Kratochvil, P. *Adv. Colloid Interface Sci.* **1976**, *6*, 201.
2. Price, C. In *Developments in Block Copolymers*; Goodman, I., Ed.; Applied Science Publishers: London, 1982; Vol. 1, p 39.
3. Riess, G; Hurtrez, G; Bahadur, P. *Encyclopedia of Polymer Science and Engineering*, 2nd ed.; Wiley: New York, 1985; Vol. 2, p 324.
4. Selb, J.; Gallot, Y. In *Developments in Block Copolymers*; Goodman, I., Ed.; Applied Science Publishers: London, 1985; Vol. 2, p 27.
5. Brown, R. A.; Masters, A. J.; Price, C.; Yuan, X. F. In *Comprehensive Polymer Science: Polymer Properties* Allen, S. G., Bevington, J. C., Booth, C., Price, C., Eds.; Pergamon Press: Oxford, 1989; Vol.2, p 155.

6. Tuzar, Z.; Kratochvil, P. In *Surface and Colloid Science*; Matijevic, E., Ed.; Plenum Press: New York, 1993; Vol. 15, p 1.
7. Alexandridis, P.; Hatton, A. *Colloids Surf., A* **1995**, *96*, 1.
8. Chu, B.; Zhou, Z. Physical Chemistry of Polyoxyalkylene Block Copolymer Surfactants. In *Nonionic Surfactants: Polyoxyalkyl Block Copolymers*; Nace, V. M., Ed.; Marcel Dekker: New York, 1996; Vol. 60, p 86.
9. *Amphiphilic Block Copolymers: Self-assembly and Applications*; Alexandridis, P., Lindman, B., Eds.; Elsevier: Amsterdam, 1997.
10. Hamley, I. W. Block Copolymers in Dilute Solution. *The Physics of Block Copolymers*; Oxford University Press: New York, 1998; Chapter 3.
11. Stigter, D. Hydration, Shape, and Charge of Micelles of Sodium Dodecyl Sulfate and Dodecyl Ammonium Chloride. In *Chemistry, Physics and Application of Surface Active Substances*; Overbeek, J. T. G., Ed.; Gordon and Breach, Science Publishers: New York, 1967; Vol. 2, pp 507-518.
12. Missell, P. J.; Mazer, N. A.; Carey, M. C.; Benedek, G. B. Thermodynamics of the Sphere-to-Rod Transition in Alkyl Sulfate Micelles. In *Solution Behavior of Surfactants: Theoretical and Applied Aspects*. Mittal, K. L., Fendler, E. J., Eds.; Plenum Press: New York, 1980; Vol. 1, pp 373-388.
13. Isrealachvili, J. N. Aggregation of Amphiphilic Molecules into Micelles, Bilayers, Vesicles, and Biological Membranes. In *Intermolecular and Surface Forces*, 2nd ed; Academic Press: London, 1992; Chapter 17.
14. Schafheutle, M. A.; Finkelmann, H. *Liq. Cryst.* **1988**, *10*, 1369.
15. Porte, G. Micellar Growth, Flexibility and Polymorphism in Dilute Solutions. In *Micelles, Membranes, Microemulsions, and Monolayers*; Gelbart, W. M., Ben-Shaul, A., Roux, D., Eds.; Springer-Verlag: New York, 1994; Chapter 2.
16. Hiemenz, P. C.; Rajagopalan, R. Colloidal Structures in Surfactant Solutions: Association Colloids. In *Principles of Colloid and Surface Chemistry*; Marcel Dekker: New York, 1997; Chapter 8.
17. Zhang, L; Eisenberg, A. *Science* **1995**, *268*, 1728.
18. Alexandridis, P.; Holmquist, P.; Olsson, U.; Lindman, B. *Colloids Surf., A* **1997**, *129*, 3.
19. Hajduk, D. A.; Kossuth, M. B.; Hillmyer, M. A.; Bates, F. S. *J. Phys. Chem. B* **1998**, *102*, 4269.
20. Regenbrecht, M.; Akari, S.; Förster, S.; Mohwald, H. *Surf. Interface Anal.* **1999**, *27*, 418.
21. Liu, G. *Curr. Opin. Colloid Interface Sci.* **1998**, *3*, 200.

22. Resendes, R.; Massey, J. A.; Dorn, H.; Power, K. N.; Winnik, M. A.; Manners, I. *Angew. Chem. Int. Ed. Engl.* **1999**, *38*, 2570.
23. Cameron, N. S.; Corbierre, M. K.; Eisenberg, A. *Can. J. Chem.* **1999**, *8*, 1311.
24. Netz, R. R. *Europhys. Lett.* **1999**, *47*, 391.
25. Naka, K.; Nakamura, T.; Ohki, A.; Maeda, S. *J. Macromol. Sci., Pure Appl. Chem.* **1997**, *A34*, 587.
26. Nagarajan, R. *Colloids Surf., B* **1999**, *16*, 55.
27. Harada, A.; Kataoka, K. *Science* **1999**, *283*, 65.
28. Lee, A. S.; Gast, A. P.; Butun, V.; Armes, S. P. *Macromolecules* **1999**, *32*, 4302.
29. Cowie, J. M. G. *Polymers: Chemistry & Physics of Modern Materials*, 2nd ed., Chapman & Hall: New York, 1991.
30. Fried, J. R. *Polymer Science and Technology*; Prentice Hall: Englewood Cliffs., NJ, 1995.
31. Hadjichristidis, N.; Tselikas, Y.; Iatrou, H.; Efstratiadis, V.; Avgropoulos, A. *J. Macromol. Sci., Pure Appl. Chem.* **1996**, *33*, 1447.
32. Zhong, Z. F.; Varshney, S. K.; Eisenberg, A. *Macromolecules* **1992**, *25*, 7160.
33. Hautekeer, J. P.; Varshney, S. K.; Fayt, R.; Jacobs, C.; Jerome, R.; Teyssie, P. *Macromolecules* **1990**, *23*, 3893.
34. Shen, H.; Eisenberg, A. *J. Phys. Chem. B* **1999**, *103*, 9473.
35. Myers, D. *Surfaces, Interfaces, and Colloids: Principles and Applications*, 2nd ed.; Wiley-VCH: New York, 1999.
36. Rosen, M. J. *Surfactants and Interfacial Phenomena*, 2nd ed.; Wiley: New York, 1989.
37. Turro, N. J.; Yekta, Y. *J. Am. Chem. Soc.* **1978**, *100*, 5951.
38. Aniansson, E. A. G.; Wall, S. N. *J. Phys. Chem.* **1974**, *78*, 1024.
39. Evans, D. F.; Wennerstrom, H. *The Colloidal Domain: Where Physics, Chemistry, Biology and Technology Meet*, 1st ed.; VCH Publishers: New York, 1994; pp 135-144.
40. Aniansson, E. A. G.; Wall, S. N.; Almgren, M.; Hoffmann, H.; Kielmann, I.; Ulbricht, W.; Zana, R.; Lang, J.; Tondre, C. *J. Phys. Chem.* **1976**, *80*, 905.
41. Lang, J.; Zana, R. In *Surfactant Solutions: New Methods of Investigation*; Zana, R., Ed.; Surfactant Science Series 22; Marcel Dekker: New York, 1987; pp 414-422.
42. Isrealachvili, J. N.; Mitchell, D. J.; Ninham, B. W. *J. Chem. Soc. Faraday Trans.* **1976**, *72*, 1525.

43. Hayashi, S.; Ikeda, S. *J. Phys. Chem.* **1980**, *84*, 744.
44. Silvander, M.; Karlsson, G.; Edwards, K. *J. Colloid Interface Sci.* **1996**, *179*, 104.
45. Robinson, B. H.; Bucak, S.; Fortana, A. *Langmuir* **2000**, *16*, 8231.
46. In, M.; Aguerre-Chariol, O.; Zana, R. *J. Phys. Chem. B* **1999**, *103*, 7747.
47. Chiruvolu, S.; Isealachvili, J. N.; Naranjo, E.; Xu, Z.; Zasadzinski, J. A. *Langmuir*, **1995**, *11*, 4256.
48. Horn, R. G. *Biochim. Biophys. Acta* **1984**, *778*, 224.
49. Egelhaff, S. U. *Curr. Opin. Colloid Interface Sci.* **1998**, *3*, 608.
50. Harada, S.; Fujita, N.; Sano, T. *J. Am. Chem. Soc.* **1988**, *110*, 8710.
51. Michels, B.; Waton, G. *J. Phys. Chem. B* **2000**, *104*, 228.
52. Farquhar, K. D.; Misran, M.; Robinson, B. H.; Steytler, D. C.; Morini, P.; Garrett, P. R.; Holzwarth, J. F. *J. Phys: Condens. Matter* **1996**, *8*, 9397.
53. Salkar, R. A.; Mukesh, D.; Samant, S. D.; Manohar, C. *Langmuir*, **1998**, *14*, 3778.
54. Brinkmann, U.; Neumann, E.; Robinson, B. H. *J. Chem. Soc. Faraday Trans.* **1998**, *9*, 1281.
55. Campbell, S. E.; Yang, H.; Patel, R.; Friberg, S. E.; Aikens, P. A. *Colloid Polym. Sci.* **1997**, *275*, 303.
56. Halperin, A.; Tirrell, M.; Lodge, T. P. *Adv. Polym. Sci.* **1992**, *100*, 31.
57. Bednár, B.; Edwards, K.; Almgren, M.; Tormod, S.; Tuzar, Z. *Macromol. Chem. Rapid Commun.* **1988**, *9*, 785.
58. Procházka, K.; Bednár, B.; Tuzar, Z.; Kocirik, M. *J. Liq. Chrom.* **1989**, *12*, 1023.
59. Honda, C.; Hasegawa, Y.; Hirunuma, R.; Nose, T. *Macromolecules* **1994**, *26*, 7660.
60. Hecht, E.; Hoffmann, H. *Colloids Surf., A.* **1995**, *96*, 181.
61. Honda, C.; Abe, Y.; Nose, T. *Macromolecules* **1996**, *21*, 6778.
62. Michels, B.; Waton, G. *Langmuir* **1997**, *13*, 311.
63. Iyama, E.; Nose, T. *Macromolecules* **1998**, *31*, 7356.
64. Kent, M. S.; Tirrell, M.; Lodge, T. P. *J. Polym. Sci., Part B: Polym. Phys.* **1994**, *32*, 1927.
65. Tsunashima, Y.; Kawamata, Y. *Macromolecules* **1993**, *26*, 4899.
66. Tian, M.; Qin, A.; Ramireddy, C.; Webber, S. E.; Munk, P.; Tuzar, Z.; Procházka, K. *Langmuir* **1993**, *9*, 1741.
67. Brown, W.; Schillén, K.; Hvidt, S. *J. Phys. Chem.* **1992**, *96*, 6038.

68. Underhill, R. S.; Ding, J.; Birss, V. I.; Liu, G. *Macromolecules* **1997**, *26*, 8298.
69. Kabanov, A. V.; Alakhov, V. Y. Micelles of Amphiphilic Block Copolymers as Vehicles for Drug Delivery. In *Amphiphilic Block Copolymers: Self-Assembly and Applications*. Alexandridis, P., Lindman, B. Eds.; Elsevier: Amsterdam, The Netherlands, 2000; Chapter 15.
70. Cha, J. N.; Stucky, G. D.; Morse, D. E.; Deming, T. J. *Nature* **2000**, *403*, 289.
71. Zhang, L.; Eisenberg, A. *J. Am. Chem. Soc.* **1996**, *118*, 3168.
72. Yu, K.; Eisenberg, A. *Macromolecules* **1996**, *27*, 6359.
73. Yu, K.; Zhang, L.; Eisenberg, A. *Langmuir* **1996**, *12*, 5984.
74. Zhang, L.; Bartels, C.; Yu, Y.; Shen, H.; Eisenberg, A. *Phys. Rev. Lett.* **1997**, *79*, 5034.
75. Yu, Y.; Zhang, L.; Eisenberg, A. *Macromolecules* **1998**, *31*, 1144.
76. Yu, K.; Eisenberg, A. *Macromolecules* **1998**, *31*, 3509.
77. Zhang, L.; Eisenberg, A. *Polym. Adv. Tech.* **1998**, *9*, 677.
78. Yu, K.; Bartels, C.; Eisenberg, A. *Macromolecules* **1998**, *31*, 9399.
79. Yu, Y.; Zhang, L.; Eisenberg, A. *Langmuir* **1997**, *13*, 2578.
80. Yu, Y.; Eisenberg, A. *J. Am. Chem. Soc.* **1997**, *119*, 8383.
81. Yu, G.; Eisenberg, A. *Macromolecules* **1998**, *31*, 5546.
82. Zhang, L.; Eisenberg, A. *Macromolecules* **1999**, *32*, 2239.
83. Shen, H.; Eisenberg, A. *J. Phys. Chem. B* **1999**, *103*, 9473.
84. Shen, H.; Zhang, L.; Eisenberg, A. *J. Phys. Chem. B* **1997**, *24*, 4697.
85. Shen, H.; Eisenberg, A. *Macromolecules* **2000**, *33*, 2561.
86. Desbaumes, L.; Eisenberg, A. *Langmuir* **1999**, *15*, 36.
87. Zhang, L.; Yu, K.; Eisenberg, A. *Science* **1996**, *272*, 1777.
88. Zhang, L.; Eisenberg, A. *Macromolecules* **1996**, *29*, 8805.
89. Zhang, L.; Shen, H.; Eisenberg, A. *Macromolecules* **1997**, *30*, 1001.
90. Shen, H.; Zhang, L.; Eisenberg, A. *J. Am. Chem. Soc.* **1999**, *121*, 2728.
91. Chen, L.; Shen, H.; Eisenberg, A. *J. Phys. Chem. B* **1999**, *103*, 9488.
92. Ding, J.; Liu, G. *Macromolecules* **1999**, *32*, 8413.
93. Ding, J.; Liu, G. *Polymer* **1997**, *38*, 5497.
94. Ding, J.; Liu, G. *Chem. Mater.* **1998**, *2*, 537.

95. Rheingans, O.; Hugenberg, N.; Harris, J. R.; Fischer, K.; Maskos, M. *Macromolecules* **2000**, *33*, 4780.
96. Maskos, M.; Harris, J. R. *Macromol. Rapid Commun.* **2001**, *22*, 271.
97. Discher, B. M.; Won, Y.-Y.; Ege, D. S.; Lee, J. C.-M.; Bates, F. S.; Discher, D. E.; Hammer, D. A. *Science* **1999**, *284*, 1143.
98. Won, Y.-Y.; Davis, H. T.; Bates, F. S. *Science* **1999**, *283*, 960.
99. Discher, B. M.; Hammer, D. A.; Bates, F. S.; Discher, D. E. *Curr. Opin. Colloid Interface Sci.* **2000**, *2*, 125.
100. Schillén, K.; Brown, W.; Johnsen, M. *Macromolecules* **1994**, *27*, 4825.
101. Lehner, D.; Lindner, H.; Glatter, O. *Langmuir* **2000**, *16*, 1689.
102. Zipfel, J.; Lindner, P.; Tsianou, M.; Alexandridis, P.; Richtering, W. *Langmuir* **1999**, *15*, 2599.
103. Svensson, B.; Olsson, U.; Alexandridis, P. *Langmuir* **2000**, *16*, 6839.
104. Prochazka, K.; Martin, T. J.; Webber, S. E.; Munk, P. *Macromolecules* **1996**, *29*, 6526.
105. Talingting, M. R.; Munk, P.; Webber, S. E. Tuzar, Z. *Macromolecules* **1999**, *32*, 1593.
106. Regenbrecht, M.; Akari, S.; Förster, S.; Mohwald, H. *Surf. Interface Anal.* **1999**, *27*, 418.
107. Liang, Y.-Z.; Li, Z.-C.; Li, F.-M. *Chem. Lett.* **2000**, *4*, 320.
108. Liang, Y.-Z.; Li, Z.-C.; Li, F.-M. *New J. Chem.* **2000**, *5*, 323.
109. Massey, J.; Power, K. N.; Manners, I.; Winnik, M. A. *J. Am. Chem. Soc.* **1998**, *120*, 9533.
110. Ræz, J.; Barjovanu, R.; Massey, J..A.; Winnik, M. A.; Manners, I. *Angew. Chem. Int. Edit.* **2000**, *39*, 3862.
111. Spatz, J. P.; Mössmer, S.; Möller, M. *Angew. Chem. Int. Ed. Engl.* **1996**, *35*, 1510.
112. Spatz, J. P.; Mössmer, S.; Möller, M.; Herzog, T.; Plettl, A.; Ziemann, P. *J. Lumin.* **1998**, *76*, 168.
113. Chernyshov, D. M.; Bronstein, L. M.; Börner, H.; Berton, B.; Antonietti, M. *Chem. Mater.* **2000**, *12*, 114.
114. Kramer, E.; Förster, S.; Goltner, C.; Antonietti, M. *Langmuir*, **1998**, *14*, 2027.
115. Jørgenseb, E. B.; Hvidt, S.; Brown, W.; Schillén, K. *Macromolecules* **1997**, *30*, 2355.

116. Kabanov, A.; Bronich, T. K.; Kabanov, V. A.; Eisenberg, A. *J. Am. Chem. Soc.* **1998**, *120*, 9941.
117. Zheng, Y.; Davis, H. T. *Langmuir* **2000**, *16*, 6453.
118. Skoog, D. A.; Leary, J. L. *Principles of Instrumental Analysis*, 4th ed.; Harcourt Brace College Publishers: Orlando, FL, 1992; pp 58-69.
119. Harris, D. A. *Light Spectroscopy*; BIOS Scientific Publishers: Oxford, 1996; pp 1-54.
120. Rochow, T. G.; Tucker, P. A. Transmission Electron Microscopy and Electron Diffraction. *Introduction to Microscopy by Means of Light, Electrons, X-Rays, or Acoustics*, 2nd ed.; Plenum Press: New York, 1994; Chapter 14.
121. Thomas, G.; Goringe, M. J. *Transmission Electron Microscopy of Materials*; John Wiley & Sons: New York, 1976; pp 5-24.

Chapter 2

Kinetics and Mechanisms of the Sphere-to-Rod and Rod-to-Sphere Transitions in the Ternary System PS₃₁₀-b-PAA₅₂ / Dioxane / Water

The introductory chapter made note of the fact that the self-assembly of asymmetric, amphiphilic block copolymers into aggregates with various morphologies in solution has recently received considerable attention from scientists all over the world. Because some of these aggregates show potential for possible applications in such areas as drug delivery and nano-technology, it is particularly important to understand the transformation process involved in the transition from one aggregate morphology to another and the properties of the system that promote such transitions.

This chapter reports on the relaxation kinetics and transition mechanisms of the sphere-to-rod and rod-to-sphere transitions occurring in polystyrene-*b*-poly(acrylic acid) (PS-*b*-PAA) aggregates that have been examined using solution turbidity measurements and transmission electron microscopy. The copolymer PS₃₁₀-*b*-PAA₅₂ has been found to self-assemble into aggregates with spherical, rod-like, and vesicular shapes in dioxane-water mixtures. Recently, the morphological phase diagram for this ternary system was constructed in order to determine the concentration boundaries associated with each aggregate architecture and the regions of morphological coexistence.¹ It was previously found that a sudden alteration of the solvent composition near one of these boundaries could induce a morphological transition.² This method has been used to investigate the kinetics and mechanisms of the sphere-to-rod and rod-to-sphere transitions. The transformation of spherical micelles to rod-like aggregates occurs through a two-step mechanism; it begins with the fast, adhesive collisions of spheres resulting in the formation of “pearl necklace” intermediate structures. This is followed by the reorganization of the necklace intermediates to form smooth rods. The rod-to-sphere transition also involves two steps. A bulb develops quickly on one or both ends of the rod and then the bulbs are slowly pinched off to release free spheres in solution. The sphere-to-rod transition occurs at comparable rates to the reverse process. The effect of the jump magnitude, the initial solvent content, and the copolymer concentration on the relaxation rates was also investigated.

2.1 Introduction

It is well known that asymmetric, amphiphilic diblock copolymers can self-assemble to form aggregates in selective solvents.³⁻⁵ Micelles with a lyophilic core and a lyophobic corona are formed in highly polar media, while aggregates with the opposite composition are present in solvents of low polarity. Diblock copolymer micelles are classified, according to their block lengths, as star-like when the length of the corona is larger than the diameter of the micellar core, while crew-cut micelles have a larger core diameter relative to the size of the corona.^{6,7}

One of the more novel properties of block copolymers is their ability, similar to that of small molecule surfactants^{8,9}, to form aggregates of a variety of different morphologies in solution.¹⁰⁻¹² The balance between the stretching of the core-forming blocks, the intercoronal interactions, and the interfacial tension between the micellar core and the solvent has been identified as having a major influence on the architecture of the block copolymer aggregates.¹³⁻¹⁵ Several other studies have revealed that multiple aggregate morphologies can be prepared by altering such factors as the relative block lengths of the copolymer,¹⁶ the solvent composition,¹⁷ the temperature,¹⁸ and the presence of additives.¹⁹ Changing any one of these factors disturbs the force balance governing the structure of the aggregates, which can lead to the transformation of one morphology into another.

Although the polymorphism demonstrated by block copolymer aggregates in solution has received considerable attention in the past few years,²⁰ physico-chemical investigations of these multiple morphologies are only beginning to appear in the literature.^{2,21,22} Since amphiphilic block copolymers often exhibit surfactant-like behavior in solution, fundamental knowledge of the solution properties of small molecule surfactants has proven to be invaluable in attempting to obtain similar information about amphiphilic block copolymers. The self-assembly process has been well studied for both types of amphiphilic systems. The aggregation of surfactant and block copolymer molecules is described as a step-wise association; the closed-association model is most frequently used to explain the mechanistic details of micellization.^{3-5,23-25}

The kinetics involved in the micellization of small molecule surfactants has been extensively investigated.^{26,27} The Aniansson and Wall theory of self-assembly, which

divides the process into two steps, is the most widely accepted kinetic description of micellization. The first step involves an increase in the aggregation number of each micelle, but the total population of aggregates does not change. The rate determining relaxation process is the simultaneous formation and decomposition of micelles with a change in the total number of aggregates as equilibrium is approached.²⁶ This involves a series of step-wise events, during which one molecule at a time associate and dissociates from an aggregate. The kinetics of block copolymer micellization has also been discussed in recent years.²⁸⁻³⁰ This process is found to have two relaxation steps, as in the case of surfactants, but occurs at a much slower rate. The mechanism of block copolymer micelle formation also resembles that of surfactant micelles.

Much is known about the kinetics and mechanism of the formation of surfactant and block copolymer aggregates, yet only a few studies have examined the details involved in the transition from one aggregate morphology to another. Most of these studies deal with structural transformations in surfactant aggregates.³¹⁻³⁶ Some of the morphological transitions that have been investigated in surfactant systems include the sphere-to-vesicle,³² the vesicle-to-sphere,³³ the sphere-to-rod,³⁴ and the lamellar-to-inverted hexagonal transition,³⁵ as well as the fusion of two vesicles to form one large vesicle³⁶.

Of particular interest, in our case, is the sphere-to-rod transition. This architectural change occurs quite rapidly, thus the kinetics has been difficult to follow. Harada et al. were the first to examine this transformation process in aqueous solutions of hexadecyltrimethylammonium bromide with the use of conductivity and ultrasonic velocity measurements.^{34a} The transformation was induced by a sudden change in the surfactant concentration near the phase boundary. This process proceeds via a growth mechanism, and the kinetics involve two relaxation steps. The fast step corresponds to the progressive addition of monomers to the spherical micelles, which occurs over tens of milliseconds. The rate-limiting process, proceeding over hundreds of milliseconds, is the overall formation and dissociation of rod-like micelles. Recently, kinetic studies were carried out with sodium dodecyl sulfate micelles in aqueous sodium chloride solutions.^{34b} The transition was brought about by a jump in the temperature of the system, and it was monitored by light scattering detection. This process was also found to evolve through a

similar mechanism as that proposed by Harada et al.^{34a} It must be noted that in the case of surfactant aggregates, the single chain concentration is high and plays an important role in the mechanisms of morphological transformations. However, in contrast, the single chain population, in block copolymer aggregate systems is low and does not contribute significantly to architectural changes.^{19b}

To date, only limited information is available regarding the kinetics and mechanisms of structural transitions occurring in block copolymer aggregate systems. In fact, only two studies have appeared in the literature. Iyama and Nose were the first to complete such an investigation on dilute solutions of polystyrene-*b*-poly(dimethylsiloxane) in mixtures of *n*-octane and methylcyclohexane.³⁷ During their investigation of the kinetics and mechanism of the self-assembly of these block copolymer aggregates, by means of time-resolved static and dynamic light scattering, they found that the aggregation of individual copolymer molecules proceeds via the formation of intermediate cylindrical aggregates, which have larger aggregation numbers than those of the final micellar structure. The transition has a two-step mechanism. During the first step, which occurs quickly, micelles form and grow into metastable cylindrical aggregates by consuming large amounts of excess free copolymer molecules in the solution. The individual chains within these intermediate structures rearrange, through the insertion and expulsion of copolymer chains, to form spherical micelles in the final rate-determining step.

Chen et al. reported on the kinetic and mechanistic details of the transformation of rod-like polystyrene-*b*-poly(acrylic acid) aggregates, formed in dioxane-water mixtures, into vesicular structures.² This particular polymer is known to self-assemble into aggregates of multiple morphologies in solution (i.e. spheres, rods, vesicles). Transmission electron micrographs indicate that near the boundary, between the rod and vesicle regions, the rods become shorter with an increase in their diameter, and a few vesicles begin to appear in the solution. A sudden jump in the water content, in this region, results in the formation of vesicles at the expense of the rods. The rod-to-vesicle transition has a two-step mechanism. Initially, the transformation involves the flattening of the short rods, forming irregular or circular lamellae. This is followed by the rate-

limiting closure of the bowl-shaped lamellae to form vesicles. The kinetics of this transition was followed by monitoring the solution turbidity as a function of time.²

The ability to transverse the morphological phase diagram (i.e. spheres to rods to vesicles), with increasing perturbation to the system, has prompted an investigation of the factors governing the morphology of PS-b-PAA aggregates in selective solvents, and the details involved in the transition from one aggregate morphology to another.¹ Zhang and Eisenberg have already explored the conditions under which the formation of aggregates with a specific morphology are determined by thermodynamics factors or by the kinetics of the system.^{19b} It was found that the solvent composition and the method used to form the aggregates (i.e. direct dissolution or slow solvent addition) greatly influence whether a given architecture is under thermodynamic or kinetic control. This knowledge has provided a basis and a motivation for examining the mechanistic and kinetic details associated with each morphological transition.

This present study is a continuation of the work started by Chen et al.² Here, we report on the kinetics and mechanisms associated with the sphere-to-rod and rod-to-sphere transition in the PS₃₁₀-b-PAA₅₂ / dioxane / water system. Changes in the solution turbidity were followed as a function of time, after a jump was made in one of the solvent components, in order to determine the kinetics of the transitions. The mechanisms were elucidated using a freeze-dry technique to trap the intermediate aggregate structures for observation using transmission electron microscopy. The discussion section of this communication is divided into four parts. First we look at the factors that determine the size and shape of the copolymer aggregates. This is followed by a description of the mechanism of both the sphere-to-rod and the rod-to-sphere transitions. The kinetic results are outlined in the next section. Finally, the effects of the initial solvent composition, the degree of solvent perturbation, and the initial polymer concentration on the morphological transitions are discussed.

2.2 Experimental Section

This study was carried out using a polystyrene-b-poly(acrylic acid) copolymer composed of blocks containing 310 and 52 repeat units respectively. It was synthesized by sequential anionic polymerization and has an overall polydispersity of 1.05.¹ A detailed description of the synthesis procedure can be found in a previous publication.³⁸

The polymer sample was fractionated to remove homopolystyrene using a standard method.^{19b} The phase behavior of PS₃₁₀-b-PAA₅₂ has also been described in an earlier communication.¹

In order to prepare the aggregates, PS₃₁₀-b-PAA₅₂ was first dissolved in dioxane, which is a solvent suitable for both copolymer blocks. The aggregation of the chains was induced by the slow addition of deionized water (0.2 wt % / min), which is a precipitant for the PS blocks. The presence of micelles was indicated by the appearance of a blue tint to the solution. The water addition was continued until the desired concentration was reached. The solution was stirred for 24 hours, after the water addition, in order to ensure that equilibrium was reached.

In order to study the solution turbidity of spheres and rods as a function of polymer concentrations, two stock solutions were prepared, one with spherical aggregates and one containing rods in dioxane-water mixtures of 9.5 and 13.5 wt % water respectively. The morphology of the aggregates was quenched by quickly adding the stock solutions to an excess of water, which resulted in the two-fold dilution of the samples. The solutions were placed in dialysis bags (Spectra/Por) with a molecular weight cutoff of 50 000 g/mol. After dialysis, the stock solutions were rotary evaporated to increase the polymer concentration. Several other samples with varying polymer concentrations were prepared by diluting the stock solution with water.

The solution turbidity was measured at 650 nm with a Varian Cary 50 spectrophotometer, because that is where both the copolymer and the aggregates have the lowest absorption. The measurements were taken at room temperature. The kinetic experiments were also done using visible spectroscopy by following the solution turbidity as a function of time at 650 nm.

The mechanistic details of the morphological transition were examined using transmission electron microscopy (TEM). After the initial addition of solvent for the jump, the polymer solution was sprayed, at given time points, onto copper grids that had been previously coated with poly(vinyl formal) (JB EM Services Inc.) and carbon respectively. The temperature of the samples was reduced to near that of liquid nitrogen in order to preserve the intermediate morphologies. The samples were then freeze-dried by allowing them to warm to room temperature while under vacuum. A Phillips EM400

microscope operating at an acceleration voltage of 80 kV was used to observe the morphologies.¹

2.3 Results and Discussion

2.3.1 Change in Aggregate Size and Shape

Before describing the kinetic and mechanistic details associated with architectural changes in block copolymer aggregates induced by a change in the solvent composition, it is important to discuss how the interactions between the solvent and the copolymer molecules affect the size and shape of the aggregates.

The interactions between the PS-*b*-PAA chains and the solvent have been found to influence the dimensions of both the aggregate core and the corona.¹³⁻¹⁵ The strength of these interactions is described by the Flory interaction parameter (χ), which is a measure of the solvent power. The better the quality of the solvent for the polymer, the lower the value of χ . The properties of dioxane make it a favorable solvent for both the PS and the PAA blocks. However, since water has a higher dielectric constant than dioxane, it interacts favorably only with the PAA blocks. The morphology of the copolymer aggregates is dictated by the balance between the effect of the PS-solvent and the PAA-solvent interactions on the three forces governing the structure of the aggregates (i.e., stretching of the core-forming blocks, the interfacial tension between the solvent and the micellar core, and the intercorona interactions). The degree of stretching of the PS chains within an aggregate is proportional to the size of the core of the aggregates. In turn, the core radius is a function of the aggregation number of the micelle (N_{agg}). The value of N_{agg} is determined by the compatibility of the solvent with each of the copolymer blocks, and so too is the degree of core-chain stretching.^{10b}

It was found that PS₃₁₀-*b*-PAA₅₂ form spherical micelles in dioxane-water mixtures with compositions between 8.5 and 11.5 wt % water (Figure 1).¹ This is the most thermodynamically favorable structure in this solvent composition range because of the relatively low interfacial energy that exists under these conditions, which results from the small value of χ . The aggregation number of each micelle has been shown to increase with water content, at a fixed polymer concentration.^{10b} In the case of PS₃₁₀-*b*-PAA₅₂ micelles, the diameter of the aggregates increases from an average value of 39 ± 1 nm for

initially formed micelles, to a value of 50 ± 2 nm near the sphere to rod morphological boundary. The core radius of a spherical micelle therefore expands as the aggregation number becomes larger. From a thermodynamic point of view, an increase in the aggregation number is favorable because it leads to a decrease in the interfacial area between the solvent and the core chains. However, this is also accompanied by an increase in the stretching of the polystyrene chains and an increase in the corona-chain repulsions. Both processes are thermodynamically unfavorable because they result in an increase in the free energy of the system. This stretching of the core chains has a greater influence on the energetics of the system than the decrease in the interfacial area or the increase in corona repulsions.¹³⁻¹⁵ The spherical micelles undergo adhesive collisions to form rod-like aggregates, with a smaller diameter than that of the spheres, because the degree of core-chain stretching and corona-chain repulsion is lower in rods. As the aggregates change their shape from spheres to rods, additional freedom is gained about the long-axis with little change in the conformation of the chains. Therefore, the transition between the two structures is thermodynamically favorable at solvent compositions of greater than 11.5 wt % H₂O for PS₃₁₀-b-PAA₅₂. However, this transition has been shown to be reversible by altering the solvent composition in favor of the dioxane content.¹

In fact, near the boundary between the S + R and the R regions (Figure 1), an increase in the dioxane content of the solvent mixture leads to the conversion of the rods back to spherical aggregates. The interaction between the solvent and the core chains becomes more favorable with an increase in the dioxane content, which reduces the degree of chain extension. The aggregation number begins to decrease as the dioxane content of the solvent increases. In turn, the interfacial area increases. These events make the rod-like aggregates energetically unstable; hence, the rods convert back to spherical aggregates to gain thermodynamic stability.¹³⁻¹⁵

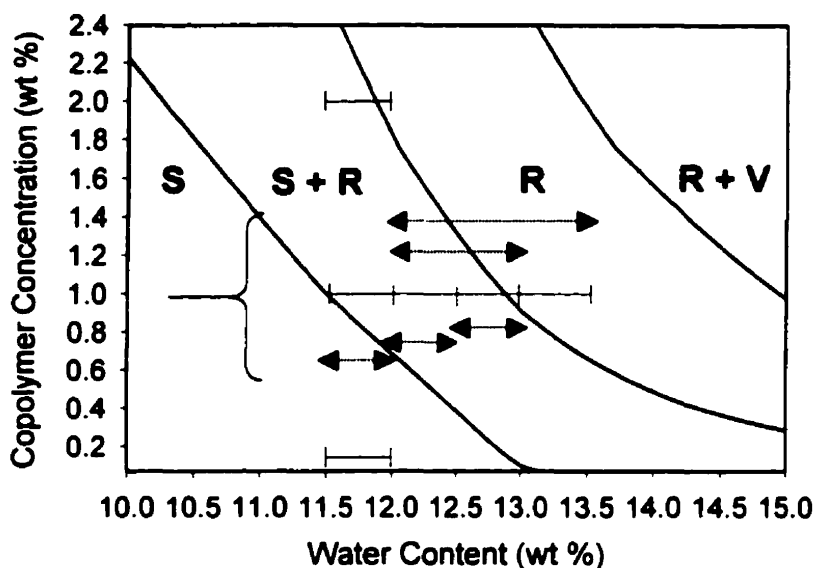


Figure 1: A partial morphological phase diagram for PS₃₁₀-b-PAA₅₂ in dioxane-water mixtures. S: spheres, S + R: spheres and rods, R: rods, R + V: rods and vesicles. The solid line scale shows the water content range covered at a given polymer concentration. The dashed lines with arrows indicate the forward and reverse solvent jumps at 1.0 wt % polymer.

It should be noted that in addition to the influence of the size and shape of the aggregates on the solution turbidity, the polymer concentration also effects the turbidity of a solution containing aggregates of a given morphology.¹ Figure 2 contains a plot of the solution turbidity for both spheres and rods as a function of polymer concentration. The plots indicate that there is a linear dependence of turbidity on polymer concentration for both aggregate morphologies within the concentration range used in the present studies. However, these plots are only representative of the aggregates formed using a particular set of conditions. For example, the spheres were prepared in a solution of 1.0 wt % polymer and 9.5 wt % water and the aggregates were kinetically trapped with their given size and shape upon quenching into water and subsequent dialysis. Thus, turbidity-concentration curves can also be prepared as a function of the size of the spheres. The same process is true for rod-shaped aggregates. However, it is believed that such plots will also be linear because the dimensional changes occur on such a small scale. It is also

concluded that the linear dependence of the solution turbidity on the polymer concentration for spheres and rods in water reflects the behavior of the system in dioxane-water mixtures because the refractive index of the medium is similar in both cases.

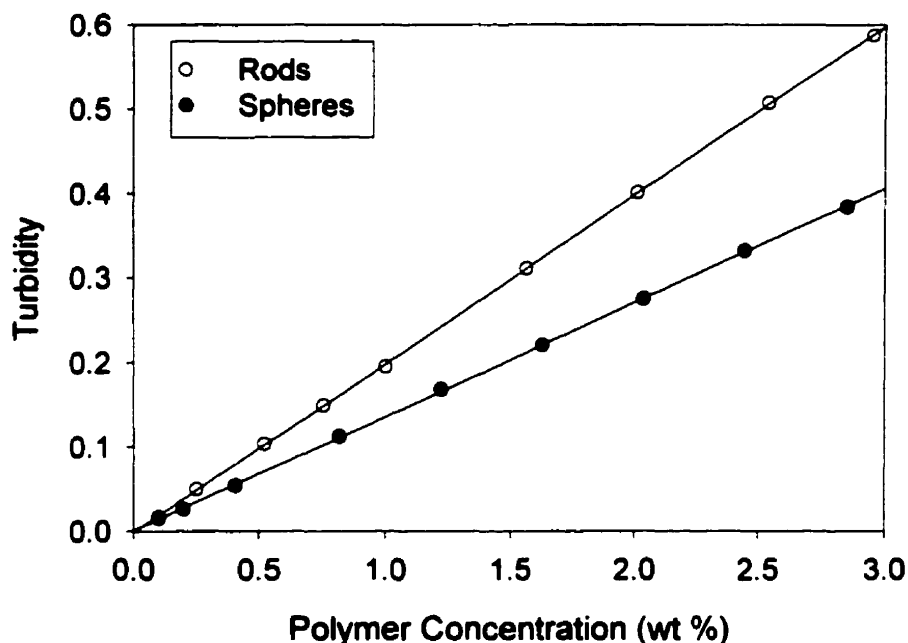


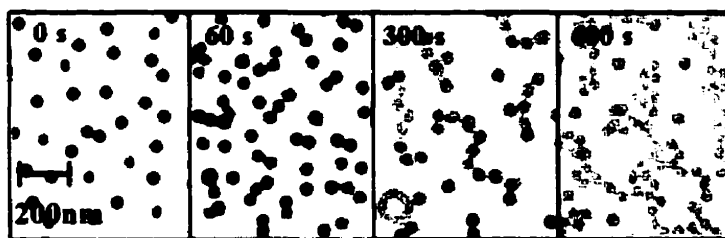
Figure 2: Dependence of the solution turbidity on the polymer concentration for spheres and rods in water. (Error in turbidity of ± 0.01 units)

2.3.2 Mechanisms

Figure 3 contains representative transmission electron micrographs of aggregate structures at different time points during the morphological transitions induced by jumps in the water content from 11.5 to 12.0 wt % and from 12.0 to 13.5 wt % in solutions consisting of 1.0 wt % PS₃₁₀-b-PAA₅₂. At 11.5 wt % H₂O, the system is at the boundary between the S and S+R regions and all of the aggregates are spherical at this point (Figure 1). Thus, the 11.5 to 12.0 wt % H₂O transition brings the system into the S + R region, while the 12.0 to 13.5 wt % H₂O transition moves the system from the S+R region to the R region. The sudden addition of water to the system makes these aggregates energetically unstable. The micrographs indicate that this leads to adhesive collisions of spherical micelles to form “pearl necklace” structures. At high enough water

contents, the pearl necklace intermediates eventually reorganize to form smooth rods with hemispherical caps in order to reduce the surface area of the aggregates. The intermediate stages of this process are shown in the last picture in the 11.5 to 12.0 wt % H₂O transition series and the first few pictures in the 12.0 to 13.5 wt % H₂O transition series. These necklace structures are believed to exist under equilibrium conditions in the water content range covered by the S+R region. The average rod diameter decreases from a value of 50 ± 2 nm, for the individual spheres within a necklace, to 37 ± 2 nm for a smooth rod. Light branching has also been observed in some of these rod structures. This transition mechanism is different from that proposed for the sphere-to-rod transition in small molecule surfactant aggregate systems. However, the clustering of smaller aggregates to form cylinders or rod-shaped structures has been observed in other cases such as aerosol agglomeration in gas particle systems,⁴² flocculation of colloids,⁴³ the aggregation of red blood cells⁴⁴ etc.

Transition from 11.5 to 12.0 wt % H₂O



Transition from 12.0 to 13.5 wt % H₂O



Figure 3: Micrographs of the aggregates at different time points during the sphere-to-rod transition occurring in solutions of 1.0 wt % PS₃₁₀-b-PAA₅₂ in dioxane-water mixtures.

The rod-to-sphere transition also has a mechanism with two observable steps. This is shown in Figure 4, which contains micrographs outlining the rod-to-sphere

transition in solutions of 1.0 wt % PS₃₁₀-b-PAA₅₂ that have initial compositions of 13.0 and 12.0 wt % H₂O respectively. The transition from 13.0 to 12.0 wt % H₂O brings the system from the boundary between the S+R and R regions to a location in the transition region. The 12.0 to 11.5 wt % H₂O transition moves the system from the transition region to the boundary between the S+R and R regions where all of the aggregates are spherical in shape. The first set of micrographs (13.0 to 12.0 wt % H₂O) indicate that the quick addition of a small quantity of dioxane to the system near the boundary between the S+R and R regions results in the development of a bulb on either or both ends of the rods forming dumbbell-like intermediates. These bulbs develop because of the need to reduce the interfacial energy of the unstable rod structures. The bulbs are progressively pinched off to release free spherical micelles. The rods continue to develop bulbs until the final release of the last two micelles.

Transition from 13.0 to 12.0 wt % H₂O



Transition from 12.0 to 11.5 wt % H₂O

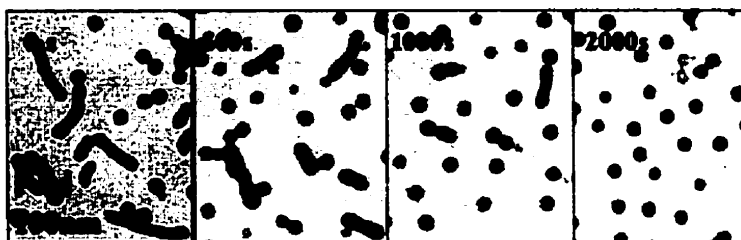


Figure 4: Micrographs of the aggregates at different time points during the rod-to-sphere transition occurring in solutions of 1.0 wt % PS₃₁₀-b-PAA₅₂ in dioxane-water mixtures.

2.3.3 Transition Kinetics

It is well known that the turbidity of the PS₃₁₀-b-PAA₅₂ solutions is dependent upon the size and shape of the copolymer aggregates. As you transect the morphological phase diagram, from spheres to vesicles, the solution turbidity increases. The kinetic

analysis of the morphological transitions under study is based upon this dependence of solution turbidity on the morphology of the aggregates. All of the turbidity-time profiles for both transitions, with exceptions at higher polymer concentrations, are best fitted by a double exponential equation. In the case of the sphere-to-rod transition, the expression is:

$$Y = C + A(1 - e^{-t/\tau_1}) + B(1 - e^{-t/\tau_2}) \quad (1)$$

while, for the rod-to-sphere transition the equation reads as follows:

$$Y = C + Ae^{-t/\tau_1} + Be^{-t/\tau_2} \quad (2)$$

In both equations, τ_1 and τ_2 are the relaxation times, t is the time, A , and B are adjustable parameters, and C is the turbidity at infinite time. Since the sum of C , A , and B is equal to the solution turbidity, the ratio of A to B indicates which relaxation process contributes more to the change in the solution turbidity for any given transition.

An analysis of the TEM micrographs is used to assign the relaxation times to specific processes that occur during the morphological transitions. For example, the first observable step in the mechanism of the sphere-to-rod transition is the adhesive collisions between spheres; one can speculate that the first relaxation time (τ_1) corresponds to this process. It is believed that the reorganization of the intermediate necklaces, which is accompanied by a reduction in the diameter of the aggregates and a slight extension about the long-axis is possibly represented by the second relaxation time (τ_2) in the sphere-to-rod transition. In the case of the rod-to-sphere transition, the first observable change in the aggregate morphology is the development of a bulb on either or both ends of the rods. Since changes in aggregate shape are known to affect the solution turbidity, it is conceivable that this process is related to the first relaxation time (τ_1). Eventually the bulbs are pinched off of the rods, which not only affects the size of the rods, but also changes the ratio of the number of spheres to the number of rods in solution. The second relaxation time (τ_2) for the rod-to-vesicle transition is believed to be a possible reflection of the effect of these changes on the solution turbidity. It must be noted that we do not have enough evidence to confirm the process that corresponds to each relaxation time and that the above assignments are believed to provide the most reasonable description.

It is apparent, from examining the morphological phase diagram (Figure 1), that the region of pure spherical aggregates (S) is separated from that of rod-like aggregates

(R) by a large difference in the solvent composition (≈ 1.5 wt % water). It has been shown that a large, sudden increase in the water content may lead to the kinetic freezing of the starting morphology because of the slow chain dynamics. In order to preserve a state of equilibrium, the transformation of aggregates from one morphology to another is accomplished with small jumps in the solvent composition as the sphere-rod coexistence region is crossed.

Since neither the forward nor reverse transitions proceed with conservation of mass (the aggregation number of rods is larger than that of spheres) it is difficult to obtain the relation between the concentration of each species and the solution turbidity that is required to determine the rate constants for each step in the transitions. Although this information can, in principle, be obtained from light scattering studies, it was not possible to complete such an investigation for the sphere-to-rod and rod-to-sphere transitions because the relaxation times are too short to obtain reliable data from the light scattering instrument. Thus, statistical treatment of the data from the TEM micrographs is required to get an estimate of the rate constants involved in these transitions.

2.3.4 Factors Influencing the Kinetics

Although the specific morphology of the block copolymer aggregates is determined by the thermodynamics of the system, the transition of one morphology to another is dependent upon the kinetics of this process under a given set of conditions. Hence, it is of interest to determine the properties of the system that influence the kinetics of morphological transformation.

2.3.4.1 Effect of Initial Solvent Composition

Previous studies have shown that the solvent composition, which influences the interaction of the polymer chains with the bulk solvent plays a major role in determining the morphology of the block copolymer aggregates. Earlier publications have reported that the slow addition of water to a solution of PS₃₁₀-b-PAA₅₂ in dioxane gradually results in the formation of spherical micelles; when the water addition is continued the micelles are systematically transformed into rods and then vesicles.^{1,2} This warrants further investigation into the effects of the initial solvent composition on the kinetics of morphological transformations.

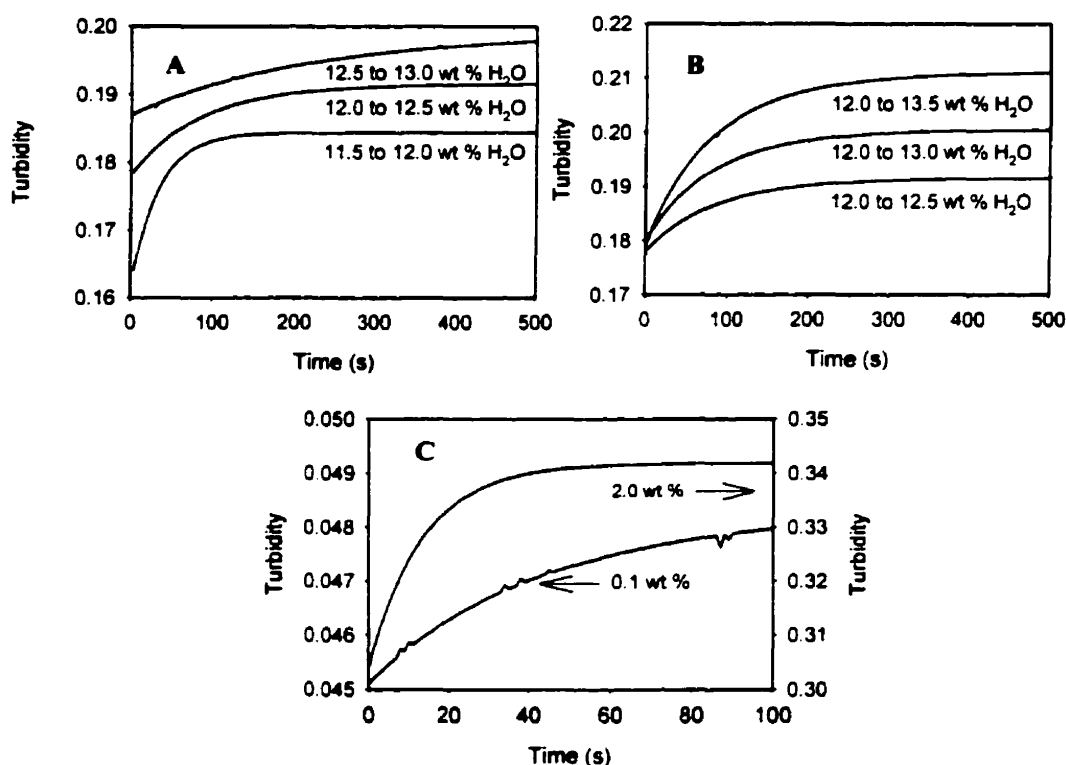


Figure 5: (A) Effect of the initial solvent composition on the kinetics of the sphere-to-rod transition in PS₃₁₀-b-PAA₅₂ aggregates in dioxane-water mixtures. The initial polymer concentration is 1.0 wt %. (B) Effect of the magnitude of the dioxane jump on the kinetics of the sphere-to-rod transition in PS₃₁₀-b-PAA₅₂ aggregates in dioxane-water mixtures. The initial polymer concentration is 1.0 wt %. (C) Effect of the initial polymer concentration on the kinetics of the sphere-to-rod transition from 11.5 to 12.0 wt % H₂O in PS₃₁₀-b-PAA₅₂ aggregates.

Table 1: Kinetic parameters for the sphere-to-rod transition in PS₃₁₀-b-PAA₅₂ aggregates in dioxane-water mixtures.

	Initial Polymer Conc. (wt %)	Initial Water Content (wt %)	$\Delta\text{H}_2\text{O}$	C	A / 10^3	B / 10^3	τ_1 (s)	τ_2 (s)	R^2
Initial	1.01	11.5	0.5	0.160	21.0	3.74	25.0	90.4	0.998
Water	0.99	12.0	0.5	0.179	10.2	2.91	74.8	136	0.997
Content	1.01	12.5	0.5	0.203	9.62	2.66	195	383	0.999
Magnitude	1.00	12.0	0.5	0.179	10.2	2.91	74.8	136	0.997
of Solvent	1.02	12.0	1.0	0.180	5.23	5.32	66.4	120	0.996
Jump	1.00	12.0	1.5	0.179	2.84	5.88	58.5	114	1.00
Initial	0.10	11.5	0.5	0.045	2.46	1.02	37.1	121	0.996
Polymer	1.01	11.5	0.5	0.160	21.0	3.74	25.0	90.4	0.998
Conc.	2.03	11.5	0.5	0.304	----	37.9	----	13.3	0.990

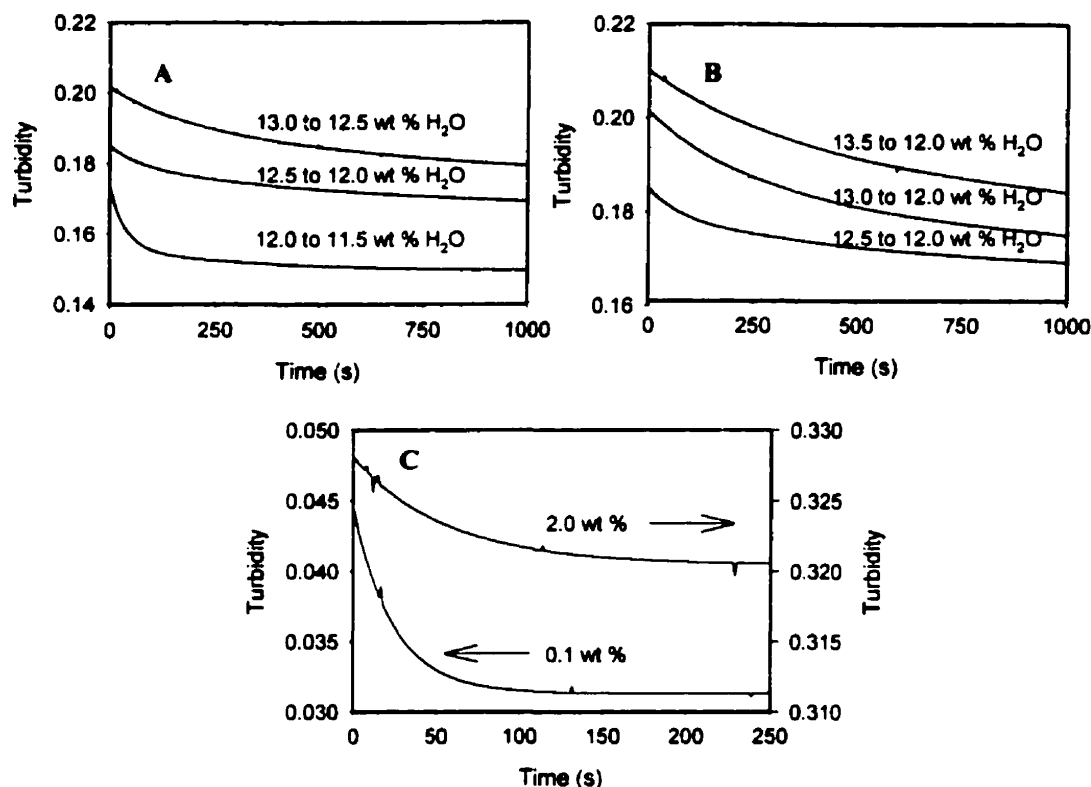


Figure 6: (A) Effect of the initial solvent composition on the kinetics of the rod-to sphere transition in PS₃₁₀-b-PAA₅₂ aggregates in dioxane-water mixtures. The initial polymer concentration is 1.0 wt %. (B) Effect of the magnitude of the dioxane jump on the kinetics of the rod-to-sphere transition in PS₃₁₀-b-PAA₅₂ aggregates in dioxane-water mixtures. The initial polymer concentration is 1.0 wt %. (C) Effect of the initial polymer concentration on the kinetics of the rod-to-sphere transition from 12.0 to 11.5 wt % H₂O in PS₃₁₀-b-PAA₅₂ aggregates.

Table 2: Kinetic parameters for the rod-to-sphere transition in PS₃₁₀-b-PAA₅₂ aggregates in dioxane-water mixtures.

	Initial Polymer Conc. (wt %)	Initial Water Content (wt %)	$\Delta\text{H}_2\text{O}$	C	A / 10^3	B / 10^3	τ_1 (s)	τ_2 (s)	R ²
Initial	1.00	12.0	-0.5	0.149	17.7	6.52	37.0	325	0.995
Water	1.02	12.5	-0.5	0.166	11.4	12.7	78.5	740	0.998
Content	1.00	13.0	-0.5	0.172	9.04	20.3	147	945	1.00
Magnitude	1.01	12.5	-0.5	0.166	11.4	12.7	78.5	740	0.998
of Solvent	1.00	13.0	-1.0	0.166	14.0	21.4	204	1140	0.999
Jump	0.99	13.5	-1.5	0.167	14.5	28.2	293	1890	0.999
Initial	0.10	12.0	-0.5	0.031	6.90	6.41	19.7	24.5	0.996
Polymer	1.00	12.0	-0.5	0.149	17.7	6.52	37.0	325	0.995
Conc.	2.01	12.0	-0.5	0.320	----	7.65	----	56.0	0.990

Figures 5a and 6a contain plots of the solution turbidity as a function of time for the sphere-to-rod and reverse transitions at different initial solvent compositions, but with the polymer concentration and the magnitude of the solvent jump held constant. It is quite clear that the composition of the solvent mixture influences the kinetics of the structural changes. The relaxation times for both steps in the transformation of spherical aggregates to rods, as well as that for rods to spheres, increase with an increase in the water content of the initial solvent composition as indicated in Tables 1 and 2. As well, the relaxation times are similar for both transitions in comparison to the relaxation times for the rod-to-vesicle and vesicles-to-rod transitions where the vesicle-to-rod transition occurs orders of magnitude faster than the forward transition.^{2,21} In order to understand the trend in the relaxation times with increasing water content, it is important to consider the experimental results in terms of the influence of each solvent composition on the dynamics of the aggregates, and the location of each initial solvent composition within the morphological transition region (Figure 1).

Near the edge of the morphological boundary between the sphere zone and the coexistence region, all of the aggregates are spherical. Thus, when water is added quickly to the system, in order to bring it into the coexistence region of the phase diagram, the initial stages of the transition involve the adhesive collisions of spheres to form dimers, trimers etc, with very little contribution from structural rearrangement of the individual chains. This is indicated by the small contribution of the second relaxation step, relative to that of the first, to the total turbidity (i.e. A / B is large). The efficiency of adhesive collisions depends upon the repulsive interactions among the aggregates and the osmotic pressure within the gap between two aggregates. The pressure results from the presence of the concentrated PAA phase in the corona shell of the micelles. The osmotic pressure is a function of the segment charge density σ .⁴²

$$P(D \rightarrow 0) = \frac{-2\sigma kT}{zeD} \quad (3)$$

Here, D is the distance between the two spheres, k is the Boltzmann constant, T is the temperature, e is the charge of a proton, and z is the charge. Hence, the osmotic pressure in the gap is inversely proportional to the water content in the corona, since the charge density increases with water content due to the fact that altering the solvent composition

in favor of water increases the dielectric constant of the medium. An increase in the repulsive interactions between the spheres is also a consequence of the higher charge density. Thus, the efficiency of the collisions decreases with an increase in the water content, contributing to the decrease in the first relaxation time, which corresponds to the collision between spherical aggregates.

In addition to the influence the initial water content has on the interaction of the solvent molecules with the PAA blocks of the corona, it also affects the PS core of the aggregates. As the water content increases, the common solvent is gradually removed from the micellar core. This leads to an increase in the viscosity of the aggregate core. The chain mobility decreases, which slows down the rearrangement of the individual chains within a necklace, and as a result, dynamics of the flow of chains within the core of a necklace decreases. This necklace-to-rod reorganization process has a greater influence on the kinetics of the transition (i.e. A / B decreases) as the initial solvent content is increased because the rate of collisions between aggregates decreases with decreasing sphere population. As the number of collisions decreases, the contribution of τ_1 to the solution turbidity also decreases.

The distance the initial water content is away from the morphological boundary also greatly influences the kinetics of the transition. The further the system is away from the boundary between the S and S + R regions (Figure 1), the smaller the initial sphere population. This means that, statistically, there will be fewer collisions of spheres with other spheres or with other aggregates. Because of the difference in the masses between aggregates of different morphologies, the rate of necklace-necklace collisions is slower than that of sphere-necklace or sphere-sphere collisions. This also contributes to the increase in τ_1 from 25 s, in a solvent with an initial water content of 11.5 wt %, to 195 s in a system initially composed of 12.5 wt % water.

The interaction of the solvent with the copolymer chains also has an impact on the two relaxation steps involved in the transformation of rods into spheres. Since the first step involves the development of a bulb on either or both ends of a rod, the chain mobility (core viscosity) under a given set of conditions will influence the rate at which these structures grow. As a result of the decrease in the chain mobility at higher water contents, the relaxation time for bulb growth increases with water content.

The value of τ_2 reflects the change in the ratio of the sphere population to that of rods and the decrease in the size of the rods as the transition processes. Thus, the second relaxation time depends upon the rate at which the bulbs are pinched off of the intermediate dumbbell aggregates. The removal of a bulb from the intermediate dumbbell structure occurs when the contact angle between the bulb and the cylindrical body decreases to a critical value. According to the JKR theory of elastic collisions between spheres, developed by Johnson, Kendal, and Roberts, the contact angle is dependent upon the interfacial energy between the two surfaces (γ), the elastic modulus (K), and the radius of the bulb (R).^{42,43}

$$a_o = \left(\frac{12\pi R^2 \gamma}{K} \right)^{1/3} \quad (4)$$

Since the contact angle is directly proportional to the interfacial energy, the rate at which a bulb is pinched off of the dumbbell is dependent upon the change in the interfacial energy throughout the transition. This energy term is directly related to χ . At higher water contents, the interaction between the core-chains and the solvent is less favorable, thus bulb removal will occur more quickly when the transition is induced to occur in systems with lower initial water contents.

Although the solvent composition has an effect on the rod-to-sphere transition kinetics, the location of the system within the coexistence region of the phase diagram also influences the kinetics. The jump in the dioxane content of the solvent drives the morphological change from rods to spherical micelles. The closer the system is to achieving this spherical architecture, the faster the process occurs (Table 2) because the aggregates have to undergo fewer structural changes as the system approaches the sphere region. For example, when the initial solvent composition is at 13.0 wt % water, the majority of the aggregates are rods. The 0.5 wt % change in the dioxane content brings the system to a state where the aggregates are still mostly rod-like. However, applying the same water jump to a system with a 12.0 wt % water content produces an aggregate population of mostly spheres because at 12.0 wt % the rods are shorter than at higher water contents, thus fewer bulb development events must occur to convert the rods to spherical micelles.

2.3.4.2 Effect of Magnitude of Solvent Jump

The effect of changing the magnitude of the solvent jump on the rate of morphological transitions was studied by following the solution turbidity as a function of time for different amounts of added solvent, while keeping the initial polymer concentration and either the initial or the final solvent composition fixed. The size of the water jump was varied between ± 0.5 to ± 1.5 wt % because smaller changes were found to have little effect on the system, while larger jumps kinetically trap the aggregates in their original morphology.

For the sphere-to-rod transition, the initial polymer concentration was held at 1.0 wt % and the solvent composition at $t = 0$ was 12.0 wt %, which lies within the coexistence region of the morphological phase diagram. Figure 5b contains a plot of the turbidity-time profiles for various water content jumps and the relaxation times are outlined in Table 2. The results indicate that the relaxation times for the sphere-to-rod transition slightly increase with increasing jump magnitude. Since the change in the solvent composition influences the force balance governing the morphology of the aggregates, the size of the jump has an effect on the driving force for the transformation. Similarly, Robinson et al. have recently shown that the overall rate constants for the transformation of surfactant micelles to vesicles are strongly dependent upon the final salt concentration, where an increase in the salt concentration provides a greater driving force for the transition.⁴⁷ It was found that the larger the salt jump, the greater the tendency to form vesicles. This was attributed to the fact that an increase in the salt concentration reduces the free energy barrier for the transformation. Thus, in the case of the sphere-to-rod transition, the relaxation times decrease with increasing degree of perturbation due, in part, to a decrease in the morphological free energy barrier.

Altering the degree of the external perturbation to the system also influences how far away the final state of the system is from equilibrium conditions. Since, the initial solvent composition is within the transition region, the larger the jump in the water content, the closer the system approaches the boundary for the existence of equilibrium rods. Hence, the closer the final water content is to the phase boundary, the faster the transition occurs because only a small degree of structural change is required to reach these conditions.

The rate at which rods breakdown to form spheres, unlike that for the formation of rods from spheres, has been found to slightly increase with the degree of perturbation imposed upon the system (Figure 6b). However, in this case, instead of maintaining a constant initial solvent composition, the final solvent composition was fixed while varying the size of the jump in the dioxane content. The final solvent composition of 12.0 wt % H₂O is located in the transition region and the aggregates are a mixture of spheres and rods. Although increasing the solvent jump increases the perturbation to the force balance controlling the morphology of the aggregates, the position of the initial solvent composition has more of an influence on the kinetics of the transition since the final solvent composition resides within the transition region. At 13.5 wt % H₂O, the system is deep in the rod region and at 13.0 wt % H₂O it is located at the boundary between the S+R and R regions, thus of the aggregates are all rod-like in both cases. However, at 12.5 wt % H₂O the system is in the transition region and the aggregate population is a mixture of spheres and rods. Therefore, the relaxation times increase with increasing water content because the aggregates must undergo more structural changes in order to resemble the system at 12.0 wt % H₂O the further the initial conditions locate the system within the rod region. Similar trends were observed in the relaxation times for the vesicle-to-rod and rod-to-vesicle transitions, but unlike the sphere-to-rod and reverse transitions, the relaxation times for the forward and reverse processes are very different.²²

2.3.4.3 Effect of Initial Polymer Concentration

Another one of the factors believed to have an influence on the kinetics of the morphological transitions under investigation, is the initial polymer concentration, not only because it effects the total aggregate population, but also because it alters the position of the phase boundaries. In order to study this effect on the kinetics, a 0.5 wt % solvent jump is imposed upon a series of solutions with different initial polymer composition ranging from 0.1 to 2.0 wt %, but with a constant initial water content of 11.5 wt % for the sphere-to-rod transitions and 12.0 wt % for the rod-to-sphere transition.

Figure 5c shows the turbidity versus time for three aggregate systems with different polymer concentrations that have been induced to undergo the sphere-to-rod transition. The data contained in Table 1 indicates that the rate of the transition is highly

dependent upon the initial polymer concentration and increases with increasing concentration. In fact, the transition occurs so rapidly at higher polymer concentrations that only one relaxation time is observed. One of the reasons for this phenomenon is that the total number of block copolymer aggregates increases with polymer concentration. This leads to a higher frequency of aggregate collisions. Since this process is thought to correspond to the first relaxation time in the sphere-to-rod transition kinetics, it is not surprising that experimental limitations prevent us from obtaining a value for τ_1 at higher polymer concentrations.

The more prominent factor governing the effect of polymer concentration on transition kinetics is the initial location of the system, at a given concentration, within the morphological phase diagram. At 1.0 wt % PS-b-PAA, the system is located at the boundary between the S and S+R regions. However, for a solution of 0.1 wt % polymer, the initial solvent composition of 11.5 wt % H₂O places the aggregates more deeply within the sphere region, while for the same solvent composition, the system lies within the transition region at a polymer concentration of 2.0 wt %. Hence, since the final state of the system, after the 0.5 wt % jump in the water content, for each polymer concentration, lies in different regions of the phase diagram with respect to the morphological boundaries (Figure 1), the location of the initial state of the system within the phase diagram influences how quickly the transition occurs. In the case of the 2.0 wt % polymer system, the initial conditions place it closer to the boundary between the S + R and R regions (Figure 1). Thus, the system is driven to reach the rod region more quickly because the aggregates have to undergo fewer architectural changes in order to reach the desired state. However, the initial and final states of the 0.1 wt % polymer system are located entirely within the sphere region. The kinetics is slower because the aggregates start out in equilibrium and water content jump only causes them to increase in diameter. It should be noted that there is still some uncertainty as to why two relaxation times are obtained for this process.

The rate of the reverse process is also influenced by the polymer concentration (Figure 6c). However, the nature of this effect is more complex. At lower polymer concentrations, two relaxation times are observed, which increase with increasing polymer concentration. When the polymer concentration is raised to 2.0 wt % the kinetics

shows a single relaxation time, which is smaller than the τ_2 value obtained for the kinetics of the systems with lower polymer concentrations. No logical explanation has emerged for these results. Hence, further investigation is warranted in this case.

2.4 Conclusions

An investigation of the kinetics and mechanism of the sphere-to-rod and rod-to-sphere transitions that occur in aggregates prepared from PS₃₁₀-b-PAA₅₂, in dioxane-water mixtures, has been completed. A sudden jump in the content of one of the solvent components was used to induce the transitions. The solution turbidity was monitored as a function of time during the transition, and the results were fitted to appropriate exponential equations. It was concluded that the transitions proceed via two relaxation steps. The relaxation time for each step was obtained from the turbidity-time profiles. The relaxation times for both the forward and reverse transitions are found to be comparable to each other, in contrast to those of the rod-to-vesicle transition and the reverse process where the forward transition is orders of magnitude slower than the backward transition.^{2,22} The kinetics associated with both morphological transitions was found to be influenced by the initial solvent composition, the magnitude of the solvent jump, and the initial polymer concentration. The initial conditions of the system, with respect their location within the morphological phase diagram, play a major role in determining how the transition kinetics are affected by a change in anyone of these parameters.

The transition mechanisms were determined from transmission electron microscopy studies. The transformation of spherical aggregates to rod-like structures occurs through the adhesive collisions of spherical micelles to form intermediate “pearl necklace” structures. The necklaces then reorganize, during the rate-limiting step, to produce a smooth rod. The reverse transition also proceeds via a two-step mechanism. In this case, a bulb develops on either or both ends of a rod. The rate-determining step involves the removal of the bulbs from the cylindrical body. This study represents the first attempt to determine the kinetics and mechanism of the transformation of spherical block copolymer aggregates into rod-like structures and the backward conversion of rods to spherical micelles in solution.

This report represents the first study of the kinetics and mechanisms of both the forward and reverse processes involved in the transition from one block copolymer aggregate morphology to another. In order to expand our knowledge of this subject area, a study of the kinetics and mechanism of the vesicle-to-rod transition was carried out and the results are reported in the next chapter. This morphological transformation is the reverse of the rod-to-vesicle transition investigated by Chen et al.² Thus, the study of the vesicle-to-rod transition completes the characterization of the conversion between rods and vesicles and increases our understanding of how to manipulate the architecture of the PS-b-PAA aggregates in solution.

2.5 References

1. Shen, H.; Eisenberg, A. *J. Phys. Chem. B* **1999**, *103*, 9473.
2. Chen, L.; Shen, H.; Eisenberg, A. *J. Phys. Chem. B* **1999**, *103*, 9488.
3. Tuzar, Z.; Kratochvil, P. *Adv. Colloid Interface Sci.* **1976**, *6*, 201.
4. Price, C. In *Developments in Block Copolymers*; Goodman, I., Ed.; Applied Science Publishers: London, 1982; Vol. 1, p 39.
5. a) Riess, G; Hurtrez, G; Bahadur, P. *Encyclopedia of Polymer Science and Engineering*, 2nd ed.; Wiley: New York, 1985; Vol. 2, p 324. b) Selb, J.; Gallot, Y. In *Developments in Block Copolymers*; Goodman, I., Ed.; Applied Science Publishers: London, 1985; Vol. 2, p 27. c) Brown, R. A.; Masters, A. J.; Price, C.; Yuan, X. F. In *Comprehensive Polymer Science: Polymer Properties* Allen, S. G., Bevington, J. C., Booth, C., Price, C., Eds.; Pergamon Press: Oxford, 1989; Vol.2, p 155.
6. deGennes, P. G. In *Solid State Physics*; Liebert, L., Ed.; Academic Press: New York, 1978; Supplement 14, p 1.
7. Halperin, A.; Tirrell, M.; Lodge, T. P. *Adv. Polym. Sci.* **1992**, *100*, 31.
8. a) Stigter, D. Hydration, Shape, and Change of Micelles of Sodium Dodecyl Sulfate and Dodecyl Ammonium Chloride. In *Chemistry, Physics, and Application of Surface Active Substances*; Overbeek, J. T. G., Ed.; Gordon and Breach, Science Publishers: New York, 1967; Vol. 2, pp 507-518. b) Missell, P. J., Mazer, N. A., Carey, M. C., Benedek, G. B. Thermodynamics of the Sphere-to-Rod Transition in Alkyl Sulfate Micelles. In *Solution Behavior of Surfactants: Theoretical and Applied Aspects*; Mittal, K. L., Fendler, E. J., Eds.; Plenum Press: New York, 1980; Vol. 1, pp 373-388.
9. a) Isrealachvili, J. N. Aggregation of Amphiphilic Molecules into Micelles, Bilayers, Vesicles, and Biological Membranes. In *Intermolecular and Surface Forces*; Academic Press: London, 1985; Chapter 16. b) Porte, G. Micellar Growth,

Flexibility and Polymorphism in Dilute Solutions. In *Micelles, Membranes, Microemulsions, and Monolayers*; Gelbart, W. M., Ben-Shaul, A., Roux, D., Eds.; Springer-Verlag: New York, 1994; Chapter 2.

10. a) Zhang, L.; Eisenberg, A. *Science* **1995**, 268, 1728. b) Zhang, L.; Eisenberg, A. *J. Am. Chem. Soc.* **1996**, 118, 3168.
11. a) Discher, B. M.; Won, Y.-Y.; Ege, D. S.; Lee, J. C.-M.; Bates, F. S.; Discher, D. E.; Hammer, D. A. *Science* **1999**, 284, 1143. b) Procházka, K.; Martin, T. J.; Webber, S. E.; Munk, P. *Macromolecules* **1996**, 29, 6526.
12. a) Antonietti, M.; Heinz, S.; Schmidt, M.; Rosenauer, C. *Macromolecules* **1994**, 27, 3276. b) Förster, S.; Antonietti, M. *Adv. Mater.* **1998**, 10, 195.
13. Shen, H.; Zhang, L.; Eisenberg, A. *J. Phys. Chem. B* **1997**, 24, 4697.
14. Zhang, L.; Eisenberg, A. *Macromolecules* **1999**, 32, 2239.
15. Shen, H.; Eisenberg, A. *Macromolecules* **2000**, 33, 2561.
16. a) Yu, K.; Zhang, L.; Eisenberg, A. *Langmuir* **1996**, 12, 5980. b) Svensson, M.; Alexandridis, P.; Linse, P. *Macromolecules* **1999**, 32, 5435. c) Svensson, B.; Olsson, U.; Alexandridis, P. *Langmuir* **2000**, 16, 6839.
17. a) Yu, Y.; Eisenberg, A. *J. Am. Chem. Soc.* **1997**, 119, 8383. b) Rheingans, O.; Hugenberg, N.; Harris, J. R.; Fischer, K.; Maskos, M. *Macromolecules* **2000**, 33, 4780. c) Liang, Y.-Z.; Li, Z.-C.; Li, F.-M. *Chem. Lett.* **2000**, 4, 320.
18. a) Desbaumes, L.; Eisenberg, A. *Langmuir* **1999**, 15, 36. b) Mortensen, K.; Pedersen, J. S. *Macromolecules* **1993**, 26, 805. c) Schillén, K.; Brown, W.; Johnsen, M. *Macromolecules* **1994**, 27, 4825.
19. a) Zhang, L.; Yu, K.; Eisenberg, A. *Langmuir* **1996**, 272, 1777. b) Zhang, L.; Shen, H.; Eisenberg, A. *Macromolecules* **1997**, 30, 1001. c) Shen, H.; Zhang, L.; Eisenberg, A. *J. Am. Chem. Soc.* **1999**, 12, 2728. d) Talingting, M. R.; Munk, P.; Webber, S. E. Tuzar, Z. *Macromolecules* **1999**, 32, 1593. e) Jørgeseb, E. B.; Hvidt, S.; Brown, W.; Schillén, K. *Macromolecules* **1997**, 30, 2355. f) Kabanov, A.; Bronich, T. K.; Kabanov, V. A.; Eisenberg, A. *J. Am. Chem. Soc.* **1998**, 120, 9941. g) Zheng, Y.; Davis, H. T. *Langmuir* **2000**, 16, 6453.
20. a) Liu, G. *Curr. Opin. Colloid Interface Sci.* **1998**, 3, 200. b) Resendes, R.; Massey, J. A.; Dorn, H.; Power, K. N.; Winnik, M. A.; Manners, I. *Angew. Chem. Int. Ed. Engl.* **1999**, 38, 2570. c) Nagarajan, R. *Colloids Surf., B* **1999**, 16, 55. d) Zipfel, J.; Lindner, P.; Tsianou, M.; Alexandridis, P.; Richtering, W. *Langmuir* **1999**, 15, 2599. e) Hajduk, D. A.; Kossuth, M. B.; Hillmyer, M. A.; Bates, F. S. *J. Phys. Chem. B* **1998**, 102, 4269.
21. Burke, S.; Eisenberg, A. submitted to *Polymer*
22. Lehner, D.; Lindner, H.; Glatter, O. *Langmuir* **2000**, 16, 1689.
23. Alexandridis, P.; Athanassiou, V.; Hatton, T. A. *Langmuir* **1995**, 11, 2442.
24. Lang, J.; Tondre, C.; Zana, R.; Bauer, R.; Hoffmann, H.; Ulbricht, W. *J. Phys. Chem.* **1975**, 79, 276.

25. Aniansson, E. A. G.; Wall, S. *J. Phys. Chem.* **1974**, *78*, 1024.
26. Aniansson, E. A. G.; Wall, S. N.; Almgren, M.; Hoffman, H.; Kielmann, I.; Ulbricht, W.; Zana, R.; Lang, J.; Tondre, C. *J. Phys. Chem.* **1976**, *80*, 905.
27. Lang, J.; Zana, R. In *Surfactant Solutions: New Methods of Investigation*; Zana, R., Ed.; Surfactant Science Series 22; Marcel Dekker: New York, 1987; pp 414-422.
28. Bednár, B.; Edwards, K.; Almgren, M.; Tormod, S.; Tuzar, Z. *Macromol. Chem. Rapid Commun.* **1988**, *9*, 785.
29. Honda, C.; Hasegawa, Y.; Hirunuma, R.; Nose, T. *Macromolecules* **1994**, *26*, 7660.
30. Hecht, E.; Hoffmann, H. *Colloids Surf., A.* **1995**, *96*, 181.
31. Egelhaff, S. U. *Curr. Opin. Colloid Interface Sci.* **1998**, *3*, 608.
32. a) Michels, B.; Waton, G. *J. Phys. Chem. B* **2000**, *104*, 228. b) Campbell, S. E.; Yang, H.; Patel, R.; Friberg, S. E.; Aikens, P. A. *Colloid Polym. Sci.* **1997**, *275*, 303. c) O'Connor, A. J.; Hatton, T. A.; Bose, A. *Langmuir* **1997**, *13*, 6931. d) Friberg, S. E.; Campbell, S.; Fei, L.; Yang, H.; Patel, R. *Langmuir* **1998**, *14*, 590. e) Campbell, S. E.; Zhang, Z.; Friberg, S. E.; Patel, R. *Langmuir* **1998**, *14*, 590.
33. Brinkmann, U.; Neumann, E.; Robinson, B. H. *J. Chem. Soc. Faraday Trans.* **1998**, *94*, 1281.
34. a) Harada, S.; Fujita, N.; Sano, T. *J. Am. Chem. Soc.* **1988**, *110*, 8710. b) Michels, B.; Waton, G. *J. Phys. Chem. B* **2000**, *104*, 228.
35. a) Köberl, M.; Hinz, H.-J.; Rappolt, M.; Rapp, G. *Phys. Chem. Chem. Phys.* **1997**, *101*, 789. b) Quinn, P. *J. Appl. Cyst.* **1997**, *30*, 733.
36. a) Lee, J. K.; Lentz, B. R. *Biochemistry* **1997**, *36*, 6251. b) Minami, H.; Inoue, T.; Shimozawa, R. *Langmuir* **1996**, *12*, 3574.
37. Iyama, K.; Nose, T. *Macromolecules* **1998**, *31*, 7356.
38. a) Zhong, Z. F.; Varshney, S. K.; Eisenberg, A. *Macromolecules* **1992**, *25*, 7160. b) Hautekeer, J. P.; Varshney, S. K.; Fayt, R.; Jacobs, C.; Jerome, R.; Teyssie, P. *Macromolecules* **1990**, *23*, 3893.
39. a) Brock, J. R. *J. Colloid Sci.* **1972**, *39*, 32. b) Gelbard, F.; Seinfeld, J. H. *J. Colloid Interface Sci.* **1979**, *68*, 173. c) Simons, S. *Phys. Lett. A* **1982**, *91*, 260.
40. Medalia, A. I. In *Surface and Colloid Science*; Matijevic, E., Ed.; Wiley-Interscience: New York, 1971; Vol. 4, p 68.
41. a) Samsel, R. W.; Perelson, A. S. *Biophys. J.* **1982**, *37*, 493. b) Perelson, A. S.; Wiegel, F. W. *Biophys. J.* **1982**, *37*, 515.
42. Isrealachvili, J. N. Adhsions. In *Intermolecular and Surface Forces* 2nd ed.; Academic Press: London, 1992; Chapter 15.
43. Johnson, K. L.; Kendall, K.; Roberts, A. D. *Proc. R. Soc. London, Ser. A* **1971**, *324*, 301.

44. Farquhar, K. D.; Misran, M.; Robinson, B. H.; Steytler, D. C.; Morini, P.; Garrett, P. R.; Holzwarth, J. F. *J. Phys.: Condens. Matter* **1996**, 8, 9397.

Chapter 3

Kinetic and Mechanistic Details of the Vesicle-to-Rod Transition in Aggregates of PS₃₁₀-b-PAA₅₂ in Dioxane-Water Mixtures

The kinetic and mechanistic study described in the previous chapter, which described the sphere-to-rod and rod-to-sphere transitions in PS-b-PAA aggregates, is the first of its kind to report on both the forward and reverse processes of a transition from one block copolymer aggregate morphology to another. It was previously shown by Shen and Eisenberg that the spheres, rods, and vesicles formed in the PS₃₁₀-b-PAA₅₂ / dioxane / water system under investigation are equilibrium structures and that the transition from one architecture to another is completely reversible. Hence, it is equally important to examine the properties of the morphological transitions in both directions. In keeping with this belief, this chapter describes the kinetics and mechanism of the vesicle-to-rod transition, which is a continuation of the study of the rod-to-vesicle transition previously carried out by Chen et al. For comparison sake, the investigation was conducted in a parallel manner to that of Chen et al. The transition was brought about by a sudden jump in the solvent composition, while the kinetics was examined as a function of the initial solvent composition, the magnitude of the solvent jump, and the polymer concentration. Thus, the study of the vesicle-to-rod transition completes the characterization of the conversion between rods and vesicles and increases our understanding of how to manipulate the architecture of the PS-b-PAA aggregates in solution.

3.1 Introduction

Asymmetric, amphiphilic, block copolymers form a variety of self-assembled structures in solution. The properties of these aggregates, both under equilibrium conditions and after quenching, have been extensively investigated.¹⁻⁸ Block copolymer aggregates are most commonly spherical in shape. Micelles with a core radius that is much smaller than the cross-sectional area of the corona are referred to as star-like. De Gennes predicted that it should be possible to form micelles with a larger core radius relative to the length of the corona.⁹ Halperin et al. were the first to use the phrase “crew-cut” to describe these aggregates.¹⁰ For block copolymers, in general, their ability to form aggregates in solution has prompted several attempts to characterize the self-assembly process in such systems. It has been shown that block copolymer micelles, as in the case of small molecule surfactants, are formed through a step-wise association.¹¹⁻¹⁵ The mechanism of block copolymer self-assembly involves two steps and is similar to that proposed by Aniansson and Wall to describe micelle formation from surfactant molecules.¹⁶ The first step involves the fast exchange of the copolymer chains between the micelles and the bulk solution. The rate-determining process includes a series of step-wise events during which copolymer molecules associate with or dissociate from the micelles.

Zhang and Eisenberg showed that crew-cut aggregates of a range of morphologies are obtained in solution from one block copolymer family.¹⁷ This is also observed for a single block copolymer.¹⁸ The materials that were used include asymmetric polystyrene-b-poly(acrylic acid) (PS-b-PAA) and polystyrene-b-poly(ethylene oxide) copolymers.¹⁷⁻²² Several other block copolymers have been found to self-assemble into aggregates of multiple morphologies.²³⁻³² Block copolymer aggregates with different architectures have been prepared from a single polymer in solution by altering such factors as the solvent composition³⁴, the relative block lengths³⁵, the temperature³⁶, and the presence of additives³⁷. These tunable parameters have an influence on the size and shape of the aggregates because they affect the balance between three of the major forces acting on the system. These include the stretching of the core-forming blocks, the inter-corona interactions, and the interfacial energy between the solvent and the micellar core. This

force balance has a strong influence on the thermodynamics governing the equilibrium morphology of these aggregates.^{20,38-40}

A continual increase in the perturbation imposed upon the system leads to a progressive change in both the size and shape of the block copolymer aggregates. Shen and Eisenberg have prepared a morphological phase diagram for the ternary system PS₃₁₀-b-PAA₅₂ / dioxane / water.¹⁸ They have shown that a gradual increase in the water content of the solvent mixture transports the aggregates from a region of purely spherical micelles to a solvent composition region where spheres coexist in equilibrium with rods, to a region where only rods exist. This is followed by a region of rod and vesicle coexistence, and then finally to a region where all of the aggregates are converted to vesicles. They have also proven that the morphological transitions are reversible by decreasing and subsequently increasing the dioxane content.¹⁸

The conversion of vesicles to rods is the topic of the present study. In order to understand why this phenomenon occurs, it is important to consider the factors that are involved in the stabilization of vesicular structures. Although the equilibrium nature of polymer vesicles is a controversial subject, Shen and Eisenberg proposed that PS₃₁₀-b-PAA₅₂ vesicles are under equilibrium control within a water content range of 28.0 to 40.0 wt %.¹⁸ Since the stability of the vesicles is dependent upon the degree of stabilization of the curvature on either side of the bilayer, they predicted that the differential pressure that maintains the curvature is balanced, as the water content is increased, by the segregation of the polydisperse corona chains within the bilayer, with the long chains on the outside and the shorter chains on the inside. Recently, this hypothesis of Shen and Eisenberg was confirmed.⁴¹ It was shown that the copolymer molecules with shorter hydrophilic block lengths do indeed segregate to the inside of the vesicle, while chains with longer hydrophilic blocks are located in the outer layer of the vesicle. This distribution of chain lengths increases the corona repulsion on the outside of the vesicles relative to that on the inside; therefore, chain segregation results in thermodynamic stabilization of the curvature.

Disturbing the equilibrium stabilization mechanism of vesicular aggregates leads to structural transformations. Although this phenomenon has been observed for vesicles formed from block copolymers^{18,20,42-44}, as well as other colloidal systems⁴⁵⁻⁵³, the

mechanistic details involved in the structural transition have only been thoroughly investigated for lipid and double-chain surfactant vesicles.⁴⁵⁻⁵³ In both of these cases, the vesicles are most commonly transformed into spherical micelles. The vesicle-to-micelle transformation induced by the addition of micelle-forming surfactants (e.g., octylglucoside, sodium cholate, C₁₂E₈, Triton X-100, hexadecyltrimethylammonium chloride, and sodium alkyl sulfates) to vesicles composed of phospholipids such as egg yolk lecithin and dipalmitoylphosphatidylcholine progress through a series of lipid-surfactant mixed assemblies formed at different molar ratios of surfactant to lipid.⁴⁵⁻⁵⁰ However, the pathway (i.e. intermediate aggregate structures) for the transition can be very different in each case. For example, with large uniform vesicles of egg lecithin, the successive addition of octylglucoside causes the breakdown of the vesicles to elongated tubules and small vesicles, then to open vesicles and long cylindrical aggregates, and finally to spherical micelles.⁴⁶ The use of sodium cholate to induce the vesicle-to-micelle transition in egg lecithin aggregates causes the transition to proceed through the formation of open vesicles, which are then transformed to bilayer sheets. The sheets are then converted to cylindrical aggregates, and the further addition of surfactant leads to the formation of spherical micelles.⁴⁹ It must be noted that cylindrical aggregates have never been observed as intermediate structures during the vesicle-to-micelle transition induced by the addition of single-chain surfactants to solutions of vesicles formed from double-chain surfactants.⁵¹⁻⁵³ Instead, small vesicles, broken vesicles, large multi-layer lamellae vesicles, bilayer sheets, and small discs have been observed in these cases.

Despite the existence of numerous reports regarding the mechanism of vesicle breakdown in different colloidal systems, few studies address the kinetics associated with these structural transitions. Farquhar et al. investigated the kinetics and mechanism of the breakdown of sodium 6-phenyltridecane sulfonate vesicles, in aqueous sodium chloride solutions, by rapid mixing of the surfactant system with a salt solution that is injected using a stop-flow device equipped with ultraviolet-visible detection.⁵¹ The transition occurs within a time range of 0.1 to 10 s and involves a three-step mechanism. The vesicles are first transformed into unstable bilayer structures in the slow step. The bilayers are quickly converted into smaller disc aggregates, which rapidly dissociate to individual surfactant molecules. Brinkmann et al. used the same procedure to study the

vesicle-to-micelle transition in sodium 6-phenyltridecane sulfate aggregates, in aqueous sodium chloride solutions, induced by the addition of sodium dodecyl sulfate (SDS).⁵³ The structural transformation involves first order kinetics and proceeds through a phase in which the SDS molecules interact with the vesicles. The rate constant is strongly dependent upon the concentration of SDS, decreasing from $k_{\text{exp}} = 0.090 \text{ s}^{-1}$ at 0.65 mM SDS to $k_{\text{exp}} = 0.023 \text{ s}^{-1}$ at 0.55 mM SDS.

There have been a few studies of the kinetics of morphological transitions in block copolymer aggregates, but only one of these studies involved vesicular structures.⁵⁴⁻⁵⁶ Chen et al. investigated the kinetics and mechanism of the rod-to-vesicle transition occurring in aggregates formed from PS₃₁₀-b-PAA₅₂ in dioxane-water mixtures.⁵⁵ The transition was induced with a jump in the water content of the solvent mixture. The kinetics was followed by measuring the solution turbidity as a function of time, and the intermediate aggregates were monitored with transmission electron microscopy. Near the morphological phase boundary, the rods become shorter and plumper, and vesicles start to appear in the solution. An increase in the water content increases the population of vesicles at the expense of the rod population. The transition mechanism is believed to involve two steps. During the fast step, the short rods are flattened forming irregular or circular bowl-shaped lamellae. The slow process is the closure of the bowl-shaped lamellae to produce vesicles. The two relaxation times have been found to depend on both the initial water content and the polymer concentration, increasing with an increase in either parameter. However, the size of the water jump is found to have little influence on the transition kinetics.⁵⁵

Here, we extend the study of Chen et al. with an investigation of the kinetics and mechanism of the vesicle-to-rod transition in aggregates prepared from PS₃₁₀-b-PAA₅₂ in dioxane-water mixtures. The morphological transformation is brought about by a sudden jump in the dioxane content of the solvent mixture near the boundary between the vesicle and vesicle-rod regions of the phase diagram. Turbidity measurements are used to follow the transition kinetics as a function of time. The intermediate aggregates are isolated by dropping the solution temperature to near that of liquid nitrogen, followed by gradually warming under vacuum to freeze-dry the aggregates, which are subsequently observed using transmission electron microscopy. The kinetics is investigated as a function of the

initial water content, the magnitude of the dioxane jump, and the initial polymer concentration. The results are compared with those obtained for the rod-to-vesicle transition.⁵⁵

3.2 Experimental

The block copolymer employed in this study is a polystyrene-*b*-poly(acrylic acid) [PS-*b*-PAA] sample that contains 310 PS and 52 PAA repeat units and has a polydispersity of 1.05.⁴⁰ The polymer was prepared by sequential anionic polymerization; the details of this procedure were outlined in previous publications.^{57,58} The copolymer sample was fractionated, using a standard procedure, to remove any homopolymer.¹⁸ This fractionation process first involved the conversion of the acrylic acid blocks to sodium acrylate with the addition of sodium hydroxide to a solution of the copolymer in THF. This led to the self-assembly of the copolymer molecules into reverse micelles with a poly(sodium acrylate) core. The addition of water to the solution resulted in phase separation. The upper solution contained the homopolymer, and the above process was repeated several times until homopolymer was not detected, by gel permeation chromatography, in the reverse micelle phase. The sodium acrylate blocks were converted back to the acrylic acid form upon treatment with hydrochloric acid and then precipitated from solution and dried under vacuum.

Aggregates with a particular morphology were prepared by first dissolving the copolymer in dioxane, which is a solvent favorable for both blocks. The copolymer molecules were driven to self-assemble with the slow addition of water to the system at a rate of 0.2 wt % per minute. The appearance of a blue tint in the solution indicated the formation of micelles. The water addition was continued until the desired solvent composition was reached.

For the study of solution turbidity as a function of polymer concentration, water was added to a solution of the polymer dissolved in dioxane until the solvent was composed of 40.0 wt % water. This solution was placed in a dialysis bag (Spectra/Por) with a molecular cut-off of 50 000 g/mol and dialyzed against distilled water for 4 days in order to remove the dioxane. The morphology of the aggregates was kinetically frozen as a result of the dialysis process. The stock solution, after dialysis, had a concentration of

3.44 wt % polymer. Several other samples with varying polymer concentration were prepared by diluting the stock solution with water. The solution turbidity was measured at 650 nm using a Varian Cary 50 spectrometer. The measurements were taken at room temperature.

The morphological transition was induced by the quick addition of dioxane to the system. A change in the size and shape of the aggregates resulted in a change in the turbidity of the solution. The kinetics of the transition was monitored by following the optical density of the transmitted light (180°) as a function of time at 650 nm and at room temperature.

Transmission electron microscopy (TEM) was performed using a Phillips EM400 microscope operating at an acceleration voltage of 80 kV. The EM copper grids used to mount the sample were first coated with a thin film of poly(vinyl formal) (JB EM Services Inc.) and one of carbon. The grids were placed on a metal block, which was kept in thermal equilibrium with liquid nitrogen. A drop of the polymer solution was deposited onto the cold grids at various time points throughout the morphological transition. The samples were then dried under vacuum for 24 hours. Some of the sample grids were shadowed with a palladium/platinum alloy at an angle of ca. 36° so that details about the height of the aggregates could be obtained. The dimensions of the aggregates were determined from the TEM negatives using a calibration map prepared from measurements taken of PS latex standards.²⁰

3.3 Results and Discussion

3.3.1 Transition Region and Aggregate Dimensions

Chen et al. have indicated in their study of the rod-to-vesicle transition that the major part of this transformation occurs above a water content of ca. 26.0 wt % and that only vesicles are observed above a water content of 27.6 wt %.¹⁸ They consider the water content range of 25.9 to 27.6 wt % to be the transition zone at a polymer concentration of 1.0 wt %. At the beginning of the transition region very few (ca. < 5 %) of the aggregates are present as vesicles. The location of these boundaries shifts to solvent compositions with smaller water content as the polymer concentration is increased. Shen and Eisenberg have shown that approaching the transition region from the vesicle side by adding

dioxane to the system results in a decrease in both the mean diameter and the wall thickness of the vesicles.⁴¹ For example, at a solvent composition of 28.0 wt % H₂O the vesicles have a mean diameter of 87.6 ± 2.3 nm when the polymer concentration is 1.26 wt %; this value changes to 84.3 ± 1.9 nm when the polymer concentration is reduced to 0.72 wt %. When the solvent composition is 40 wt % in water, the mean vesicle diameter is 96.7 ± 2.7 and 90.2 ± 2.1 nm at polymer concentrations of 1.80 and 0.60 wt % respectively. It must also be noted that an approach to the transition region from the rod zone leads to a decrease in the length and an increase in the diameter of the rods. At the boundary between the rod and the transition region, the average length of a rod is ca. 400 nm and a diameter of ca. 20 nm.⁵⁵

It has previously been shown that these dimensional changes are reflected in the solution turbidity, with the turbidity increasing as the aggregates, of a given morphology, grow in size.²⁰ However, the concentration of the aggregates also affects the solution turbidity. Figure 1 contains a plot of concentration dependence of the solution turbidity for vesicular aggregates. The vesicles were prepared in a mixture of 30.0 wt % H₂O-70.0 wt % dioxane, but the solution was quenched in water and then dialyzed against water to remove the dioxane. This kinetically trapped the aggregates so that they remained as vesicles when the solution was diluted. The plot indicates that there is a linear dependence of turbidity of vesicles on polymer concentration below ca. 1.0 wt % polymer. The turbidity-concentration curve for rods is also linear in the concentration range covered in this investigation.⁵⁶ These studies were carried out for aggregates with a given size. However, this behavior is also expected for aggregates of different sizes since the size differences are compared on such a small scale. As well, the linear dependence of turbidity on polymer concentration in water should also be observed in water-dioxane mixtures because of the similarity of the refractive index of the two media.

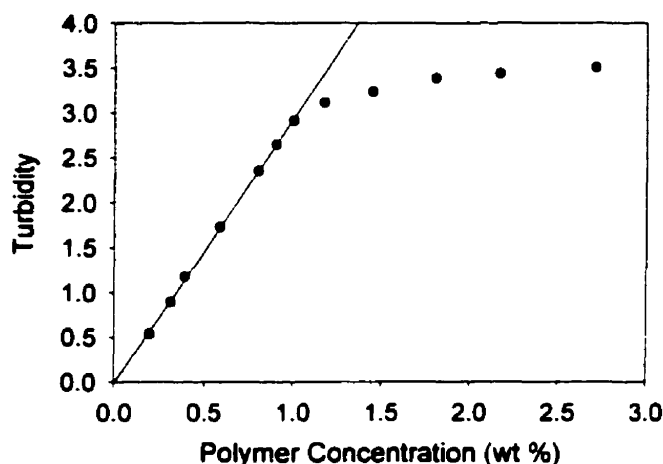


Figure 1: Dependence of the solution turbidity on the polymer concentration for vesicular aggregates in water. The line illustrates the linear fit at lower concentrations. (error in turbidity of ± 0.01 units)

3.3.2 Interpretation of Dimensional and Structural Changes

The structure of PS₃₁₀-b-PAA₅₂ aggregates is affected by the interfacial energy between the aggregate core and the solvent, the repulsive interactions among the corona chains, and the core-chain stretching. It is the balance between these forces that dictates the morphology of the aggregates under a given set of conditions. Perturbing the system with a sudden change in the solvent composition alters this equilibrium between the three forces, leading to morphological change.^{20,37-39}

The stability of vesicles prepared from block copolymers, like those composed of lipids or other small amphiphiles, is dependent on the curvature energy.⁵⁹ The degree of curvature is determined by the force balance governing the aggregates.⁴¹ Hence, the stability of the vesicles is influenced by the solvent composition of the system. Increasing the dioxane content of the solvent decreases the stretching of the PS blocks in the core of the bilayer and also decreases the repulsive interactions among the corona chains, which leads to a reduction in the interfacial energy between the core and the solvent. These favorable energy changes contribute to a reduction in the mean diameter of the aggregates. However, there is only a slight decrease in the thickness of the bilayer. In order to compensate for this imbalance in the dimensional changes, the degree of vesicle

curvature increases. The resulting rise in the curvature energy makes the vesicles unstable; therefore, they change their morphology in order to relieve this strain.

3.3.3 Mechanism of Morphological Change

The images obtained from the TEM studies suggest that the vesicle-to-rod transition proceeds through a complex, multi-step mechanism. Figure 2 contains a series of micrographs corresponding to the structural changes that occur during the jump from 29.0 to 26.4 wt % H₂O in a solution with an initial polymer concentration of 1.0 wt %. The beginning stages of the structural transformation involve a reduction in the mean vesicle diameter of the polydisperse sample and the reorganization of the vesicular structures yielding bowtie shaped (two connected spheres) aggregates. Some of the samples (not shown) were shadowed with a Pt/Pd alloy in order to get an indication of the thickness of these aggregates. It is concluded from this study that the bowties are not bilayer structures. The volume of a bowtie (V_b) is approximately equal to that of a vesicle (V_v) ($V_b = 5.1 \pm 0.7 \times 10^5 \text{ nm}^3$, $V_v = 5.4 \pm 0.5 \times 10^5 \text{ nm}^3$), although the size distribution of both populations is quite broad. It is not likely that the bowtie aggregates directly result from the collapse of vesicles. One might speculate that the bowties are actually two small adjoining vesicles; however, a core has ever been observed in these aggregates. If one did exist, it is estimated, from volume calculations (assuming the wall thickness remains the same), to be approximately 20 nm, which would certainly be observable with transmission electron microscopy. Considering that the aggregates are seen only in two-dimensions and that the sample handling procedure prevents us from obtaining micrographs of the first few seconds of the transition, it is likely that there is another intermediate aggregate morphology that appears prior to the bowtie structure. As the transition progresses, the bowties begin to elongate into aggregates resembling dumbbells. The long axis of these aggregates lengthens at the expense of the size of the bulbs on either end. The final rods are ca. 300 nm in length and have a diameter of 25 nm. The vesicles, rods, and intermediate structures are all of similar volume; thus, it is concluded that one vesicle is converted to one rod or vice-versa, as is the case for the rod-to-vesicle transition.

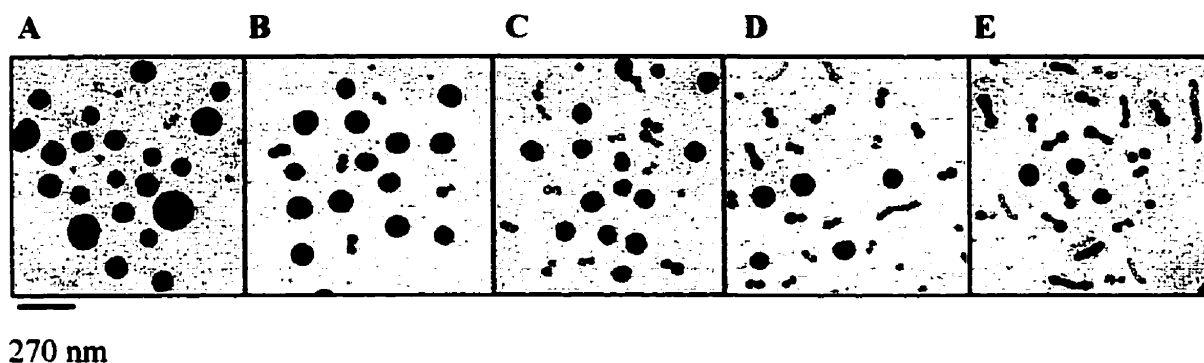


Figure 2: Micrographs of the aggregate morphologies at various time points during the transition from 29.0 to 26.4 wt % H₂O in a 1.0 wt % PS₃₁₀-b-PAA₅₂ solution. (A: 0s, B: 5s, C: 11s, D: 17s, E: 25s).

3.3.4 Transition Kinetics

The kinetics of structural transitions in colloidal aggregate systems have most often been studied using relaxation methods utilizing temperature, concentration, and pressure jump techniques.^{51-55,60} In this particular study, a jump in the dioxane content of the dioxane-water solvent system is employed to induce the vesicle-to-rod transition in aggregates of PS₃₁₀-b-PAA₅₂. The transformation is followed by monitoring the solution turbidity as a function of time because the turbidity has been shown to be sensitive to changes in the size and shape of the aggregates.²⁰

All of the turbidity curves associated with this transition have been found to fit best to a single exponential equation.

$$Y = C + Ae^{-t/\tau} \quad (1)$$

Here, Y is the turbidity, C and A are adjustable parameters, t is the time, and τ is the relaxation time. It is interesting to note that the value of C is equal to the turbidity of the solution at infinite time. The fact that there is a single relaxation time is inconsistent with the details outlined for the transition mechanism. The transformation of vesicle into rods appears to involve multiple steps beginning with the reduction in the mean diameter of the vesicles, followed by the reorganization of the vesicles to form a non-bilayer bowtie aggregate and then these bowties elongate to form rods. As mentioned earlier, the bowtie structure is not a logical step in the morphological evolution of the aggregates from the

vesicular state because it is unlikely that a spherical bilayer aggregate can collapse to form a non-bilayer aggregate with a bowtie structure. This hypothesis, coupled with the fact that a single relaxation time is obtained for the kinetics of what is obviously a multi-step process, leads to the conclusion that experimental limitations possibly prevent us from detecting the relaxation process of the fastest step(s) in the transition, and that the relaxation time that is obtained corresponds to the expansion of the bowties in the direction of the long-axis. This conclusion is justified considering the short time scale over which the transition occurs. Because of this uncertainty in the kinetic data, it is more appropriate to discuss the transition in terms of relaxation time instead of simplifying the results in order to obtain a rate constant.

3.3.5 Factors Effecting the Transition Kinetics

3.3.5.1 The Initial Solvent Composition

Figure 3A contains turbidity-time profiles for the vesicle-to-rod transition induced at different solvent compositions; they suggest that this parameter of the system has a slight influence on the transition kinetics. This effect was studied by applying a 0.5 wt % jump in the dioxane content to a series of solutions with different solvent compositions, and with a 1.0 wt % polymer concentration. The starting position was varied from 28.2 to 27.4 wt % H₂O. The relaxation times increase with a rise in the initial water content (Table 1). This phenomenon must be considered in terms of where the initial conditions place the system within the morphological phase diagram. At 28.2 wt % H₂O, the system is located within the vesicle region and is further away from the transition boundary than the starting position of any other experiment. The kinetics is slower for this transition because all of the aggregates are equilibrium vesicles, thus the aggregates must undergo a larger degree of structural rearrangement as they progress toward rods, than the aggregates in those systems that start out already within the transition region (i.e. 27.6 and 27.4 wt % H₂O). The mean vesicle diameter expands with increasing water content in the solvent, but the wall thickness is relatively constant.¹⁸ This indicates that the hollow regions of the vesicles are able to hold more solvent. Hence, the kinetics progressively slow down with increasing initial water content because more solvent must be expelled from the vesicle core in order for it to reorganize to become a non-bilayer aggregate.

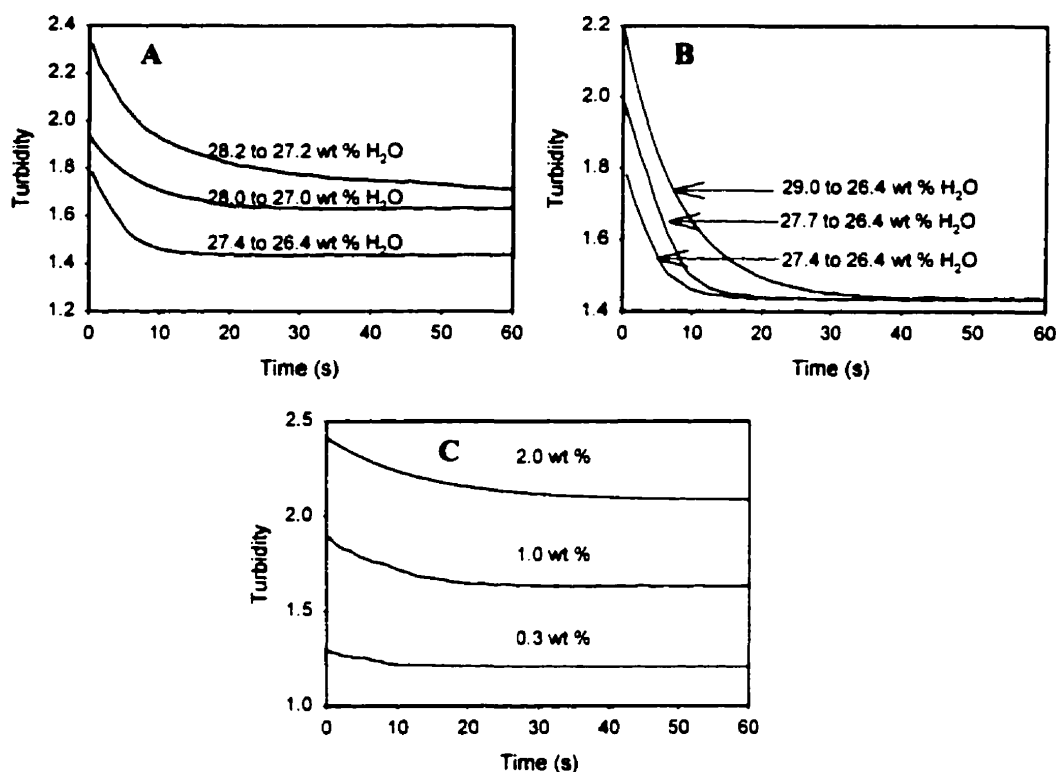


Figure 3: (A) Effect of the initial solvent composition on the kinetics of the vesicle-to-rod transition in PS₃₁₀-b-PAA₅₂ aggregates in dioxane-water mixtures. The initial polymer concentration is 1.0 wt %. (B) Effect of the magnitude of the dioxane jump on the kinetics of the vesicle-to-rod transition in PS₃₁₀-b-PAA₅₂ aggregates in dioxane-water mixtures. The initial polymer concentration is 1.0 wt %. (C) Effect of the initial polymer concentration on the kinetics of the vesicle-to-rod transition from 28.0 to 27.0 wt % H₂O in PS₃₁₀-b-PAA₅₂ aggregates.

The relaxation times for the rod-to-vesicle transition also increase with increasing water content.⁵⁵ This is attributed to the fact that the slow step in the transition, the closure of the lamellae or bowls to form vesicles, contributes more to the turbidity change than the fast initial formation of the lamellae from rods at higher water contents. It is noteworthy that the rod-to-vesicle, transition occurs much more slowly than the opposite, vesicle-to-rod transition in spite of the fact that it is induced at higher water contents. A high ratio of water to dioxane in the solvent can kinetically trap the morphology of the

aggregates by affecting the mobility of the copolymer chains. This factor does not influence the kinetics of the transitions because the difference in the starting solvent composition between the forward and reverse transitions is small relative to the composition range covered by the morphological phase diagram.

Table 1: Kinetic Results for Vesicle to Rod Transition of PS₃₁₀-b-PAA₅₂ Aggregates in Dioxane / Water Mixtures

	Initial Polymer Conc.	Initial H ₂ O content	Δ H ₂ O	C	A	τ (s)	R ²
Initial Water Content	1.01	28.2	-1.0	1.66	0.465	7.22	0.999
	1.00	28.0	-1.0	1.63	0.409	6.13	0.999
	1.02	27.6	-1.0	1.46	0.329	4.72	0.997
	1.01	27.4	-1.0	1.44	0.309	3.97	0.997
Jump Magnitude	1.03	29.0	-2.6	1.44	0.765	7.86	1.00
	1.01	27.7	-1.3	1.44	0.584	5.65	0.995
	1.01	27.4	-1.0	1.44	0.309	3.97	0.997
Polymer Concentration	0.30	28.0	-1.0	1.21	0.093	5.88	0.990
	1.00	28.0	-1.0	1.63	0.409	6.13	0.999
	2.02	28.0	-1.0	2.08	0.332	12.8	0.996

3.3.5.2. The Size of the Dioxane Content Jump

Altering the solvent composition affects the force balance governing the aggregate morphology, and is used to drive the morphological transition. In order to gain a better understanding of the vesicle-to-rod transition, it is important to determine how the degree of perturbation imposed on the system influences the transition kinetics. This is accomplished by applying different dioxane content jumps, ranging from 1.0 to 2.6 wt %, to solutions with a polymer concentration of 1.0 wt % (Fig. 3B). The initial solvent composition is varied, depending on the size of the jump, so that the final solvent composition is 26.4 wt % H₂O-73.6 wt % dioxane in all cases.

The relaxation time becomes slightly longer with an increase in the magnitude of the dioxane jump as outlined in Table 1. This result is attributed to the initial conditions of the system, and the location of each system within the phase diagram. Since the drive is toward the formation of rods, it will take longer to reach this desired state the further

the system resides to the right of the transition region because the aggregates must proceed through more structural rearrangement steps and more solvent must be expelled from the core of the vesicles before they begin to resemble rods. At water contents above 28.0 wt %, the vesicles are considered to be equilibrium structures. Thus, the larger the magnitude of the perturbation imposed on these aggregates the further they are driven away from their initial equilibrium state, and the longer it takes for the aggregates to reach a new state of equilibrium.

The kinetics of the rod-to-vesicle transition, like that of the vesicle-to-rod transition has a slight dependence on the magnitude of the solvent jump. Chen et al. argue that the reason for this result is that the Gibbs activation energy is not strongly influenced by the size of the solvent jump.⁵⁵ However, there is a very large difference in the relaxation times for these opposing transitions, with the vesicle-to-rod transition occurring more quickly than the reverse transition when the same degree of perturbation is applied to both systems.

3.3.5.3. The Initial Polymer Concentration

By keeping the solvent composition and the size of the dioxane jump constant, it is possible to explore the effect that the initial polymer concentration has on the kinetics of the transition. Figure 3C contains turbidity curves for three systems with polymer concentrations ranging from 0.3 to 2.0 wt %. A 1.0 wt % jump in the dioxane content is used to induce the transition.

The relaxation time for the transition becomes longer as the polymer concentration is increased. The effect is more pronounced at higher polymer concentration; there is a two-fold increase in the value of τ in going from 1.0 to 2.0 wt % PS-b-PAA. The phase diagram studies indicate that the transition boundaries are shifted to lower water content with increasing polymer concentration. The boundary between the vesicle and transition regions is situated at a solvent composition of ca. 24.0 wt % H₂O when the polymer concentration is 2.0 wt %. This is increased to 27.6 wt % and ca. 28.5 wt % for polymer concentrations of 1.0 wt % and 0.3 wt % respectively. Hence, the starting conditions place the system within the vesicle region when the polymer concentration is 1.0 and 2.0 wt %, but within the transition region when the polymer concentration is only 0.3 wt %. The mean diameter of the vesicles also increases with a

rise in the polymer concentration, but the bilayer thickness remains constant. Thus, not only are the aggregates initially all vesicles at 2.0 wt % polymer, but they also contain a larger amount of solvent in their core. The transition kinetics are slower at higher polymer concentrations because the systems is deeper within the vesicle region, causing the aggregates to have to undergo more reorganization, and expel more solvent from the core in order for them to become non-bilayer structures. There is only a slight difference in the relaxation times in going from 0.3 to 1.0 wt % polymer. The initial parameters place these systems approximately the same distance away, but on opposite sides of the transition boundary, so their starting conditions are more closely related than those at 2.0 wt % polymer. The same trend is observed for the effect of the initial polymer concentration on the rod-to-vesicle transition. Chen et al. attribute this to an increase in the activation energy with increasing polymer concentration.⁵⁵

3.3.6 Comparison of the Results with those of other PS-b-PAA Aggregate Transitions

To date, the kinetics and mechanism of four morphological transitions that occur in aggregates prepared from PS₃₁₀-b-PAA₅₂ in dioxane-water mixtures have been investigated.^{55,56} These include the sphere-to-rod, the rod-to-sphere, the rod-to-vesicle, and the vesicle-to-rod transitions. Although the exact mechanistic details are different for each transition, the morphological transformations can be compared in terms of the kinetics and the more fundamental aspects of the transition process. The accumulation of this information can lead to better insight into how to control the morphology of the block copolymer aggregates. A complete understanding of the morphological behavior of block copolymer aggregates is useful not only for its own sake, but also if these aggregates are to be employed in potential applications in such areas as pharmaceuticals, agriculture, and personal care products.

The sphere-to-rod transition proceeds through a two-step mechanism.⁵⁶ As the transition boundary is approached; the spherical micelles become energetically unstable because of core-chain stretching. This results in the adhesive collisions between the spheres leading to the formation of “pearl necklace” intermediates in order to reduce the energy of the system. During the rate-determining step, the individual chains within a

necklace reorganize to produce a smooth rod with a smaller diameter than that of the original spherical aggregates. The reverse transition, rod-to-sphere, also has a two-step mechanism.⁵⁶ In this case, a bulb quickly grows on one or both ends of a rod. The bulbs are extruded from the rod to release free spheres during the rate-limiting step.

An increase in the water content of the solvent within the rod region leads to the shortening of the length of the rods accompanied by an increase in the diameter.⁵⁵ A sudden jump in the water content near this transition boundary initiates the transformation of rods into vesicles beginning with the flattening of the rods to form circular or irregular shaped lamellae. The lamellae then slowly become bowl-shaped, and eventually close to form vesicles. As discussed earlier, the vesicle-to-rod transition has a more complex mechanism for which not all of the details are clear. However, the transformation appears to progress from small vesicles to non-bilayer aggregates with a bowtie shape. Growth occurs at the ends of these aggregates to form dumbbell intermediate structures. The expansion of the long-axis continues at the expense of the bulbs on either end until a smooth rod is formed.

The above description of the transition mechanisms reveals two trends in the results. The forward and reverse transitions between rods and vesicles both occur without a change in the aggregation number; one rod is converted to one vesicle and vice versa. On the other hand, the sphere-to-rod and rod-to-sphere transitions both proceed without conservation of aggregate mass in that many spheres form one rod. It is also noteworthy that the mechanism of three of the four transitions involves only two transformation steps. Despite this fact, the transition kinetics can easily be compared.

Examining the kinetic results for the forward and reverse transition between two aggregate morphologies indicates that the relaxation times for the sphere-to-rod and rod-to-sphere transitions are of the same order of magnitude. However, in the case of rods and vesicles, the relaxation time for the vesicle-to-rod transition is two orders of magnitude shorter than the τ values for the rod-to-vesicle transition. Although the turbidity-time profiles for most of the kinetic experiments are fitted to the same double exponential equation, all of those for the vesicle-to-rod and one experiment from both the sphere-to-rod and rod-to-sphere transition studies yield a single exponential equation.

Table 2 contains a summary of the effect of varying the initial solvent composition, the magnitude of the solvent jump, and the initial polymer concentration on the general trends in the relaxation times for each transition. In all cases, the relaxation times become longer with an increase in the water content of the solvent mixture. This phenomenon is related to the location that each set of parameters places the system within the morphological phase diagram and how this position impacts the progress of the transition. The size of the solvent jump has the opposite effect on the relaxation times of the forward and reverse transitions for both types of morphological transformations, but the trend is the same in both cases. Increasing the size of the water content jump leads to slightly faster kinetics for both the sphere-to-rod and rod-to-vesicle transitions, while increasing the magnitude of the dioxane content jump leads to longer relaxation times for the reverse processes. This result must be considered in terms of the experimental design. For those transitions induced by a jump in the water content, the initial solvent composition was held constant, but for those transitions induced with dioxane, the final solvent composition was constant. The copolymer concentration has a strong influence on the kinetics of morphological change. However, the explanation of the observed trends is more complex. The relaxation times become longer with higher polymer concentration for the rod-to-vesicle and vesicle-to-rod transitions. However, the relaxation times decrease with an increase in the polymer concentration for the sphere-to-rod transition, but the trend is more complex for the rod-to-vesicle transition. These results are related to both the change in the activation energy for the morphological change and the transition boundaries with varying polymer concentration.

Table 2: General Trend in the Relaxation Times

Transition	General Trend in the Relaxation Time(s)		
	↑ Water Content	↑ Jump Magnitude	↑ Polymer Concentration
Sphere-to-Rod	Increase	Decrease	Decrease
Rod-to-Sphere	Increase	Increase	Increase / Decrease
Rod-to-Vesicle	Increase	Slight Decrease	Increase
Vesicle-to-Rod	Slight Increase	Slight Increase	Increase

This series of studies of the kinetics and mechanisms of morphological transitions in block copolymer aggregates in solution represents the most extensive investigation of its kind for copolymer systems. However, the complex and diverse nature of the morphological changes in block copolymer aggregates warrants further study in order to completely understand such phenomena.

3.4 Conclusions

The kinetics and mechanism of the vesicle-to-rod transition has been examined in aggregate systems prepared from the ternary system PS₃₁₀-b-PAA₅₂ / dioxane / water. The transition was induced by a jump in the dioxane content of the solvent mixture and was followed by monitoring the solution turbidity as a function of time. A single relaxation time was obtained from the turbidity-time curves. The mechanism was investigated by rapidly quenching to low temperature and subsequently freeze-drying solution samples at various time points during the transitions. This traps the intermediate aggregate morphologies, which are observed using transmission electron microscopy. Approaching the transition boundary from the vesicle region results in a decrease in the mean diameter of the vesicles with little change in the bilayer thickness. This increases the degree of curvature of both the inner and outer vesicle bilayers leading to a rise in the curvature energy. The instability of these vesicles causes them to undergo structural rearrangement. The first intermediate structures observed are in the shape of a bowtie. The bowties grow to develop into dumbbells. The long-axis expands at the expense of the bulbs on either end of the dumbbells resulting in the formation of rods. The reduction in the stretching of the core-chains in going from vesicles to rods is expressed in the smaller diameter of the rods relative to that of the bilayer. It is concluded, based upon the fact a single relaxation time was obtained for the kinetics of the multi-step transition and that bowties, which do not likely form directly from vesicles, are the first intermediate structures observed, that one or more steps in the transition are not detected as a result of experimental limitations. In any event, the kinetics of the transition is influenced by the initial solvent composition, the magnitude of the dioxane content jump, and the initial polymer concentration. The relaxation time becomes slightly longer with an increase in

both the water content of the solvent mixture and the degree of solvent perturbation. The kinetics has a greater dependence on the polymer concentration than the other two parameters investigated.

The phenomenon of morphological change occurring in PS₃₁₀-b-PAA₅₂ aggregates in dioxane-water mixtures is the focus of this dissertation. It is well known that varying the ratio of the two solvent components effects the architecture of the aggregates.²⁰⁻²² The kinetics and mechanisms of the sphere-to-rod, rod-to-sphere, and vesicle-to-rod transitions were investigated by employing a change in the solvent composition to induce the morphological transformations. However, the solvent composition is just one factor known to influence the morphology of aggregates composed of PS-b-PAA molecules. In the next chapter the ability of the small molecule surfactant sodium dodecyl sulfate to interact with the PS-b-PAA chains in a way that promotes morphological change in the copolymer aggregates is discussed. The use of this surfactant species provides an additional means of controlling the morphology of PS-b-PAA aggregates and the enhanced versatility of the system makes it more viable for potential applications.

3.5 References

1. Price, C.; Woods, D. *Eur. Polymer J.* **1973**, *9*, 827.
2. Tuzar, Z.; Kratochvil, P. *Adv. Colloid Interface Sci.* **1976**, *6*, 201.
3. Price, C. In *Developments in Block Copolymers*; Goodman, I., Ed.; Applied Science Publishers: London, 1982; Vol. 1, p 39.
4. Elis, H. G. In *Light Scattering from Polymer Solutions*; Huglin, M. B., Ed. Academic Press: London, 1972; Chapter 9.
5. Riess, G; Hurtrez, G; Bahadur, P. *Encyclopedia of Polymer Science and Engineering*, 2nd ed.; Wiley: New York, 1985; Vol. 2, p 324.
6. Selb, J.; Gallot, Y. In *Developments in Block Copolymers*; Goodman, I., Ed.; Applied Science Publishers: London, 1985; Vol. 2, p 27.
7. Brown, R. A.; Masters, A. J.; Price, C.; Yuan, X. F. In *Comprehensive Polymer Science: Polymer Properties* Allen, S. G., Bevington, J. C., Booth, C., Price, C., Eds.; Pergamon Press: Oxford, 1989; Vol.2, p 155.
8. Tuzar, Z.; Kratochvil, P. In *Surface and Colloid Science*; Matijevic, E., Ed.; Plenum Press: New York, 1993; Vol. 15, p 1.

9. de Gennes, P. G. In *Solid State Physics*; Liebert, L., Ed.; Academic Press: New York, 1978; supplement 14, p1.
10. Halperin, A.; Tirrell, M.; Lodge, T. P. *Adv. Polym. Sci.* **1992**, *100*, 31.
11. Bednar, B.; Edwards, K.; Almgren, M.; Tormod, S.; Tuzar, Z. *Makromol. Chem. Rapid Commun.* **1988**, *9*, 785.
12. Honda, C.; Hasegawa, Y.; Hirunuma, R.; Nose, T. *Macromolecules* **1994**, *27*, 7660.
13. Hecht, E.; Hoffmann, H. *Colloids Surf., A.* **1995**, *96*, 181.
14. Iyama, K.; Nose, T. *Macromolecules* **1998**, *31*, 7356.
15. Michels, B.; Waton, G.; Zana, R. *Langmuir* **1997**, *13*, 3111.
16. Aniansson, E. A. G.; Wall, S. N. *J. Phys. Chem.* **1974**, *78*, 1024.
17. Zhang, L.; Eisenberg, A. *Science* **1995**, *268*, 1728.
18. Shen, H.; Eisenberg, A. *J. Phys. Chem. B* **1999**, *103*, 9473.
19. Yu, K.; Eisenberg, A. *Macromolecules* **1998**, *31*, 3509.
20. Zhang, L.; Eisenberg, A. *Polym. Adv. Tech.* **1998**, *9*, 677.
21. Cameron, N. S.; Corbierre, M. K.; Eisenberg, A. *Can. J. Chem.* **1999**, *77*, 1311.
22. Burke, S.; Eisenberg, A. *High Performance Polymers* **2000**, *12*, 535.
23. Ding, J.; Liu, G. *Polymer* **1997**, *38*, 5497.
24. Hajduk, D. A.; Kossuth, M. B.; Hillmyer, M. A.; Bates, F. S. *J. Phys. Chem. B* **1998**, *102*, 4269.
25. Discher, B. M.; Won, Y.-Y.; Ege, D. S.; Lee, J. C.-M.; Bates, F. S.; Discher, D. E.; Hammer, D. A. *Science* **1999**, *284*, 1143.
26. Prochazka, K.; Martin, T. J.; Webber, S. E.; Munk, P. *Macromolecules* **1996**, *29*, 6526.
27. Spatz, J. P.; Mössmer, S.; Möller, M. *Angew. Chem. Int. Ed. Engl.* **1996**, *35*, 1510.
28. Massey, J.; Power, K. N.; Manners, I.; Winnik, M. A. *J. Am. Chem. Soc.* **1998**, *120*, 9533.
29. Kramer, E.; Förster, S.; Goltner, C.; Antonietti, M. *Langmuir*, **1998**, *14*, 2027.
30. Jørgenseb, E. B.; Hvidt, S.; Brown, W.; Schillén, K. *Macromolecules* **1997**, *30*, 2355.
31. Liu, G. *Curr. Opin. Colloid Interface Sci.* **1998**, *3*, 200.
32. Liu, T.; Zhou, Z.; Wu, C.; Chu, B. *J. Phys. Chem. B* **1997**, *101*, 8808.
33. Mortensen, K.; Talmon, Y.; Gao, B.; Kops, J. *Macromolecules* **1997**, *30*, 6764.
34. a) Yu, Y.; Eisenberg, A. *J. Am. Chem. Soc.* **1997**, *119*, 8383. b) Rheingans, O.; Hugenberg, N.; Harris, J. R.; Fischer, K.; Maskos, M. *Macromolecules* **2000**, *33*, 4780. c) Alexandridis, P.; Olsson, U.; Lindman, B. *Langmuir* **1998**, *14*, 2627.

35. a) Yu, K.; Zhang, L.; Eisenberg, A. *Langmuir* **1996**, *12*, 5980. b) Svensson, M.; Alexandridis, P.; Linse, P. *Macromolecules* **1999**, *32*, 5435. c) Svensson, B.; Olsson, U.; Alexandridis, P. *Langmuir* **2000**, *16*, 6839.
36. a) Desbaumes, L.; Eisenberg, A. *Langmuir* **1999**, *15*, 36. b) Mortensen, K.; Pedersen, J. S. *Macromolecules* **1993**, *26*, 805. c) Schillén, K.; Brown, W.; Johnsen, M. *Macromolecules* **1994**, *27*, 4825.
37. a) Zhang, L.; Yu, K.; Eisenberg, A. *Science* **1996**, *272*, 1777. b) Zhang, L.; Shen, H.; Eisenberg, A. *Macromolecules* **1997**, *30*, 1001. c) Shen, H.; Zhang, L.; Eisenberg, A. *J. Am. Chem. Soc.* **1999**, *121*, 2728. d) Talingting, M. R.; Munk, P.; Webber, S. E. Tuzar, Z. *Macromolecules* **1999**, *32*, 1593. e) Jørgenseb, E. B.; Hvidt, S.; Brown, W.; Schillén, K. *Macromolecules* **1997**, *30*, 2355. f) Kabanov, A.; Bronich, T. K.; Kabanov, V. A.; Eisenberg, A. *J. Am. Chem. Soc.* **1998**, *120*, 9941. g) Zheng, Y.; Davis, H. T. *Langmuir* **2000**, *16*, 6453.
38. Shen, H.; Zhang, L.; Eisenberg, A. *J. Phys. Chem. B* **1997**, *101*, 4697.
39. Zhang, L.; Eisenberg, A. *Macromolecules* **1999**, *32*, 2239.
40. Shen, H.; Eisenberg, A. *Macromolecules* **2000**, *33*, 2561.
41. Luo, L.; Eisenberg, A. *J. Am. Chem. Soc.* **2001**, *123*, 1012.
42. Yu, K.; Bartels, C.; Eisenberg, A. *Langmuir* **1999**, *15*, 7157.
43. Schillén, K.; Bryskhe, K.; Mel'nikova, Y. S. *Macromolecules* **1999**, *32*, 6885.
44. Koňák, C.; Oupický, D.; Chytrý, V.; Ulbrich, K. *Macromolecules* **2000**, *33*, 5318.
45. Vinson, P. K.; Talmon, Y.; Walter, A. *Biophys. J.* **1989**, *56*, 669.
46. Walter, A.; Vinson, P. K.; Kaplun, A.; Talmon, Y. *Biophys. J.* **1991**, *60*, 1315.
47. Edwards, K.; Almgren, M. *J. Colloid Interface Sci.* **1991**, *147*, 1.
48. Edwards, K.; Almgren, M.; Bellare, J.; Brown, W. *Langmuir* **1989**, *5*, 473.
49. Edwards, K.; Gustafsson, J.; Almgren, M.; Karlsson, G. *J. Colloid Interface Sci.* **1993**, *161*, 299.
50. Silvander, M.; Karlsson, G.; Edwards, K. *J. Colloid Interface Sci.* **1996**, *179*, 104.
51. Farquhar, K. D.; Misran, M.; Robinson, B. H.; Steytler, D. C.; Morini, P.; Garrett, P. R.; Holzwarth, J. F. *J. Phys.: Condens. Matter* **1996**, *8*, 9397.
52. Danino, D.; Talmon, Y.; Zana, R. *J. Colloid Interface Sci.* **1997**, *185*, 84.
53. Brinkmann, U.; Neumann, E.; Robinson, B. H. *J. Chem. Soc. Faraday Trans.* **1998**, *94*, 1281.
54. Iyama, K.; Nose, T. *Macromolecules* **1998**, *31*, 7356.
55. Chen, L.; Shen, H.; Eisenberg, A. *J. Phys. Chem. B* **1999**, *103*, 9488.
56. Burke, S. E.; Eisenberg, A. *submitted to Langmuir*
57. Hautekeer, J. P.; Varshney, S. K.; Fayt, R.; Jacobs, C.; Jerome, R.; Teyssie, P. *Macromolecules* **1990**, *23*, 3893.

58. Zhong, X. F.; Varshney, S. K.; Eisenberg, A. *Macromolecules* **1992**, *25*, 7160.
59. Inoue, T. In *Vesicles*; Rosoff, M., Ed.; Surfactant Science Series 62; Marcel Dekker: New York, 1996; Chapter 5.
60. Aniansson, E. A. G.; Wall, S. N.; Almgren, M.; Hoffmann, H.; Kielmann, I.; Ulbricht, W.; Zana, R.; Lang, J.; Tondre, C. *J. Phys. Chem.* **1976**, *80*, 905.

Chapter 4

Effect of Sodium Dodecyl Sulfate on the Morphology of Polystyrene-*b*-Poly(Acrylic Acid) Aggregates in Dioxane-Water Mixtures

The phenomenon of morphological change occurring in PS₃₁₀-*b*-PAA₅₂ aggregates in dioxane-water mixtures is the focus of this dissertation. It is well known that varying the ratio of the two solvent components affects the architecture of the aggregates. The kinetics and mechanisms of the sphere-to-rod, rod-to-sphere, and vesicle-to-rod transitions were investigated by employing a change in the solvent composition to induce the morphological transformations. However, the solvent composition is just one factor known to influence the morphology of aggregates composed of PS-*b*-PAA molecules. In this chapter the ability of the small molecule surfactant sodium dodecyl sulfate to interact with the PS-*b*-PAA chains in a way that promotes morphological change in the copolymer aggregates is discussed. The use of this surfactant species provides an additional means of controlling the morphology of PS-*b*-PAA aggregates and the enhanced versatility of the system makes it more viable for potential applications. This study represents the first in a series of investigations that are required to fully characterize the influence of small molecule surfactants on block copolymer aggregates in solution.

4.1 Introduction

Asymmetric, amphiphilic block copolymers self-assemble into crew-cut aggregates in solution when the core-forming block is much longer than the corona-forming segment.^{1,2} In the case of polystyrene-*b*-poly(acrylic acid) copolymers, stable crew-cut aggregates are usually prepared in a solvent mixture either by direct dissolution or by first dissolving the copolymer in a solvent suitable for both blocks and then adding water, which is a precipitant for the long block, but which is simultaneously a good solvent for the short segment.³ It has also been reported that the aggregates can be prepared in a single solvent.⁴ In any case, the equilibrium structure of these aggregates is found to be governed by a balance between three major forces acting on the system: the stretching of the core blocks, the interfacial tension between the core and the solvent, and the intercorona interactions.^{3b,5-8}

In 1995, Zhang and Eisenberg published the first report on the systematic formation of crew-cut aggregates of multiple morphologies in solution.⁵ Subsequent studies by this group and by others have revealed that a variety of aggregate morphologies can be obtained under equilibrium and non-equilibrium conditions.⁹⁻¹¹ The architecture of these aggregates was changed by altering the force balance that controls the equilibrium structure of the aggregates, which is affected by such parameters as the solvent composition¹², the relative block lengths¹³, the temperature^{4,14}, and the presence of added species including salt, acid, base, and homopolymer.¹⁵

Although it is well known that small molecule surfactants can interact with polymers to form intricate aggregate structures in solution¹⁶⁻¹⁸, the influence of surfactants on the solution behavior of block copolymer aggregates has only recently been investigated.¹⁹⁻³⁰ Many of these studies describe the interaction of surfactants with the family of block copolymers poly(ethylene oxide)-*b*-poly(propylene oxide)-*b*-poly(ethylene oxide) (PEO_x-*b*-PPO_y-*b*-PEO_x), which are commonly referred to as Pluronics.¹⁹⁻²³ The surfactant molecules penetrate into the copolymers micelles forming mixed spherical aggregates. In some cases the self-assembly of the copolymer is suppressed because the surfactant molecules bind to the individual polymer chains and form micelles along the polymer backbone. In addition, both cationic and anionic

surfactants were found to interact with polystyrene-*b*-poly(ethylene oxide) to form mixed aggregates corresponding to micelles, micellar clusters, and supermicellar aggregates.^{24,25}

A number of other studies have focused on the formation of polymer-surfactant aggregates prepared from the complexation of ionomers with surfactants of opposite charge.²⁶⁻²⁷ Many of these block ionomer complexes (BIC) form soluble spherical particles in solution. In addition to spherical micelles, Kabanov et al. also reported on the spontaneous formation of vesicles from BIC of poly(ethylene oxide)-*b*-poly(sodium methacrylate) and cationic surfactants.²⁷ This represented the first example of the preparation of aggregates of multiple morphologies from BIC systems in solution.

Two other recent studies have shown that surfactant can induce structural changes in block copolymer aggregates in solution.^{28,29} Egger et al. showed that cylindrical aggregates of polybutadiene-*b*-poly(ethylene oxide) can be converted to spherical micelles upon addition of dodecyltrimethylammonium bromide.²⁸ Similar behavior was observed by Zheng and Davis in their system of poly(ethylene oxide)-*b*-poly(ethylethylene)-*b*-poly(ethylene oxide) cylindrical aggregates and the surfactant poly(oxy ethylene (5)) dodecyl ether (C₁₂E₅). This group also observed a reduction in the diameter of the spherical aggregates prepared from poly(ethylene oxide)-*b*-polybutadiene in the presence of C₁₂E₅.²⁹

Here, we report on the ability of the small molecule surfactant, sodium dodecyl sulfate (SDS), to induce a series of morphological transitions in aggregates prepared from PS₃₁₀-*b*-PAA₅₂ in dioxane-water mixtures. This particular polymer was chosen because a great deal is known about the morphological phase behavior of its aggregates in dioxane-water mixtures.⁸ A diagram was constructed to map out the morphology of the aggregates at different SDS concentrations and solvent compositions. The nature of the influence that SDS exercises over the copolymer aggregates was determined by comparing the results with those obtained for the addition of the ionic species sodium chloride (NaCl) and the organic acid tridecanoic acid (TDA), which has a C12 linear alkyl chain and a carboxylic head group, to the aggregates of the PS-*b*-PAA in dioxane-water mixtures. The interactions of both the hydrophobic chain and the micro ions of the surfactant head group with the block copolymer molecules effect the architecture of the copolymer aggregates. Thus, the amphiphilic character of SDS enhances the ability to

tailor the morphology of the aggregates, which is the motivation behind the present study. The interaction of the copolymer aggregates and SDS was investigated at different solvent compositions and copolymer concentrations. The method of solution preparation was found to have an effect on the initial self-assembly process, possibly as a result of slow kinetics and premicellar association between the copolymer chains and the surfactant molecules.

4.2 Experimental

The PS-*b*-PAA copolymer used in this study was prepared by sequential anionic polymerization and fractionated to remove homopolymer. The details of these procedures are outlined in a previous publication.^{3a} The sample has 310 PS and 52 PAA units with an overall polydispersity of 1.05.

Two methods of solution preparation were used in this study. In the first case, samples were prepared by dissolving a given amount (0.7 to 2.0 wt %) of the copolymer in dioxane, which is a solvent for both copolymer blocks. Self-assembly was induced by adding deionized water (a precipitant for the PS blocks) slowly to a vigorously stirred copolymer solution.⁵ Micellization was indicated by the appearance of a blue tint in the solution. The additives (Sigma) were introduced to the system in small aliquots, which contained the additive dissolved in a solvent mixture with the same dioxane-water content as that of the polymer solution. In the second case, the copolymer was dissolved in dioxane and then SDS was added to the solution. This was followed by the slow addition of an aqueous SDS solution with the same concentration of SDS as the copolymer-SDS solution.

The turbidity measurements were performed on a Cary 50 spectrophotometer (Varian). The turbidity was monitored at 650 nm where the absorption is lowest for both the polymer and the aggregates.⁸ The measurements were taken 25 minutes after the addition of each aliquot and the experiment was performed at room temperature.

The aggregate morphologies were observed by transmission electron microscopy (TEM) using a JEOL JEM-2000 microscope operating at an acceleration voltage of 80 kV. Each sample was prepared by depositing a drop of the solution on an EM copper grid which had been pre-coated with a layer of poly(vinyl formal) (J.B. EM Services) and one of carbon. The samples were then quenched by reducing the temperature to near that of

liquid nitrogen. The samples were subsequently freeze-dried, as they gradually warmed to room temperature, under vacuum.

4.3 Results and Discussion

The results and discussion section is divided into three parts. The first part provides a general description of how the structure of sodium dodecyl sulfate enables it to interact with the PS-*b*-PAA chains and the effect these interactions have on the morphology of the aggregates formed from the copolymer molecules. Several trends are observed in the phase diagram, constructed as a function of the solvent composition and copolymer concentration, resulting from the polymer-surfactant interactions. These trends are discussed in the next section. The last section compares the morphological phase behavior of aggregates prepared using two different methods of solution preparation.

4.3.1 General Description of the Effect of SDS

Figure 1 contains a series of micrographs of aggregates prepared in solutions of 11.5 wt % water-88.5 wt % dioxane at a fixed polymer concentration of 1.0 wt %, but with varying concentrations of SDS. In the absence of SDS, this system contains spherical micelles with a diameter of 50 ± 2 nm.³⁰ Thus, it is apparent that sodium dodecyl sulfate can induce morphological changes in the PS₃₁₀-*b*-PAA₅₂ aggregates at water contents well below those required in the absence of SDS.⁸ Although the effect of SDS on the architecture of the PS-*b*-PAA aggregates is obvious, the origin of the interaction is more complex. Sodium dodecyl sulfate, like PS₃₁₀-*b*-PAA₅₂, is amphiphilic. Each SDS molecule has an ionic head group composed of a sulfate ion and a sodium counter ion, while the surfactant tail is a linear C12 alkyl chain. It must be noted that although SDS is amphiphilic, it does not undergo self-assembly in the solvent mixtures used throughout this study.³¹ In order to determine how the chemical properties of SDS influence the block copolymer aggregates, it is important to know the effect that simple electrolytes and small nonpolar species have on the PS-*b*-PAA aggregates. A study of the effect of NaCl on the PS₃₁₀-*b*-PAA₅₂ aggregates was carried out in parallel to the study with SDS to analyze the nature of the interaction of the micro ions with poly(acrylic acid) chains and to determine how this interaction effects the morphology of the block copolymer aggregates. Similarly, tridecanoic acid was added to solutions containing the

copolymer aggregates to investigate the effect of the linear hydrocarbon chain, containing a weakly acidic head group, on the behavior of the aggregates.

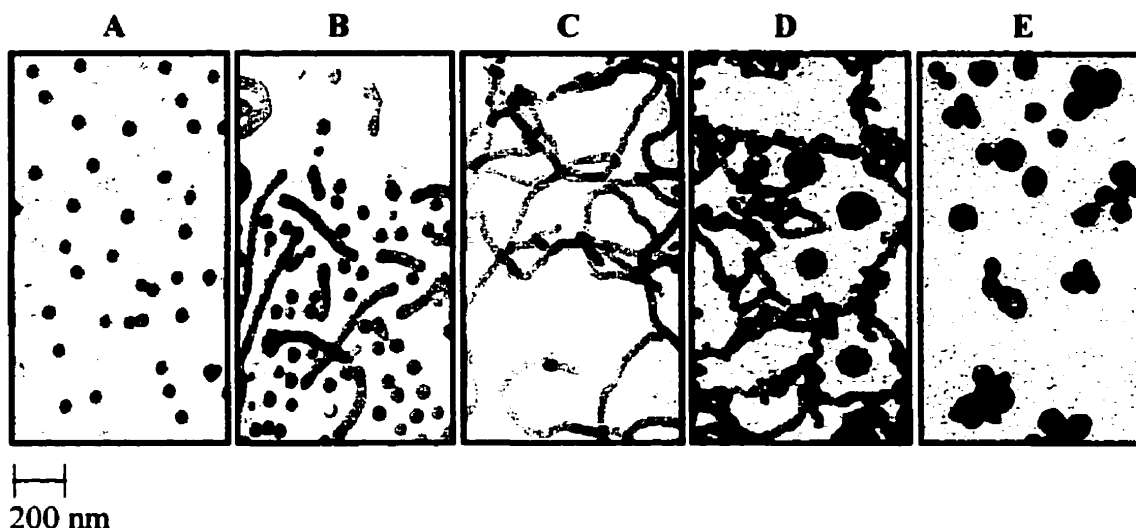


Figure 1: Micrographs of the morphologies observed for aggregates prepared from 1.0 wt % PS₃₁₀-*b*-PAA₅₂ aggregates in solutions of 11.5 wt % H₂O and increasing concentrations of SDS. (A: 2.0 mM, B: 5.1 mM, C: 9.2 mM, D: 11.0 mM, E: 17.1 mM)

Zhang and Eisenberg have previously shown that millimolar quantities of NaCl can alter the morphology of PS-*b*-PAA (i.e., PS₄₁₀-*b*-PAA₂₅, PS₄₁₀-*b*-PAA₁₃, PS₆₆₀-*b*-PAA₂₄) aggregates formed in *N,N*-dimethylformamide-water mixtures from that observed in the pure state.^{15a,15b} It is believed that this phenomenon occurs because the Na⁺ and Cl⁻ ions are able to screen the electrostatic field generated by the partially charged PAA segments. The reduction in the repulsion among the corona chains leads to an increase in the aggregate size in order to decrease the interfacial energy between the core and the solvent. However, the increase in the core size is hindered by an entropic penalty resulting from the stretching of the PS blocks. At some point, the aggregates change their morphology in order to reduce the free energy of the system.^{15a,15b} A similar investigation was carried out using the system currently under investigation, PS₃₁₀-*b*-PAA₅₂ in dioxane-water mixtures, so that comparisons could be drawn between these results and those obtained from the study involving SDS.

Table 1 summarizes the effect of NaCl on the morphological phase boundaries of PS₃₁₀-*b*-PAA₅₂ in solvent mixtures with different dioxane-water compositions. When the

water content of the solvent is low, NaCl has no observable effect on the morphology of the block copolymer aggregates because NaCl is only slightly soluble (e.g. less than 3 mM) in the solvent compositions since the dielectric constant of the medium is low at low water contents.³¹ In addition, the PAA chains of the corona are only slightly ionized at reduced water contents. Thus, the slight interaction between NaCl and PAA is not strong enough to be a driving force for morphological change in the copolymer aggregates. As the water content is increased, NaCl begins to have a stronger influence on the structure of the aggregates. The morphological boundaries are shifted to lower concentrations of NaCl (i.e. molar ratios of NaCl to acrylic acid repeat units) with increasing water content.⁸ There is a higher degree of ionization of the PAA chains at higher water contents, thus the extent to which the shielding of the electrostatic field of the corona by the Na⁺ and Cl⁻ ions influence the morphology of the aggregates increases with an increase in water content.

Table 1: Comparison of the morphological boundaries between the regions of spheres (S), spheres + rods (S+R), rods (R), rods + vesicles (R+V), and vesicles (V) for aggregates prepared from 1.0 wt % PS₃₁₀-*b*-PAA₅₂ in the presence of various additives in dioxane-water mixtures.

Starting Morphology	Water Content (wt %)	Additive	Morphological Boundaries mM of Additive ^a (molar ratio of additive to AA units per chain)			
			S → S+R	S+R → R	R → R+V	R+V → V
Spheres	10.0	SDS	3.16(1.28)	6.32(2.56)	8.36(3.56)	12.1(4.87)
	10.0	NaCl	-----	-----	-----	-----
	10.0	TDA	28.8(11.8)	56.4(23.0)	75.0(30.6)	115(47.0)
Spheres +	12.5	SDS	-----	7.10(2.97)	8.95(3.74)	14.3(6.27)
	12.5	NaCl	-----	8.54(3.32)	13.1(5.47)	16.8(7.02)
Rods	12.5	TDA	-----	38.1(15.9)	64.9(3.97)	99.2(41.5)
Rods	15.0	SDS	-----	-----	9.73(4.16)	16.1(7.85)
	15.0	NaCl	-----	-----	8.74(3.73)	10.6(4.53)
	15.0	TDA	-----	-----	24.4(10.4)	48.3(20.6)

^a relative uncertainty of ± 0.7 %

One might infer from the phenomenon mentioned above that the effect of SDS on the morphology of the PS-*b*-PAA aggregates is merely a result of the electrostatic

shielding properties of the sulfate and sodium ions. However, the results from experiments conducted with SDS, using aggregates prepared by increasing the SDS concentration at a fixed solvent composition, in parallel to those with NaCl (Table 1), indicate that SDS is effective at inducing morphological changes in the block copolymer aggregates at solvent compositions at which NaCl is ineffective. This is attributed, in part, to the fact that SDS is more soluble in the solvent mixtures than NaCl. However, the strength of the effect of SDS on the aggregate structure decreases with increasing water content, unlike that observed for NaCl. Since the trends in the results obtained for SDS and NaCl are not that similar, the shielding effect of the surfactant ions cannot be the only means of interaction between the SDS molecules and the block copolymer chains. The hydrophobic tail of the SDS molecules is believed to have an additional effect on the morphology of the block copolymer aggregates.

In order to characterize the nature of the effect of the linear C12 chain of SDS on the copolymer aggregates, a series of studies were carried out to examine the influence of tridecanoic acid on the copolymer aggregates. This organic acid also contains a linear C12 chain, but in this case the chain is terminated with a carboxylic acid group. It is only slightly soluble in water, and does not form aggregates in the solvent mixtures used in this study. The small molecule species promote morphological transitions in PS-*b*-PAA aggregates in the three solvent mixtures used in the investigation. Because TDA molecules are not able to shield the electrostatic repulsions among the PAA chains, like NaCl and SDS, it is believed that they promote architectural changes by inserting their hydrophobic chain into the core of the aggregates. They act as spacers leading to an increase in the size of the core of the aggregates. Bronstein et al. observed similar behavior in systems of polystyrene-*b*-poly(ethylene oxide) aggregates in the presence of SDS.²⁵ The degree of PS stretching increases in response to the increase in the core diameter. This increased chain stretching is subject to an entropic penalty, and the aggregates undergo morphological changes in order to relieve this energy strain.⁹ The morphological boundaries are located at progressively lower TDA concentrations as the water content is increased. This occurs because the reduced solubility of the TDA at higher water contents makes it thermodynamically more favorable for these molecules to

partition into the hydrophobic environment of the core of the block copolymer aggregates.

It is generally observed that more TDA is required to induce the various morphological transitions than either NaCl or SDS. This phenomenon possibly suggests that the shielding of the electrostatic charge of the corona by the micro ions has a greater influence on the force balance governing the structure of the aggregates than the partitioning of the hydrophobic species into the core of the PS-*b*-PAA aggregates. However, it would seem from this argument that the dual nature of the effect of SDS on the block copolymer aggregates makes SDS a better morphogenic agent than NaCl or TDA. Although this is true for SDS in comparison to TDA, it is not always the case when the effect of SDS is compared to that of NaCl. At higher water contents, lower molar ratios of NaCl are required to bring about the morphological transformations compared to those of SDS. This outcome may result because the partitioning of the surfactant molecules into the core of the aggregates increases the charge density of the corona. This, in turn, occurs because the partitioning of the hydrocarbon tail of the surfactant anchors the sulfate head group at the interface between the core and the corona. The sulfate group is anionic and therefore repels the surrounding PAA ions. This increase in the charge density counters the promotion of the morphological transitions by the electrostatic shielding action of the microions and the partitioning of the hydrocarbon tail into the aggregate core. The charge density increases with an increase in the number of surfactant chains that partition into the aggregates, which increase with increasing water content in the solvent.

4.3.2 Effect of SDS at Different Solvent Compositions and Polymer Concentrations

Since a few properties are known about the effect of SDS on the force balance that controls the morphology of the PS-*b*-PAA aggregates, it is possible to suggest some reasons for the trends observed in the morphological phase boundaries with varying dioxane-water compositions and copolymer concentrations.

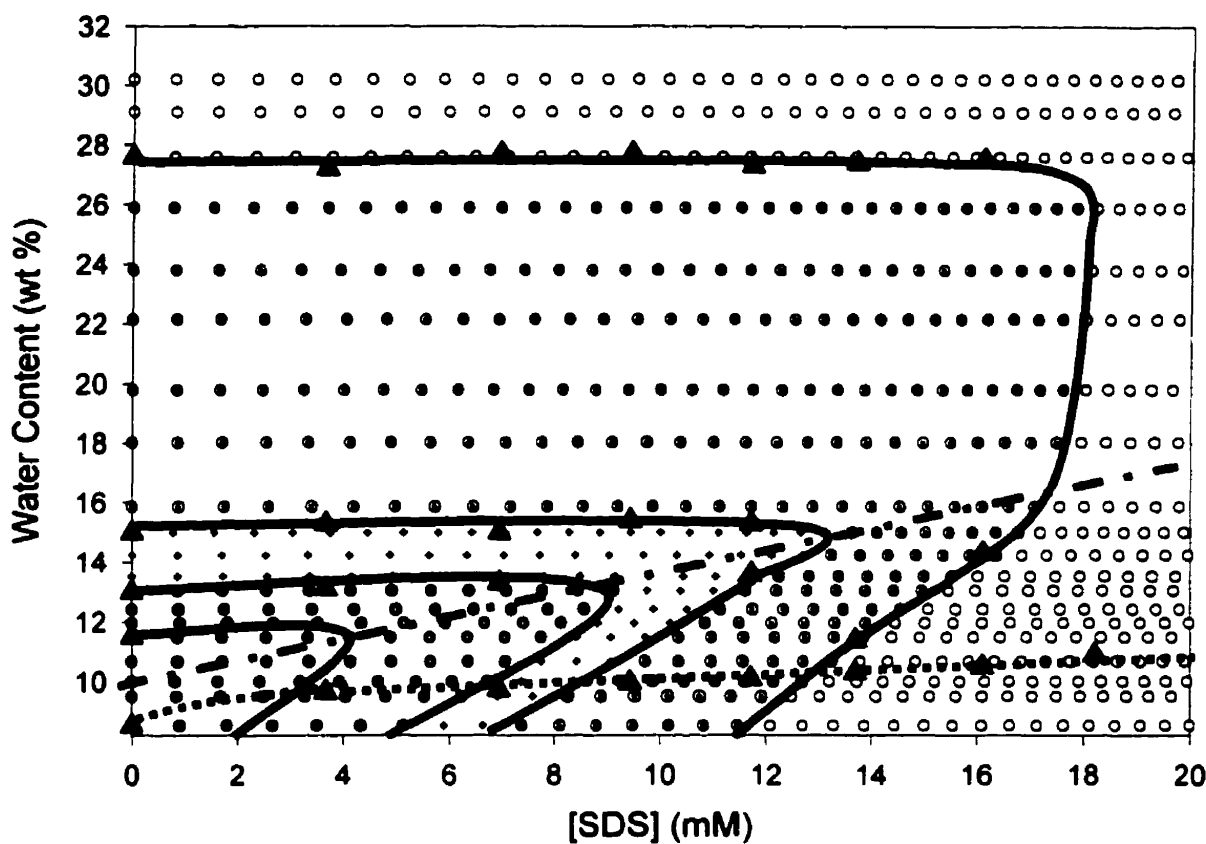


Figure 2: Morphological phase diagram for aggregates prepared from PS₃₁₀-*b*-PAA₅₂ in dioxane-water mixtures in the presence of SDS. The small symbols represent points obtained from turbidity studies (● spheres, ◐ spheres and rods, ⊕ rods, ⊙ rods and vesicles, ○ vesicles). The ▲ symbol represents the position of phase boundaries determined from increasing water content. The solid lines represent the phase boundaries determined from turbidity and TEM studies. The dashed lines are visual guides.

The phase diagram in Figure 2 summarizes the morphology of the aggregates formed in solutions of 1.0 wt % PS₃₁₀-*b*-PAA₅₂ at different SDS concentrations and at different water contents. These studies were performed in two different ways. In the first case, the solution turbidity was monitored as the SDS concentration was increased while maintaining a constant polymer concentration and solvent composition. Hence, the aggregates were already present in the system before the SDS was added. In fact, at zero

SDS spherical aggregates exist in the water content range of 8.5 to 11.5 wt % H₂O, spheres and rods coexist from 11.5 to 12.9 wt % H₂O, only rods are formed from 13.0 to 14.9 wt % H₂O, while rods and vesicles are present between 15.0 and 27.6 wt % H₂O, and vesicles are the only aggregates observed at water contents above 27.6 wt % H₂O.⁸ It should be noted that the addition of SDS to solutions in which the water component of the solvent composition was below the critical water content (cwc) of 8.5 wt %, required for aggregate formation, did not result in the formation of aggregates.⁸ In the second method of study, the solution turbidity was monitored as the water content was increased in solutions of constant polymer and surfactant concentrations; the aggregates were formed in the presence of SDS. In both cases, the morphology of the aggregates was confirmed with TEM studies. The small symbols in Figure 2 represent the experimental results obtained from the turbidity studies carried out as a function of increasing SDS concentration. The large triangles mark the position of the phase boundaries determined from the studies in which the turbidity was followed with increasing water content at fixed surfactant concentrations. The solid lines trace the location of the morphological boundaries that have been established from the results of the three different investigations.

The studies carried out by increasing the SDS concentration at fixed solvent compositions indicates that although morphological changes can be induced at lower water contents in the presence of SDS than in its absence, the morphological boundaries are shifted to higher concentrations of SDS as the water content in the solvent mixture is increased. This is attributed, in part, to the increase in the number of surfactant molecules that partition into the core of the aggregates with rising water content. As mentioned earlier, this partitioning process anchors sulfate anions at the core-corona interface, leading to an increase in the charge density of the corona. The stronger corona repulsion caused by the presence of the sulfate ions at the interface counters the ability of the surfactant molecules to promote morphological change by screening the corona repulsions with their micro ions, and by increasing the core size with the partitioning of the surfactant tails into the core of the aggregates.⁸

Similar studies were carried out at different polymer concentrations, and the results are summarized in Table 2. The aggregates were induced to undergo architectural

transitions at lower water contents than those required in the absence of additives at all polymer concentrations examined. The most notable result is that the molar ratio of SDS required to bring about structural changes in the aggregates decreases with an increase in the polymer concentration. However, the polymer concentration has also been found to influence the force balance governing the structure of the aggregates.⁸ The morphological boundaries are moved to lower water contents as the polymer concentration is increased; this is partially responsible for the trends in the morphological boundaries with increasing polymer concentration in the presence of SDS.

Table 2: *Effect of polymer concentration on the morphological boundaries between the regions of spheres (S), spheres + rods (S+R), rods (R), rods + vesicles (R+V), and vesicles (V) for PS₃₁₀-*b*-PAA₅₂ aggregates in the presence of SDS.*

Polymer Conc. (wt %)	Morphological Boundaries ^a in millimoles of SDS (and molar ratio of SDS to AA units)			
	S → S+R	S+R → R	R → R+V	R+V → V
0.71	2.13(1.28)	5.78(3.33)	8.72(5.03)	9.89(5.70)
1.01	3.16(1.24)	6.32(2.56)	8.36(3.56)	10.8(4.37)
1.52	4.66(1.22)	9.47(2.50)	11.5(3.08)	12.3(3.29)
2.00	4.82(0.98)	9.72(1.97)	13.2(2.67)	14.0(2.83)

^a Relative uncertainty of ± 0.5 %

4.3.3 Effect of Solution Preparation Method

As mentioned earlier, two methods of solution preparation were employed to study the effect of SDS on the solution behavior of the block copolymer aggregates. The first method involved gradually adding SDS to solutions with fixed polymer concentrations and solvent compositions containing aggregates of a given morphology. In the second method of solution preparation, the water content of the system was increased while maintaining constant SDS and polymer concentrations.

In principle, if the system is under equilibrium conditions, the morphology of the aggregates at a given solvent composition and SDS concentration should not depend on the method of solution preparation. Thus, the purpose of using the two preparation methods is to test the equilibrium nature of the system. The results in Figure 2 indicate that, for the most part, the morphological phase behavior of the aggregates is independent

of the solution preparation method; therefore, the system is under thermodynamic control. This is indicated by the fact that the triangular points generated by increasing the water content of the system fall on the phase boundary lines determined from increasing the SDS concentration at fixed polymer concentrations and solvent compositions. This is also clearly illustrated by the plot in Figure 3, which outlines the change in the solution turbidity as a function of water content for a system with a fixed surfactant concentration of 11.7 mM. In this case, both rods and vesicles are formed in the solution upon self-assembly of the copolymer chains. There is an initial rise in the turbidity because an increasing number of the rods are converted to vesicles, and vesicles scatter light more than rods. At ca. 12.2 wt % H₂O, the turbidity begins to decline because the vesicles are transformed back into rods. A region of pure rods is observed from 13.1 to 15.2 wt % H₂O. After this point, the turbidity increases because vesicles start to form again in solution. This continues until a water content of 27.5 wt %, above which only vesicles are present in the system. The arrows mark the morphological boundaries determined from the results of the studies carried out by increasing the SDS concentration while maintaining the solvent composition; there is good agreement between the two results.

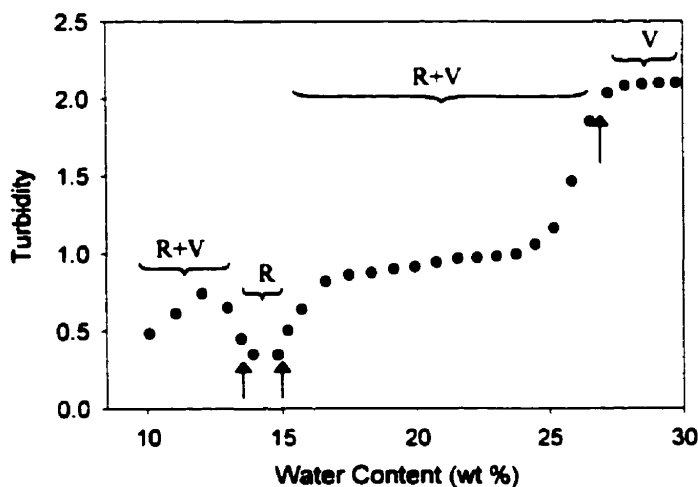


Figure 3: Morphological transitions examined by turbidity measurements for 1.0 wt % PS₃₁₀-*b*-PAA₅₂ in dioxane-water mixtures with a fixed SDS concentration of 11.7 mM. The arrows indicate the transition boundaries determined from experiments in which the solvent composition was held constant while the SDS concentration was increased.

It is interesting to note that the system is not in a state of equilibrium at lower water contents. The initial aggregation process of the block copolymer chains appears to be dependent on the solution preparation method. When the aggregates are formed by first adding water to the solutions of copolymer in dioxane and then adding SDS, the critical water content at which the aggregates initially form is found to be 8.5 wt %. When the aggregates are prepared by adding water to solutions containing copolymer and SDS in dioxane, the critical water content is increased, as shown by the dotted line in Figure 2. For example, in the presence of 9.4 mM of SDS, the copolymer solution did not become turbid, marking the onset of aggregation, until a water content of 10.0 wt % was reached. Therefore, the first morphological region of rod and vesicle coexistence from ca. 8.5 to ca. 11.0 wt % H₂O, determined from the studies of increasing the SDS concentration at constant solvent composition, was not observed when the study was carried out at constant SDS concentration and increasing water content (i.e. only rods were present. This was confirmed with TEM studies. It is speculated that the differences in the results obtained with the two methods of solution preparation may possibly be a result of very slow kinetics of aggregate formation at lower water contents in the presence of SDS. Hence, the system is governed by kinetics in the region of low water content and by thermodynamics at higher water contents. As well, surfactant molecules have been reported to impede block copolymer micellization as a result of the interaction of the surfactant molecules with the individual copolymer chains prior to aggregate formation.^{20,23} This interaction often involves the formation of small surfactant aggregates along the polymer chains. This may explain why the aggregation of PS₃₁₀-*b*-PAA₅₂ molecules occurs at higher water contents in the presence of SDS than in the absence of surfactant. In any event, the further study is required to determine the factors that influence the self-assembly process when the block copolymer aggregates are prepared using both methods of solution preparation.

Another interesting observation is made when the phase diagram in Figure 2 is divided diagonally from ca. 10.0 wt % H₂O on the left to ca. 17.5 wt % H₂O on the right of the diagram as indicated by the dash-dot line. Below this diagonal line the morphology of the aggregates appears to be dictated mostly by the effect of SDS on the force balance controlling the architecture of the copolymer aggregates. However, above this line the

aggregate morphology appears to be almost independent of the SDS concentration except at high concentrations of SDS (e.g. above 18.0 mM). This is apparent from the fact that the morphological phase boundaries in the presence of SDS were found to be the same as in the absence of additive at higher water contents. Although this phenomenon is not well understood, it is believed to be a result of the balance between the effect of SDS and that of water on the morphology of the aggregates. It is possible that the influence of SDS is more prominent at lower water contents and is enhanced with increasing SDS concentration, but that the increasing concentration of water in the system eventually overwhelms the effect of SDS on the morphology of the copolymer aggregates. This phenomenon requires further investigation.

4.4 Conclusions

Turbidity measurements and transmission electron microscopy were employed to investigate the effect of sodium dodecyl sulfate on the behavior of PS₃₁₀-*b*-PAA₅₂ aggregates in dioxane-water mixtures. It was found that SDS causes these aggregates to undergo morphological transitions at water contents lower than those normally required for the same structural changes in the absence of any additives.⁸ A parallel investigation of the effect of NaCl and tridecanoic acid on the copolymer aggregates indicated that the nature of the morphogenic effect of SDS is attributed to the ability of the surfactant micelles to screen the electrostatic field created by the partially charged PAA chains of the corona, as well as the partitioning of the surfactant tails into the core of the aggregates. Both of these factors alter the force balance controlling the morphology of the aggregates leading to structural changes. A morphological phase diagram was constructed to map out the architectural boundaries produced by increasing the SDS concentration in the copolymer solutions. The complex nature of the interaction of SDS with the copolymer aggregates results in an increase in the concentration of SDS required to induce the morphological transitions as the water content in the solvent is increased. However, the molar ratio of SDS to PAA at the morphological boundaries decreases slightly with an increase in the copolymer concentration. Although NaCl is more effective at inducing morphological changes at higher water contents, SDS proves to be a better morphogenic agent at lower water contents. One of the more interesting results obtained from this

study is the ability to convert PS-*b*-PAA aggregates from one morphology to another and than back again by increasing the water content at one SDS concentration. This is the first time this phenomenon has been observed in PS-*b*-PAA aggregate systems. It provides an additional degree of versatility to the system and hence provides better control over the aggregate architecture, which is important for any potential application of these systems.

4.5 References

1. a) de Gennes, P. G. In *Solid State Physics*; Liebert, L., Ed.; Academic Press: New York, 1978; supplement 14, p1. b) Halperin, A.; Tirrell, M.; Lodge, T. P. *Adv. Polym. Sci.* **1992**, *100*, 31.
2. a) Gao, Z.; Varshney, S. K.; Wong, S.; Eisenberg, A. *Macromolecules* **1994**, *27*, 7923. b) Honda, C.; Sakaki, K.; Nose, T. *Polymer* **1994**, *35*, 5309. c) Zhang, L.; Barlow, R. J.; Eisenberg, A. *Macromolecules* **1995**, *28*, 6055.
3. a) Zhang, L.; Shen, H.; Eisenberg, A. *Macromolecules* **1997**, *30*, 1001. b) Zhang, L.; Eisenberg, A. *Macromolecules* **1999**, *32*, 2239.
4. Desbaumes, L.; Eisenberg, A. *Langmuir* **1999**, *15*, 36.
5. Zhang, L.; Eisenberg, A. *Science* **1995**, *268*, 1728.
6. Shen, H.; Zhang, L.; Eisenberg, A. *J. Phys. Chem. B* **1997**, *101*, 4697.
7. Shen, H.; Eisenberg, A. *Macromolecules* **2000**, *33*, 2561.
8. Shen, H.; Eisenberg, A. *J. Phys. Chem. B* **1999**, *103*, 9473.
9. a) Zhang, L.; Eisenberg, A. *Poly. Adv. Technol.* **1998**, *9*, 677. b) Cameron, N. S.; Corbierre, M. K.; Eisenberg, A. *Can. J. Chem.* **1999**, *8*, 1311. c) Burke, S.; Eisenberg, A. *High Performance Polymers* **2000**, *12*, 535.
10. a) Ding, J.; Liu, G. *Polymer* **1997**, *38*, 5497. b) Hajduk, D. A.; Kossuth, M. B.; Hillmyer, M. A.; Bates, F. S. *J. Phys. Chem. B* **1998**, *102*, 4269. c) Discher, B. M.; Won, Y.-Y.; Ege, D. S.; Lee, J. C.-M.; Bates, F. S.; Discher, D. E.; Hammer, D. A. *Science* **1999**, *284*, 1143. d) Prochazka, K.; Martin, T. J.; Webber, S. E.; Munk, P. *Macromolecules* **1996**, *29*, 6526. e) Spatz, J. P.; Mössmer, S.; Möller,

- M. *Angew. Chem. Int. Ed. Engl.* **1996**, *35*, 1510. f) Massey, J.; Power, K. N.; Manners, I.; Winnik, M. A. *J. Am. Chem. Soc.* **1998**, *120*, 9533.
11. a) Kramer, E.; Förster, S.; Goltner, C.; Antonietti, M. *Langmuir*, **1998**, *14*, 2027. b) Jørgenbseb, E. B.; Hvidt, S.; Brown, W.; Schillén, K. *Macromolecules* **1997**, *30*, 2355. c) Liu, G. *Curr. Opin. Colloid Interface Sci.* **1998**, *3*, 200. d) Rheingans, O.; Hugenberg, N.; Harris, J. R.; Fischer, K.; Maskos, M. *Macromolecules* **2000**, *33*, 4780. e) Liang, Y.-Z.; Li, Z.-C.; Li, F.-M. *Chem. Lett.* **2000**, *4*, 320.
12. a) Yu, Y.; Eisenberg, A. *J. Am. Chem. Soc.* **1997**, *119*, 8383. b) Rheingans, O.; Hugenberg, N.; Harris, J. R.; Fischer, K.; Maskos, M. *Macromolecules* **2000**, *33*, 4780.
13. a) Yu, K.; Zhang, L.; Eisenberg, A. *Langmuir* **1996**, *12*, 5980. b) Svensson, M.; Alexandridis, P.; Linse, P. *Macromolecules* **1999**, *32*, 5435. c) Svensson, B.; Olsson, U.; Alexandridis, P. *Langmuir* **2000**, *16*, 6839.
14. a) Mortensen, K.; Pedersen, J. S. *Macromolecules* **1993**, *26*, 805. b) Schillén, K.; Brown, W.; Johnsen, M. *Macromolecules* **1994**, *27*, 4825.
15. a) Zhang, L.; Yu, K.; Eisenberg, A. *Science* **1996**, *272*, 1777. b) Zhang, L.; Eisenberg, A. *Macromolecules* **1996**, *29*, 8805. c) Shen, H.; Zhang, L.; Eisenberg, A. *J. Am. Chem. Soc.* **1999**, *121*, 2728. d) Talingting, M. R.; Munk, P.; Webber, S. E. Tuzar, Z. *Macromolecules* **1999**, *32*, 1593. e) Jørgenbseb, E. B.; Hvidt, S.; Brown, W.; Schillén, K. *Macromolecules* **1997**, *30*, 2355. f) Kabanov, A.; Bronich, T. K.; Kabanov, V. A.; Eisenberg, A. *J. Am. Chem. Soc.* **1998**, *120*, 9941. g) Zheng, Y.; Davis, H. T. *Langmuir* **2000**, *16*, 6453.
16. a) Goddard, E. D. *Colloid Surf.* **1986**, *19*, 255. b) Winnik, F. M.; Regismond, S. T. A. *Colloid Surf. A* **1996**, *118*, 1. c) Lindman, B.; Thalberg, K. *Adv. Coll. Int. Sci.* **1992**, *41*, 149. d) Hansson, P.; Lindman, B. *Current. Opin. Colloid Interface Sci.* **1996**, *1*, 604.
17. a) Xu, B.; Yekta, A.; Li, L.; Masoumi, Z.; Winnik, M. A. *Colloid Surf., A* **1996**, *112*, 239. b) Anthony, O.; Zana, R. *Langmuir* **1996**, *12*, 3590. c) Everaars, M. D.; Nieuwkerk, A. C.; Denis, S.; Marcelis, A. T.; Sudhölter, E. J. *Langmuir* **1996**, *12*,

4042. d) Bakeev, K. N.; Ponomarenko, E. A.; Shishkarova, T. V.; Tirrell, D. A.; Zezin, A. B.; Kabanov, V. A. *Macromolecules* **1995**, *28*, 2886.
18. a) *Interactions of Surfactants with Polymers and Proteins*; Goddard, E. D., Annthapadmanabhan, K. P., Eds.; CRC: Boca Raton, FL, 1993. b) *Surfactants and Polymers in Aqueous Solutions*; Jonsson, B.; Lindman, B.; Holmberg, K.; Kronberg, B., Eds.; Wiley: Chichester, UK, 1998. c) *Principles of Polymer Science and Technology in Cosmetics and Personal Care*; Goddard, E. D.; Gruber, J. L., Eds. Dekker: New York, 1999. d) *Polymer-Surfactant Systems*; Kwak, J.C.T., Ed.; Surfactant Science Series 77; Dekker: New York, 1998.
19. Almgren, M.; van Stam, J.; Lindblad, C.; Li, P.; Stilbs, P.; Bahadur, P. *J. Phys. Chem.* **1991**, *95*, 5677.
20. a) Hecht, E.; E.; Hoffmann, H. *Langmuir* **1994**, *10*, 86. b) Hecht, E.; Mortensen, K.; Gradzielski, M.; Hoffmann, H. *J. Phys. Chem.* **1995**, *99*, 4866.
21. Zhang, K.; Lindman, B.; Copppola, L. *Langmuir* **1995**, *11*, 538.
22. Kositza, M. J.; Rees, G. D.; Holzwarth, A.; Holzwarth, J. F. *Langmuir* **2000**, *16*, 9035.
23. a) Li, Y.; Xu, R.; Bloor, D. M.; Holzwarth, J. F.; Wyn-Jones, E. *Langmuir* **2000**, *16*, 10515. b) Li, Y.; Xu, R.; Couderc, S.; Bloor, D. M.; Wyn-Jones, E.; Holzwarth, J. F. *Langmuir* **2001**, *17*, 183.
24. Bronstein, L. M.; Chernyshov, D. M.; Timofeeva, G. I.; Bubrovina, L. V.; Valetsky, P. M.; Obolonkova, E. S.; Khokhlov, A. R. *Langmuir* **2000**, *16*, 3626.
25. Bronstein, L. M.; Chernyshov, D. M.; Timofeeva, G. I.; Dubrovina, L. V.; Valetsky, P. M.; Khokhlov, A. R. *J. Colloid Interface Sci.* **2000**, *230*, 140.
26. a) Bronich, T. K.; Kabanov, A. V.; Kabanov, V. A.; Yu, K.; Eisenberg, A. *Macromolecules* **1997**, *30*, 3519. b) Lysenko, E. A.; Bronich, T. K.; Eisenberg, A.; Kabanov, V. A.; Kabanov, A. V. *Macromolecules* **1998**, *31*, 4516. c) Bronich, T. K.; Popov, A. M.; Eisenberg, A.; Kabanov, V. A.; Kabanov, A. V. *Langmuir* **2000**, *16*, 481.

27. Kabanov, A. V.; Bronich, T. K.; Kabanov, V. A.; Yu, K.; Eisenberg, A. *J. Am. Chem. Soc.* **1998**, *120*, 9941.
28. Egger, H.; Nordskog, A.; Lang, P. *Macromol. Symp.* **2000**, *162*, 291.
29. Zheng, Y.; Davis, H. T. *Langmuir* **2000**, *16*, 6453.
30. Burke, S. E.; Eisenberg, A. *to be submitted*
31. Panda, L.; Behera, G. B. *J. Indian Chem. Soc.* **1985**, *LXII*, 44.

Chapter 5

Conclusions, Contributions to Original Knowledge, and Suggestions for Future Work

5.1 Conclusions and Contributions to Original Knowledge

The work summarized in this thesis explored some of the physico-chemical properties of aggregates of multiple morphologies prepared from PS₃₁₀-b-PAA₅₂ in dioxane-water mixtures. The following discussion is a summary of the notable experimental results that have been described throughout this dissertation with particular attention paid to the original aspects of these findings. This section is divided into two parts beginning with the conclusions drawn from the kinetic and mechanistic studies of three morphological transitions occurring in PS₃₁₀-b-PAA₅₂ aggregates in solution. The second part focuses on the effect that sodium dodecyl sulfate was found to have on the morphology of the copolymer aggregates.

5.1.1 Kinetics and Mechanisms of Morphological Transitions

Chapter 2 describes the kinetics and mechanisms associated with both the sphere-to-rod and the rod-to-sphere transitions that occur in aggregates formed in the PS₃₁₀-b-PAA₅₂ / dioxane / water system. A similar investigation was used to study the vesicle-to-rod transition that takes place in the same copolymer system, the details of which were discussed in chapter 3. Chen et al. were the first to study the kinetics and mechanisms associated with the architectural changes, observed in block copolymer aggregates in solution, with their study of the rod-to-vesicle transition in the PS₃₁₀-b-PAA₅₂ aggregates.¹ Hence, the results described in chapters 2 and 3 provide additional knowledge about the details involved in morphological transformations, and this information is important to have if control is to be exercised over these aggregates in potential applications in such areas as pharmaceutical and personal care products.

The transformations were induced by a jump in the content of one of the solvent components near the morphological boundaries. The solvent compositions at the boundaries were obtained from the morphological phase diagram that was constructed by Shen and Eisenberg for the PS₃₁₀-b-PAA₅₂ / dioxane / water system.² The solution

turbidity was monitored as a function of time in order to study the kinetics, and the intermediate aggregate structures were observed by transmission electron microscopy. This information was used to propose transition mechanisms.

The sphere-to-rod transition was found to proceed via a two-step mechanism. The first step, which is the fast process, entailed a series of adhesive collisions between spherical micelles to form “pearl necklace” intermediates. The rate-limiting step involved the reorganization of the necklaces to form smooth rods. The resulting rods had a smaller diameter than the spherical micelles from which they were formed. Within the transition region, the ratio of the rods to spheres increased with rising water content. The reverse process, the rod-to-sphere transition, also involved two relaxation steps. The fast step was ascribed to the formation of a bulb on either or both ends of the rods. These bulbs were slowly pinched off to release free spheres in solution during the rate-determining process.

Since neither the sphere-to-rod nor the rod-to-sphere transition proceeded with conservation of mass (i.e. the aggregation number of rods is larger than that of spheres), it was not possible to obtain rate constants for the steps in each mechanism. However, the turbidity-time profiles were fitted best to a double exponential equation (with exceptions at higher polymer concentrations) from which relaxation times were obtained. The rate of both the forward and reverse transitions were comparable. The kinetic results indicated that the relaxation times for both transitions increased with an increase in the initial water content of the solvent mixture. When the magnitude of the solvent jump was increased, the sphere-to-rod transition occurred more quickly, while the rate of the rod-to-sphere transition became slower. Increasing the initial copolymer concentration resulted in a decrease in the relaxation times for the sphere-to-rod transition, but a more complex trend was observed in the τ values of the rod-to-sphere transition.

In order to extend the study of the rod-to-vesicle transition led by Chen et al., the kinetics and mechanism of the vesicle-to-rod transition were investigated.¹ As the transition region was approached from the vesicle side, the mean diameter of the aggregates decreased with little change in the vesicle wall thickness, which resulted in an increase in the curvature energy. This made the vesicles energetically unstable and subsequently prone to structural transformation. The first intermediate aggregates observed were in the shape of “bowties” (two adjoining spheres). The bowties grew into

“dumbbell” shaped structures. The dumbbells extended about the long-axis at the expense of the bulbs on either end until smooth rods were formed. The average volume of the vesicles and the rods was quite similar, which suggests that this transition involved the conversion of one vesicle into one rod and vice-versa, as was observed in the case of the rod-to-vesicle transition.¹

The kinetic data obtained for this multi-step transition yielded a single relaxation time. This result, coupled with the fact that the non-bilayer bowtie intermediate structures were not likely formed directly from vesicles, suggests that experimental limitations prevented us from acquiring information about one or more of the faster steps in the transition. However, the kinetic results that were obtained shows that the relaxation time for the vesicle-to-rod transition increased slightly with an increase in both the initial water content of the solvent mixture and the magnitude of the dioxane content jump. The relaxation time also increased with increasing polymer concentration, and the effect was much more pronounced than in the case of the other two parameters.

5.1.2 Effect of Sodium Dodecyl Sulfate on Block Copolymer Aggregates in Solution

A study of the effect of sodium dodecyl sulfate (SDS) on the solution behavior of aggregates prepared from PS₃₁₀-b-PAA₅₂ in dioxane-water mixtures was described in chapter 4. It was found that the SDS molecules interact with the copolymer chains, and that these interactions cause the block copolymer aggregates to undergo morphological transitions at lower water contents than those required in the absence of surfactant.² The polymer-surfactant interactions were found to be multi-dimensional because of the amphiphilic character of SDS. The micro ions of the surfactant molecules screened the electrostatic field generated by the partially charged corona chains, while the surfactant tails partitioned into the aggregates, which resulted in an increase in the core diameter. These processes led to architectural transformations because they disturb the force balance that governs the morphology of the aggregates. The details of the interaction of SDS with PS-b-PAA were confirmed from parallel studies carried out with sodium chloride and tridecanoic acid in order to isolate the effects of the micro ions and of the linear alkyl chain.

A morphological phase diagram was constructed to determine the structural boundaries. The concentration of SDS required to induce the morphological changes increased with rising water content. This was attributed to the fact that the surfactant molecules that partition into the aggregates can hinder the transition process by increasing the degree of corona repulsion. Thus, the morphological boundaries were determined by the balance between the factors that promote structural change and those that hinder the process.

The phase diagram studies were performed using two methods of solution preparation in order to test the equilibrium nature of the system. In one case the concentration of SDS was increased while the solvent composition and copolymer concentration were fixed, while in the second method the water content was increased and the polymer and SDS concentrations were held constant. It was found that the system is under equilibrium control, except at lower water contents where the kinetics of the system influenced the morphology of the aggregates to a greater extent than the thermodynamics.

5.2 Suggestions for Future Work

The aim of this section is to provide some insight into how to build upon the studies described throughout this thesis. The discussion begins with some suggestions for the expansion of the investigation of the kinetics and mechanisms of morphological transitions occurring in block copolymer aggregates. This is followed with a few ideas for studies that may prove useful for learning more about how to tailor the structure of block copolymer aggregates with small molecule surfactants.

5.2.1 Suggestions for Research on Kinetics and Mechanisms of Morphological Change

The studies presented in chapters 2 and 3 provide the kinetic and mechanistic details associated with three morphological transitions (sphere-to-rod, rod-to-sphere, and vesicle-to-rod). There are many other transitions for which the kinetics and mechanisms are yet to be explored such as the bilayer-to-vesicle³, the bi-continuous rod-to-vesicle⁴, the vesicle-to-hexagonally packed hollow hoops⁵, the vesicle-to-large compound

micelle⁶, and several others. The reversibility of many of these morphological changes makes it viable to explore the details of the reverse transitions.²

Although our studies have focused on the influence that changing the initial solvent composition, the magnitude of the solvent jump, and the initial polymer concentration have on the kinetics of the morphological transitions, a number of other system parameters are known to effect the architecture of the aggregates and may also influence the transformation processes. These factors include the type of nonspecific solvent employed (i.e. THF or DMF instead of dioxane)⁷, the temperature⁸, the length of the copolymer blocks³, the nature of the repeat units in the copolymer⁹, and the presence of additives⁶. Among these factors, the temperature is of particular interest because lower temperatures are likely to slow down the transition kinetics, and since we were not able to obtain a complete picture of the kinetics and mechanism of the vesicle-to-rod transition, repeating the study at lower temperatures may provide more information about this process. In addition, it may be possible to determine the activation energy associated with each transitions step from a detailed study of the kinetics at different temperatures. However, it must be noted that in order to examine the structural transformations at a lower temperature, the morphological boundaries must first be evaluated at the new temperature.

Since changing such parameters as the temperature, the nature of the solvent, and the presence of additives effect the morphology of the copolymer aggregates, it would also be fruitful to carry out kinetic and mechanistic studies using one of these factors to induce the transitions in much the same way as jumps in either the water or dioxane content were employed in the studies discussed in this thesis.

Expanding the investigation of the kinetics and mechanisms of morphological transitions in block copolymer aggregates in solution in anyone of the above mentioned directions would shed new light on how to control these systems and may provide some ideas for potential applications of these systems.

5.2.2 Suggestions for Future Work on the Effect of Surfactants on PS-b-PAA Aggregates

The work presented in chapter 4 is the first study of the interaction of PS-b-PAA aggregates with surfactants of the same charge in dilute solution. Thus, many aspects of this work are yet to be examined. The first step for the continuation of this project is to further characterize the nature of the association between SDS and the PS₃₁₀-b-PAA₅₂ aggregates. It may be possible to determine the number of SDS molecules required to bring about each morphological transition. This can be attempted by using sodium NMR studies or by electrochemical analysis with a surfactant selective electrode, after dialysis of the copolymer-surfactant solutions to remove unassociated SDS.^{10,11} In addition, since the behavior of the system at lower water contents is dependent on the method of solution preparation, an examination of the mechanism, thermodynamics, and kinetics of micelle formation in the presence of SDS may prove to be valuable from both an academic and an industrial standpoint.

Once the characteristics and properties of the interaction of SDS and PS-b-PAA aggregates are more understood, it would be interesting to try to tailor the influence of the ionic interactions and hydrocarbon tail partitioning on the morphology of the aggregates by completing parallel studies using surfactants with different structural properties such as those with two head groups, a zwitterionic head group, a double chain tail, and a styrene based tail. This tailoring process may also be possible by using both nonionic surfactants and simple electrolytes together to induce morphological change.

5.3 References

1. Chen, L.; Shen, H.; Eisenberg, A. *J. Phys. Chem. B* **1999**, *103*, 9488.
2. Shen, H.; Eisenberg, A. *J. Phys. Chem. B* **1999**, *103*, 9473.
3. Shen, H.; Eisenberg, A. *Macromolecules* **2000**, *33*, 2561.
4. Zhang, L.; Eisenberg, A. *J. Polym. Sci. B: Polym. Phys.* **1999**, *37*, 1469.
5. Zhang, L.; Bartels, C.; Yu, Y.; Shen, H.; Eisenberg, A. *Phys. Rev. Lett.* **1997**, *79*, 5034.
6. Zhang, L.; Eisenberg, A. *Macromolecules* **1996**, *29*, 8805.

7. Yu, Y.; Zhang, L.; Eisenberg, A. *Macromolecules* **1998**, *31*, 1144.
8. Desbaumes, L.; Eisenberg, A. *Langmuir* **1999**, *15*, 36.
9. Cameron, N. S.; Corbierre, M. K.; Eisenberg, A. *Can. J. Chem.* **1999**, *77*, 1311.
10. Stilbs, P. NMR Studies of Polymer-Surfactant Systems. In *Polymer-Surfactant Systems*, Kwak, J. C.T., Ed., Surfactant Science Series 77, Marcel Dekker: New York, 1998; pp 239-266.
11. Li, Y.; Xu, R.; Couderc, S.; Bloor, D. M.; Wyn-Jones, E.; Holzwarth, J. F. *Langmuir* **2001**, *17*, 183.